

REPORT No. 610

TESTS OF RELATED FORWARD-CAMBER AIRFOILS IN THE VARIABLE-DENSITY WIND TUNNEL

By EASTMAN N. JACOBS, ROBERT M. PINKERTON, and HARRY GREENBERG

SUMMARY

A recent investigation of numerous related airfoils indicated that positions of camber forward of the usual location resulted in an increase of the maximum lift. As an extension of this investigation, a series of forward-camber airfoils has been developed, the members of which show airfoil characteristics superior to those of the airfoils previously investigated.

The primary object of the report is to present fully corrected results for airfoils in the useful range of shapes. With the data thus made available, an airplane designer may intelligently choose the best possible airfoil-section shape for a given application and may predict to a reasonable degree the aerodynamic characteristics to be expected in flight from the section shape chosen.

For airfoils of moderate thickness, the optimum camber position was found to correspond to that of the N. A. C. A. 23012 section. A discussion is included concerning the choice of the best thickness and camber for full-scale applications depending on specific design conditions. Data to assist in the choice of the optimum section for a design using split flaps were obtained by testing some of the better sections with trailing-edge split flaps.

INTRODUCTION

The well-known airfoil-section investigations in the N. A. C. A. variable-density wind tunnel have been directed toward studies of the effects of variations of airfoil-section shape. Such studies are intended to determine the range within which the best possible section shapes for any given application will generally be found. With the data thus made available, an airplane designer may intelligently choose the best possible airfoil-section shape for a given application and may predict to a reasonable degree the aerodynamic characteristics to be expected in flight from the section shape chosen.

The first investigation of this series (reference 1) gave comparable data from the standard large Rey-

nolds Number tests in the variable-density tunnel, which were considered as representative within the flight range, for related airfoils covering section-shape variations in the neighborhood of commonly used airfoils. A subsequent investigation (references 2 and 3), covered by this report, deals with airfoil sections differing from those commonly used in that the camber occurs farther forward, i. e., nearer the leading edge. The desirability of this shape characteristic was indicated by the first investigation.

After the mean-line shape designated 230 had been found to be near the optimum (reference 2), an airfoil having the N. A. C. A. 23012 section was tested in the N. A. C. A. full-scale tunnel to verify the superiority of its characteristics over those of commonly used airfoils (reference 4). This and other tests (references 5 and 6) in the full-scale tunnel also provided valuable data on which to base an interpretation of the variable-density-tunnel data as applied to flight. In addition, a selected group of the related airfoils has been tested over a wide range of values of the Reynolds Number. The results of this investigation (reference 6) provided the information needed to apply the standard variable-density-tunnel airfoil data to flight at any particular value of the flight Reynolds Number.

Aside from the presentation of the important section characteristics fully corrected for application to flight at the standard value of the Reynolds Number (effective Reynolds Number approximately 8,000,000) for all the forward-camber series of airfoils tested, one object of the present report is to consider possible improvements of the N. A. C. A. 23012 section. This possibility was investigated by an analysis of test results for a number of airfoils, the shape of which varied systematically from the N. A. C. A. 23012. Finally, several airfoils within the most useful range of shapes were investigated to provide data for the various airfoils that may be chosen as most efficient in particular applications.

The airfoils developed in the variable-density-tunnel investigations have been designated by numbers having four or more digits. As explained in reference 1, the maximum ordinate of the mean line is called the "camber" and the position of the maximum ordinate is called the "position of the camber." The airfoils reported in reference 1 were designated by a number having four digits. The first digit indicated the camber in percent of chord; the second, the shape of the mean line as indicated by the position of the camber in tenths of the chord from the leading edge; and the last two, the maximum thickness in percent of the chord. The extension of the investigation to the forward-camber airfoils presented herein (including the airfoils in references 2 and 3) necessitated an extension of the designation numbers to cover the new mean-line shapes. As before, the first digit indicates the relative magnitude of the camber; but the second has been replaced by a pair of digits, which together indicate the mean-line shape for which position of camber is one of the parameters; and the last two, as before, indicate the thickness of the airfoil section. The camber, the mean-line shape designation, the corresponding values of camber, and the position of camber for these forward-camber airfoils are given in the following table.

Mean-line shape designation (second and third digits)		10	20	30	40	50
Camber designation (first digit)	Position of camber, percent of chord	5	10	15	20	25
(Actual camber in percent of chord)						
2		1.1	1.5	1.8	2.1	2.3
3		2.3	2.8	3.1	—	—
4		3.1	3.7	4.2	—	—
6		4.6	5.5	6.2	—	—

The table thus indicates, for example, that the N. A. C. A. 230 -- airfoil has the camber 1.8 percent of the chord at 0.15c behind the leading edge.

The airfoils designated by both the four and the five digit numbers have only one form of thickness variation. Changes in the form of the thickness variation made by altering the leading-edge radius and the position of maximum thickness (see reference 7) have been designated by appending two additional digits separated by a dash from the basic airfoil designation. The first of these two digits indicates the relative magnitude of the leading-edge radius and the second indicates

the position of the maximum thickness in tenths of the chord from the leading edge. The significance of the leading-edge radius designation is given below:

- 0 designates sharp leading edge.
- 3 designates one-fourth normal leading-edge radius.
- 6 designates normal leading-edge radius.
- 9 designates three or more times normal leading-edge radius.

The complete system of airfoil designation is illustrated by the following examples: The N. A. C. A. 2212 (reference 1) has a camber of 2 percent of the chord at 0.2 of the chord from the leading edge and a thickness of 12 percent of the chord. The N. A. C. A. 0012 (reference 1) is a symmetrical airfoil having a thickness of 12 percent of the chord. The N. A. C. A. 24012 (reference 2) has a camber of approximately 2 percent of the chord (actually 2.1 of the chord, see table I) at 0.2 of the chord from the leading edge and a thickness of 12 percent of the chord. It will be noted that the N. A. C. A. 2212 and the N. A. C. A. 24012 have practically the same camber, camber position, and thickness; however, the shapes of the mean-camber lines, designated by the digit 2 in one case and 40 in the other, are entirely different. Finally the N. A. C. A. 0012-64 is a symmetrical airfoil having a normal leading-edge radius and the maximum thickness at 0.4 of the chord from the leading edge. The N. A. C. A. 24012-33 has the same mean line and thickness as the N. A. C. A. 24012 but has a leading-edge radius one-fourth the normal and the maximum thickness at 0.3 of the chord from the leading edge.

The scope of the present investigation is best indicated by figure 1, which gives the profiles of the airfoils tested. Of the airfoils of 12 percent thickness, there are included a group of increasing camber: 00, 230, 330, 430, and 630; a group of varying camber position: 210, 220, 230, 240, and 250; and some variations of camber position for airfoils more highly cambered than the 230 series. From the results of these tests, the camber position corresponding to the series 230, 430, and 630 appeared to be best, so that in most cases variations of section thickness are included only for these mean-line shapes and for the symmetrical airfoils. Some variations of thickness distribution are included, and also some of the more interesting airfoils with a high-lift device consisting of a 20-percent-chord full-span split flap.

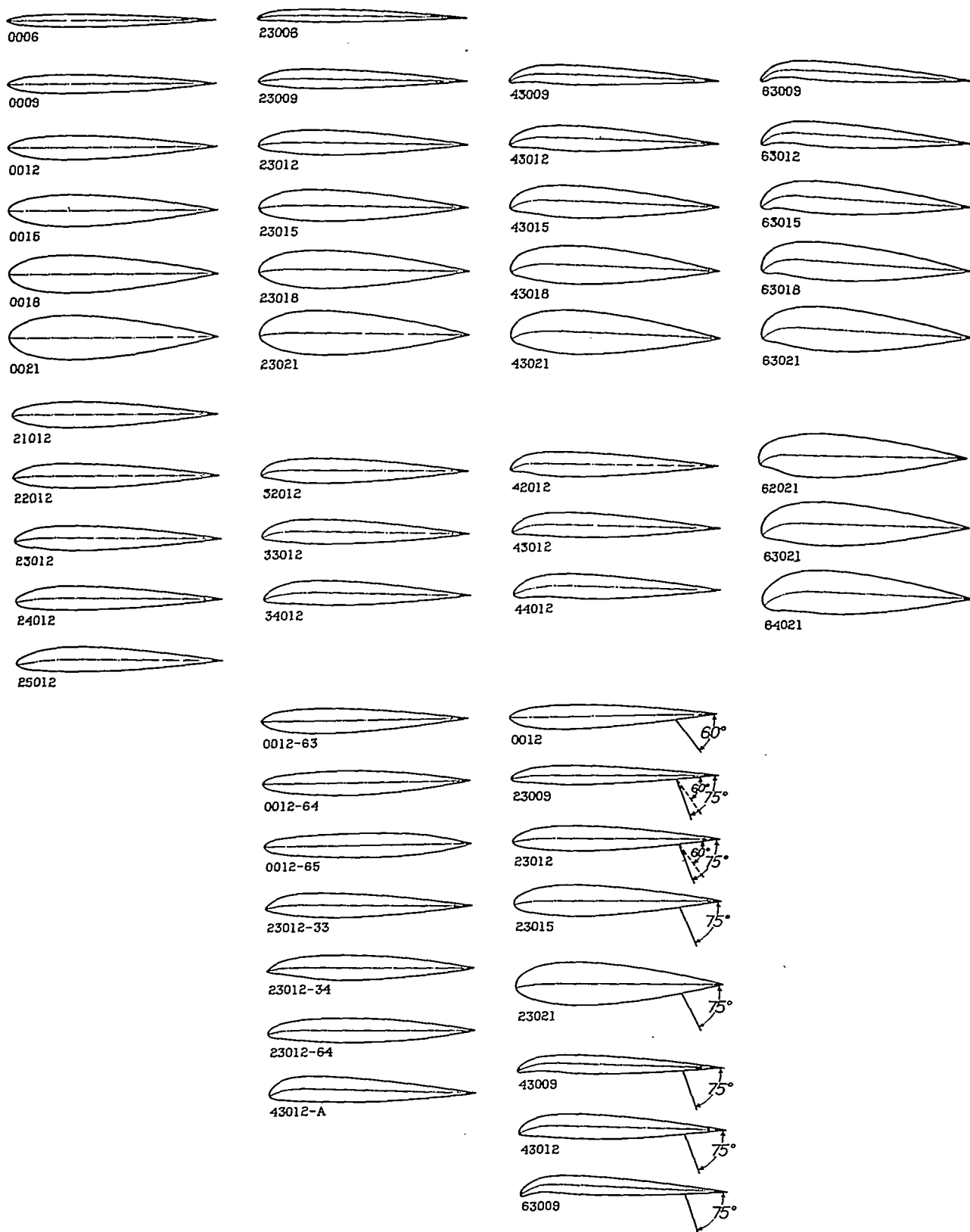


FIGURE 1.—N. A. C. A. airfoil profiles.

DESCRIPTION OF AIRFOILS

The thickness variations of the airfoils are given in references 1 and 7. The cambered airfoils have mean lines of the form given in reference 2. Profiles of all the airfoils presented herein are shown in figure 1.

The models are of 5-inch chord and 30-inch span, of rectangular plan form, and are constructed of duralumin as explained in reference 8.

APPARATUS AND METHOD

The variable-density wind tunnel, in which the tests were made, is described in reference 8. Routine measurements of the lift, drag, and pitching moment were made at an effective Reynolds Number of approxi-

and to the "blocking effect" of the model in the tunnel. These errors have since been investigated (see the appendix of reference 6) and have been eliminated by correcting the manometer settings used in fixing the tunnel air speed. Other errors mentioned in reference 1 have been somewhat reduced.

RESULTS

The data are presented (figs. 2 to 51) in a manner that is a slight modification of the standard graphic form used in previous reports. The left-hand portion of the plot presents the test data in the usual standard form for rectangular airfoils of aspect ratio 6. Included also are the airfoil profile, the table of ordinates,

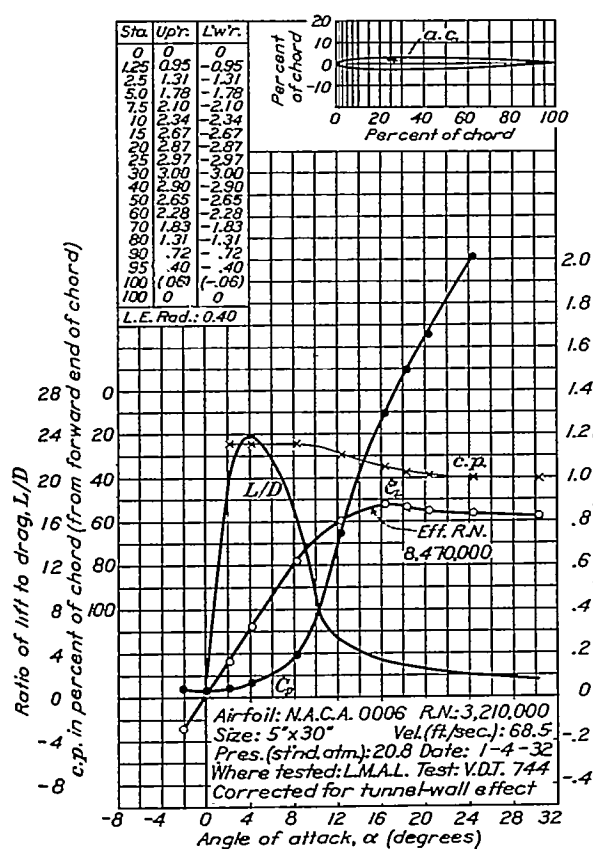
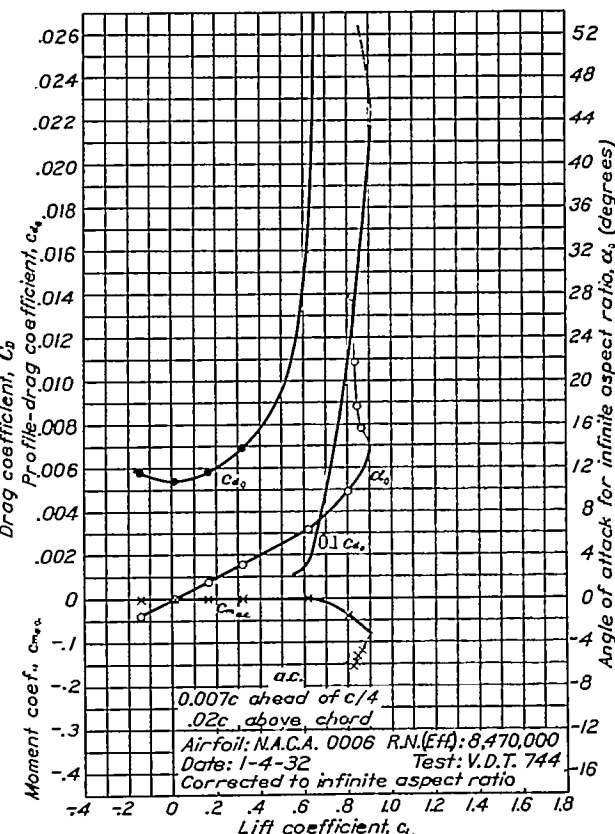


FIGURE 1.—N. A. O. A. 0006 airfoil.

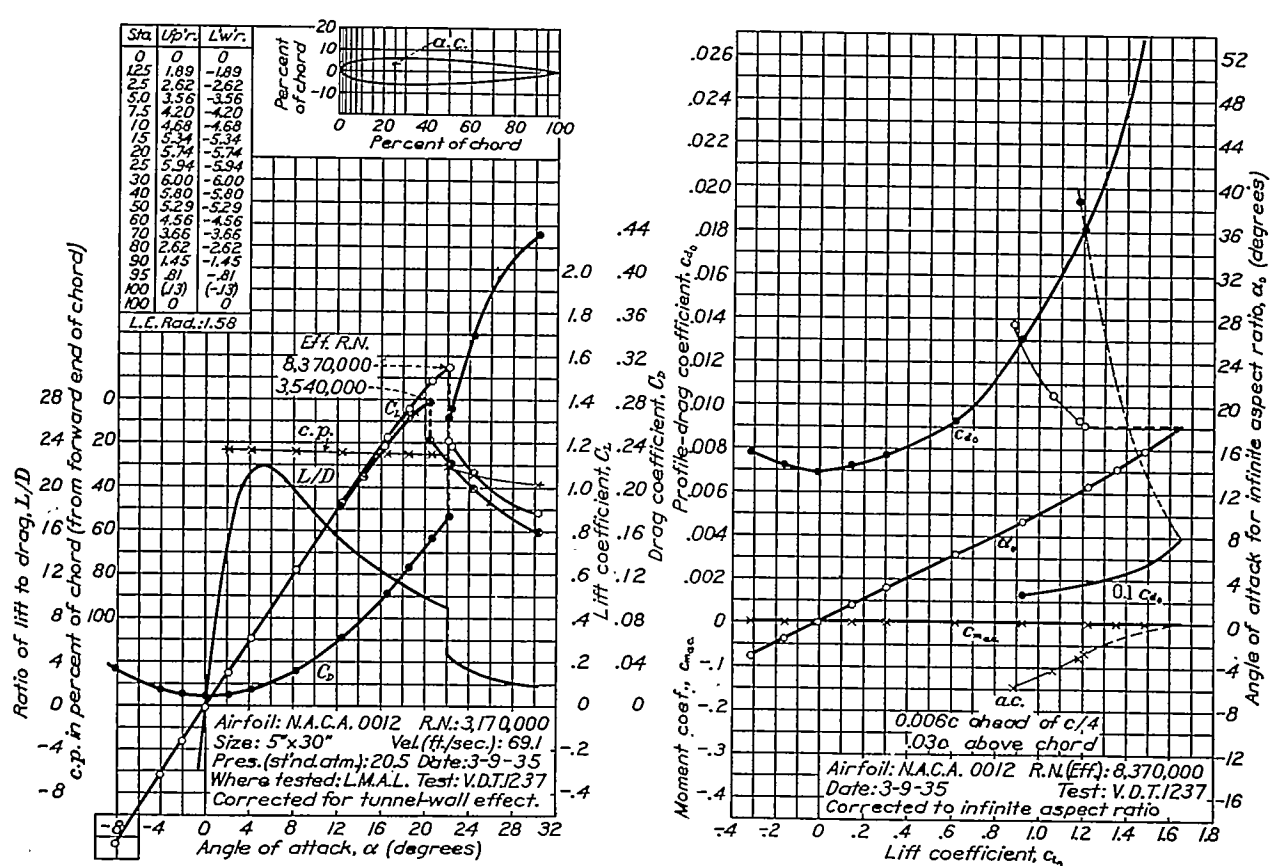
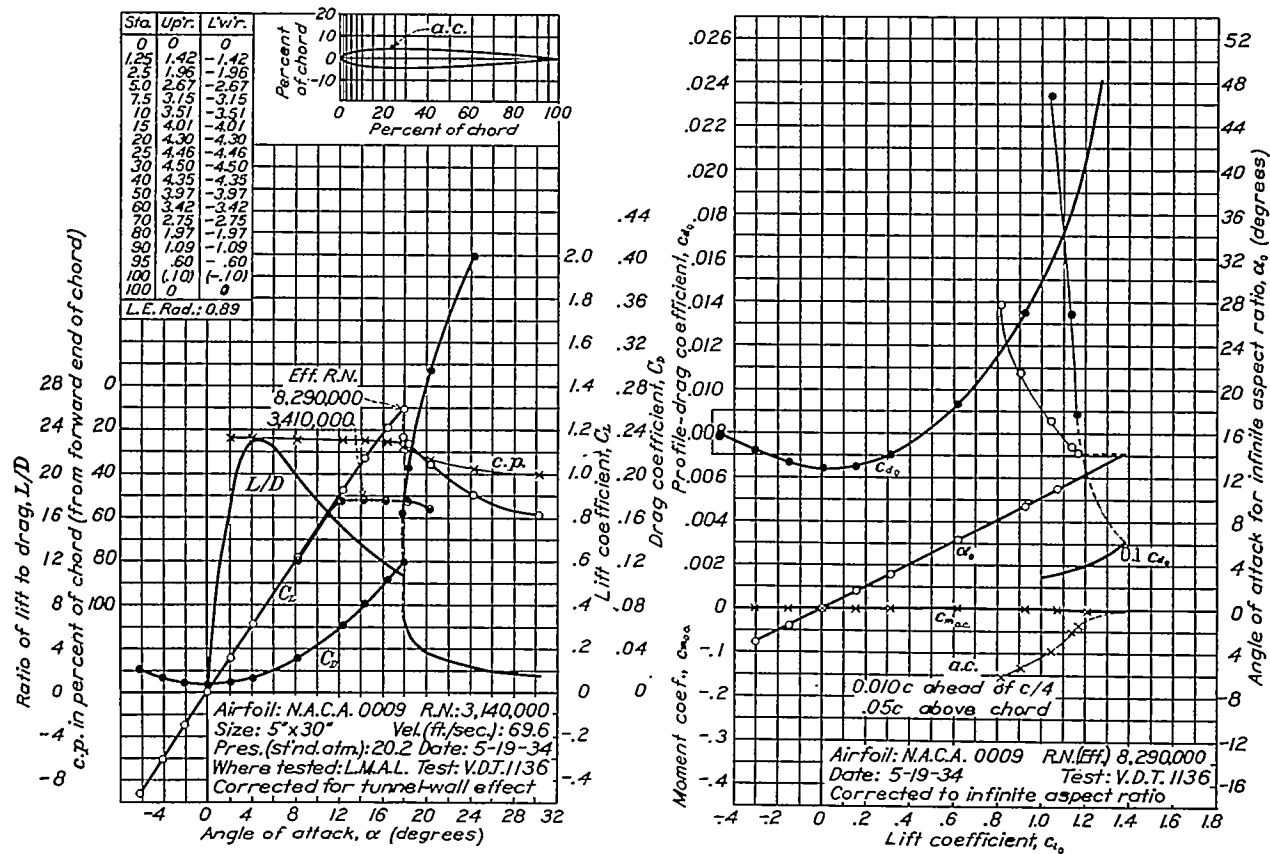
mately 8,000,000 (tank pressure 20 atmospheres). In addition, for most of the airfoils, measurements of lift in the neighborhood of maximum lift were made at an effective Reynolds Number of approximately 3,800,000, obtained by running at reduced speed with a tank pressure of 20 atmospheres.

The discussion of precision in reference 1 points out certain errors in the velocity measurements due to a change in the apparent density of the manometer fluid with a change in the tank pressure from atmospheric



and a portion of the lift curve in the neighborhood of maximum lift obtained at a reduced Reynolds Number. The right-hand portion of the plot presents the section characteristics derived from the experimental data and fully corrected for turbulence and tip effects, as explained in reference 6.

In addition to the graphic form of presentation, the most important characteristics, fully corrected, are presented for each section in table I. The three columns on classification are explained in references 6 and 9.



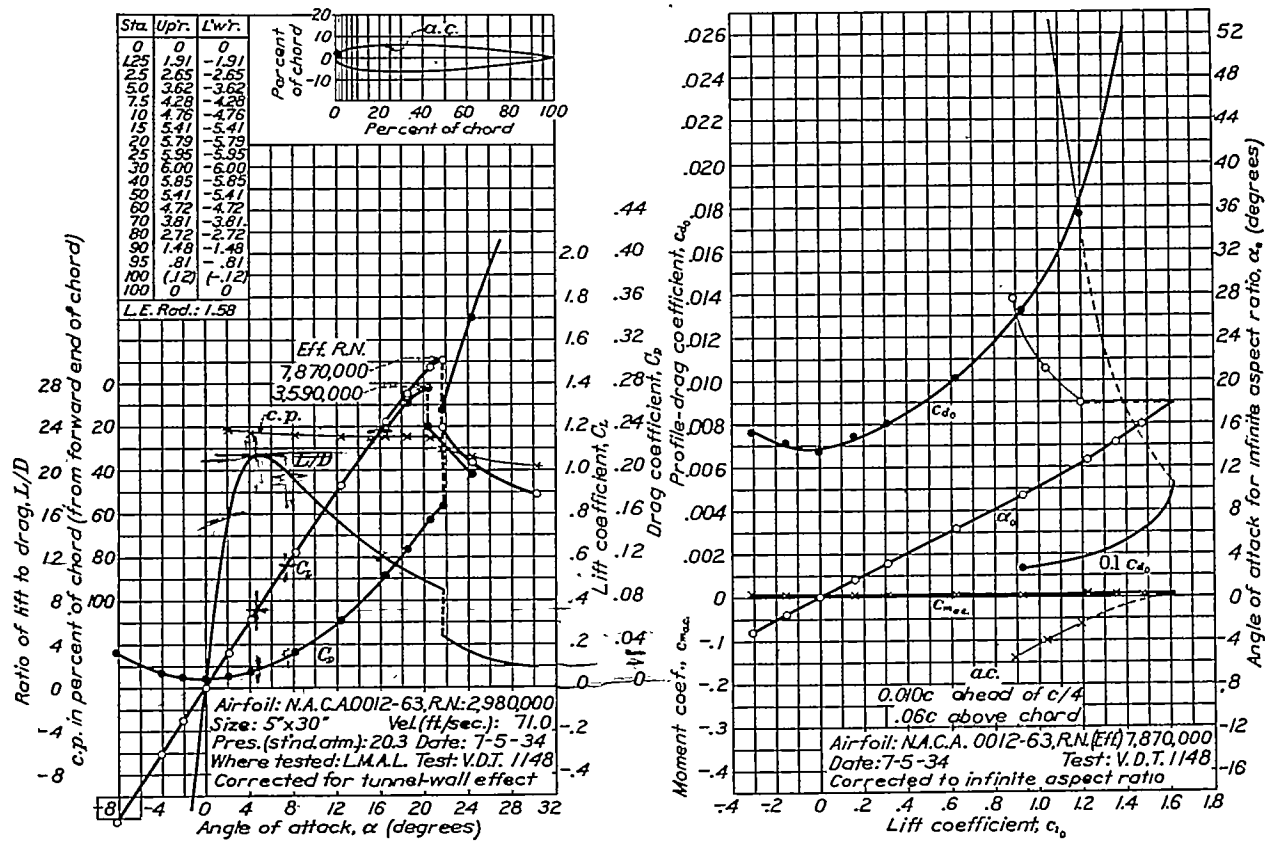


FIGURE 5.—N. A. C. A. 0012-63 airfoil.

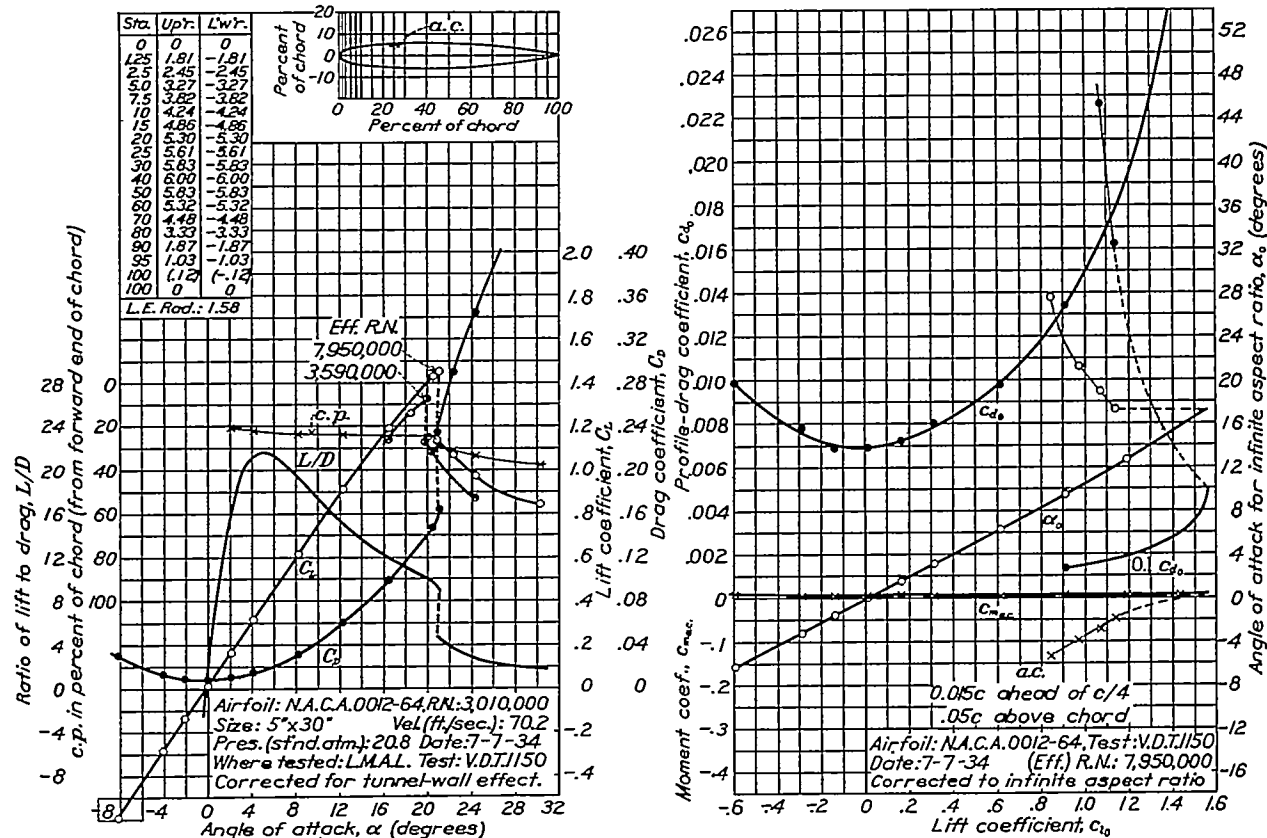


FIGURE 6.—N. A. C. A. 0012-64 airfoil.

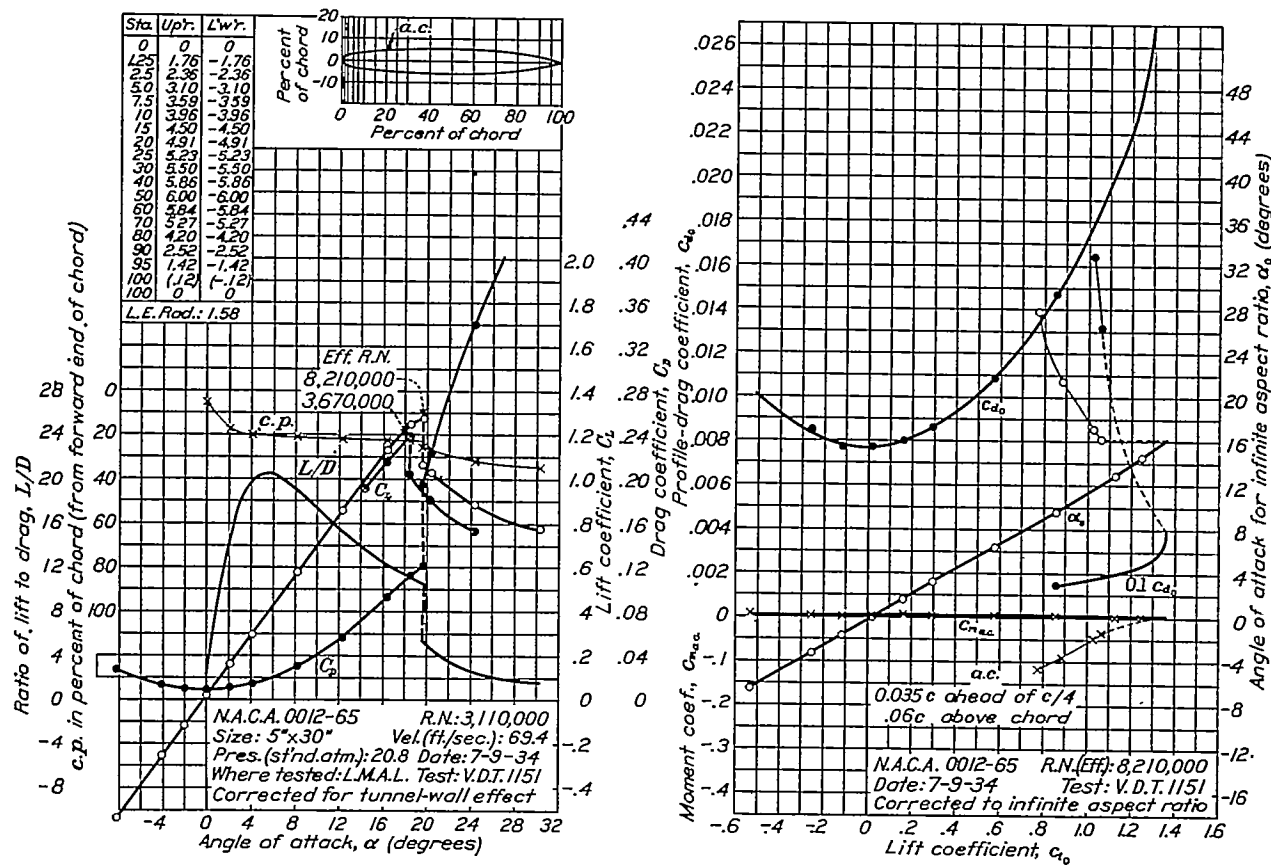


FIGURE 7.—N. A. C. A. 0012-65 airfoil.

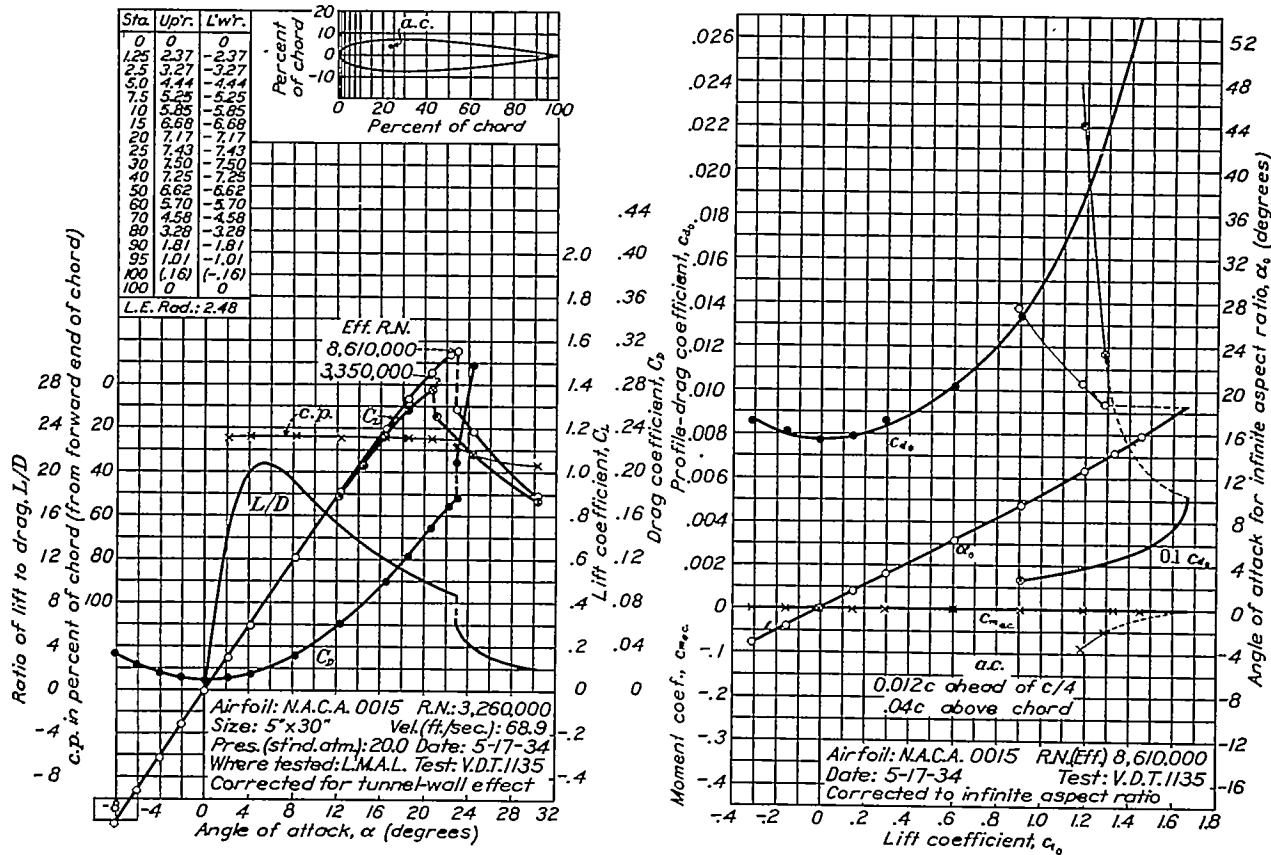


FIGURE 8.—N. A. C. A. 0015 airfoil.

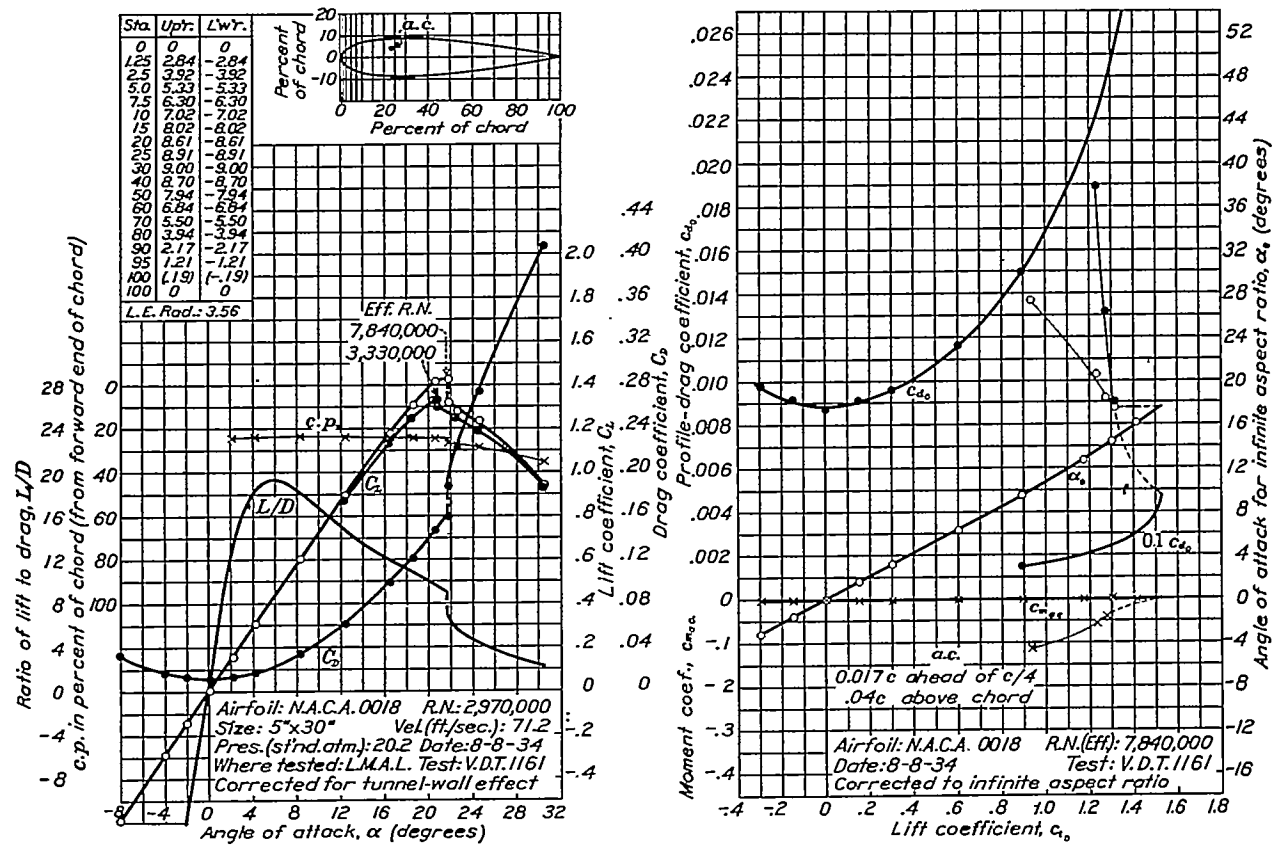


FIGURE 9.—N. A. C. A. 0018 airfoil.

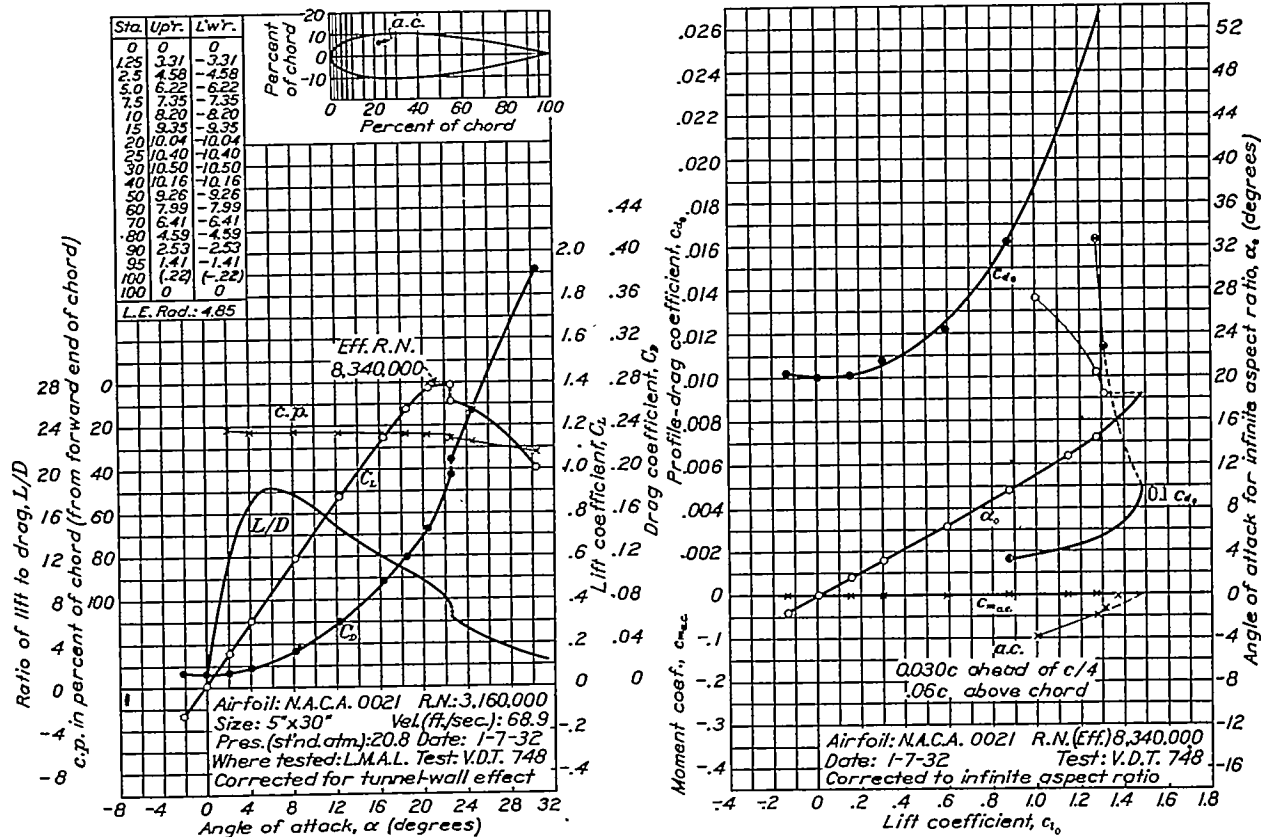


FIGURE 10.—N. A. O. A. 0021 airfoil.

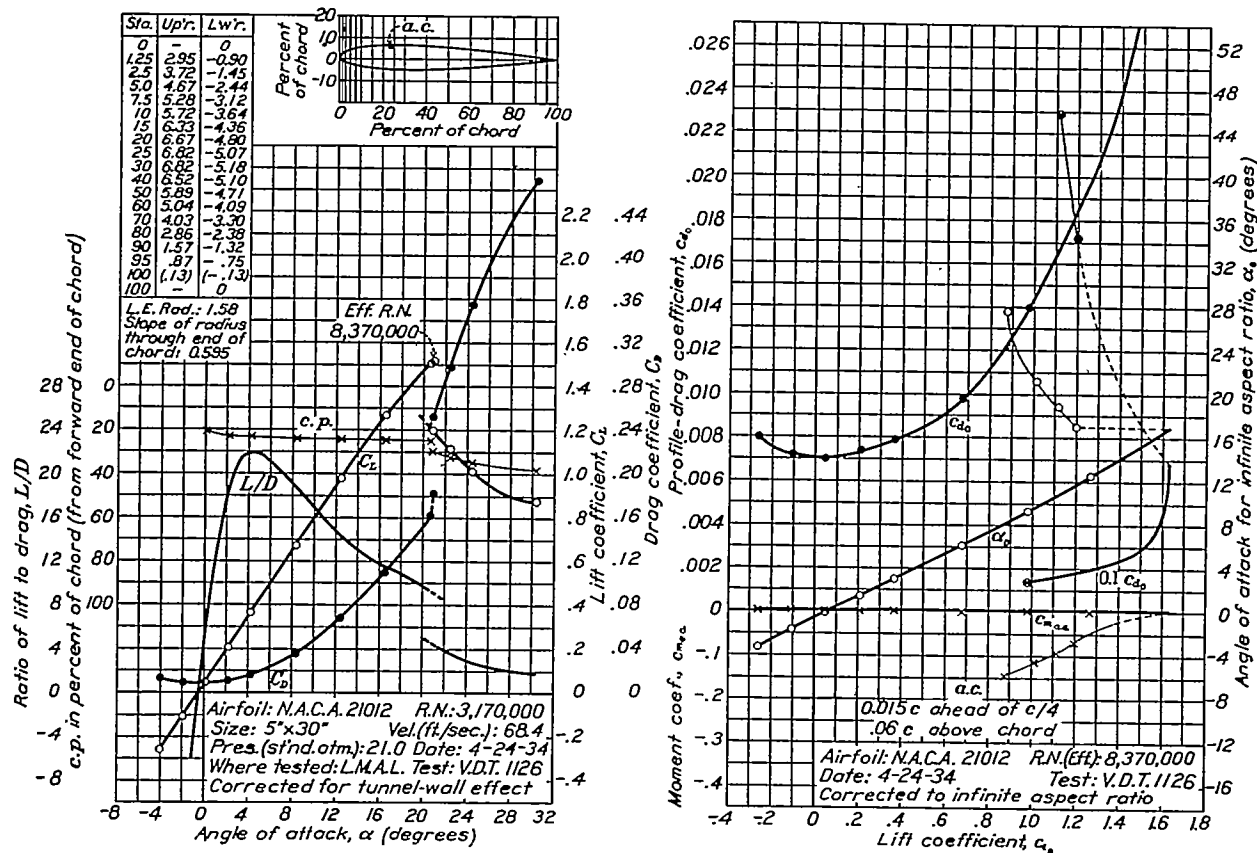


FIGURE 11.—N. A. O. A. 21012 airfoil.

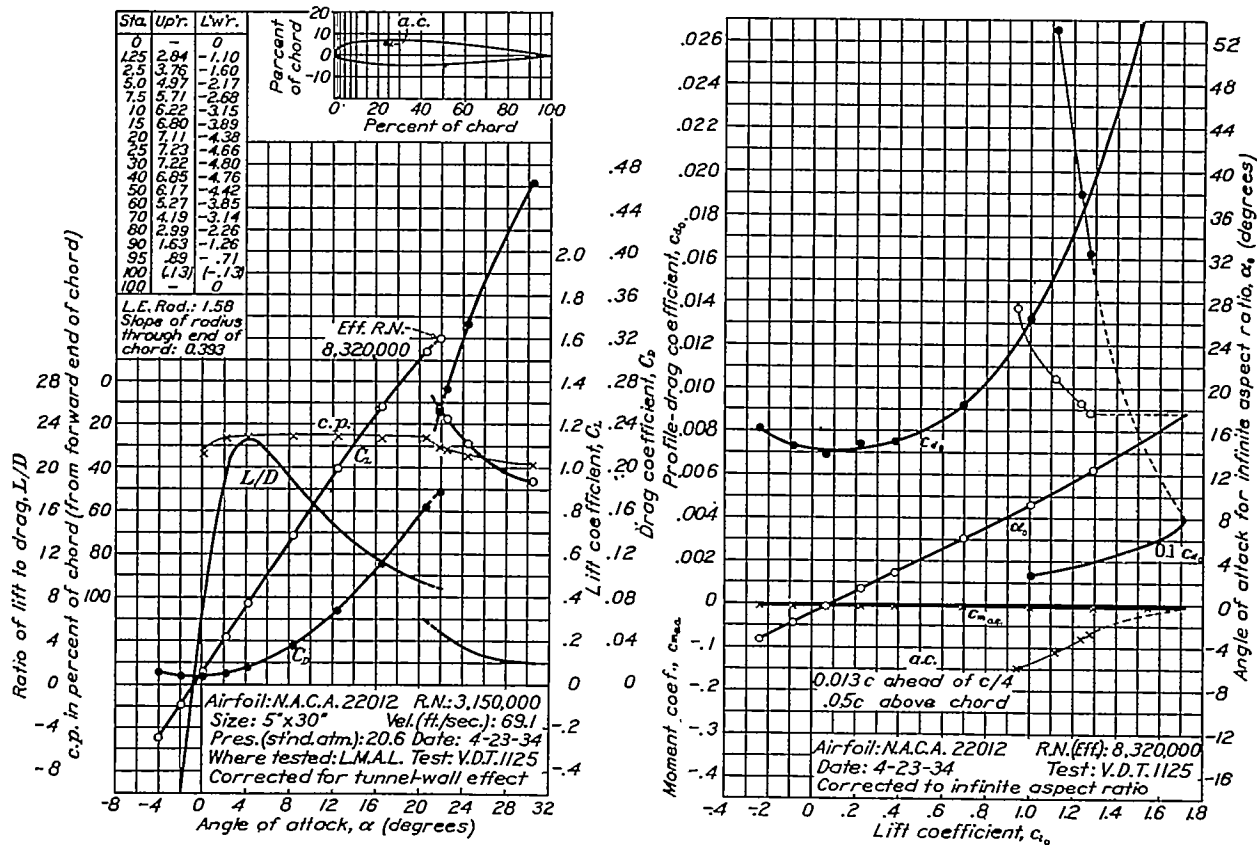


FIGURE 12.—N. A. O. A. 22012 airfoil.

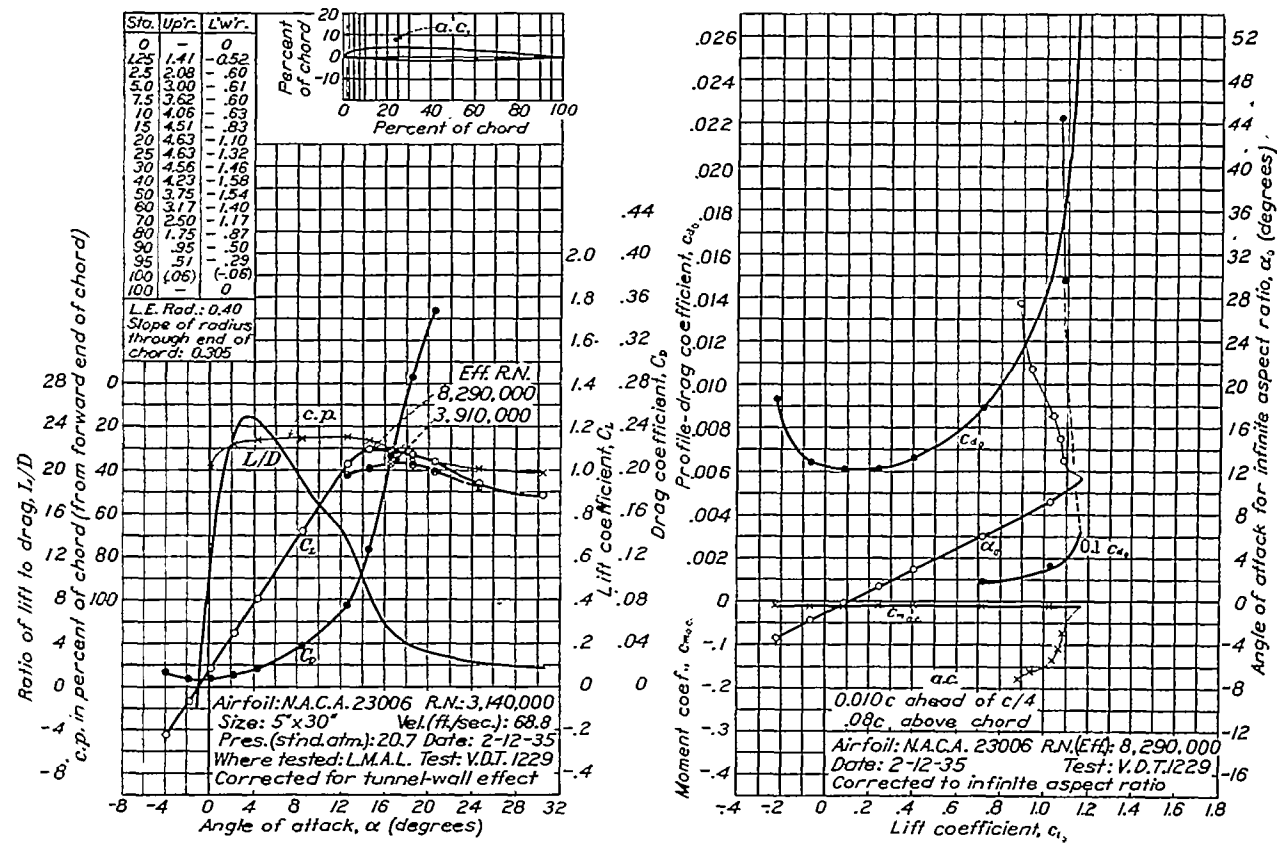


FIGURE 13.—N. A. C. A. 23006 airfoil.

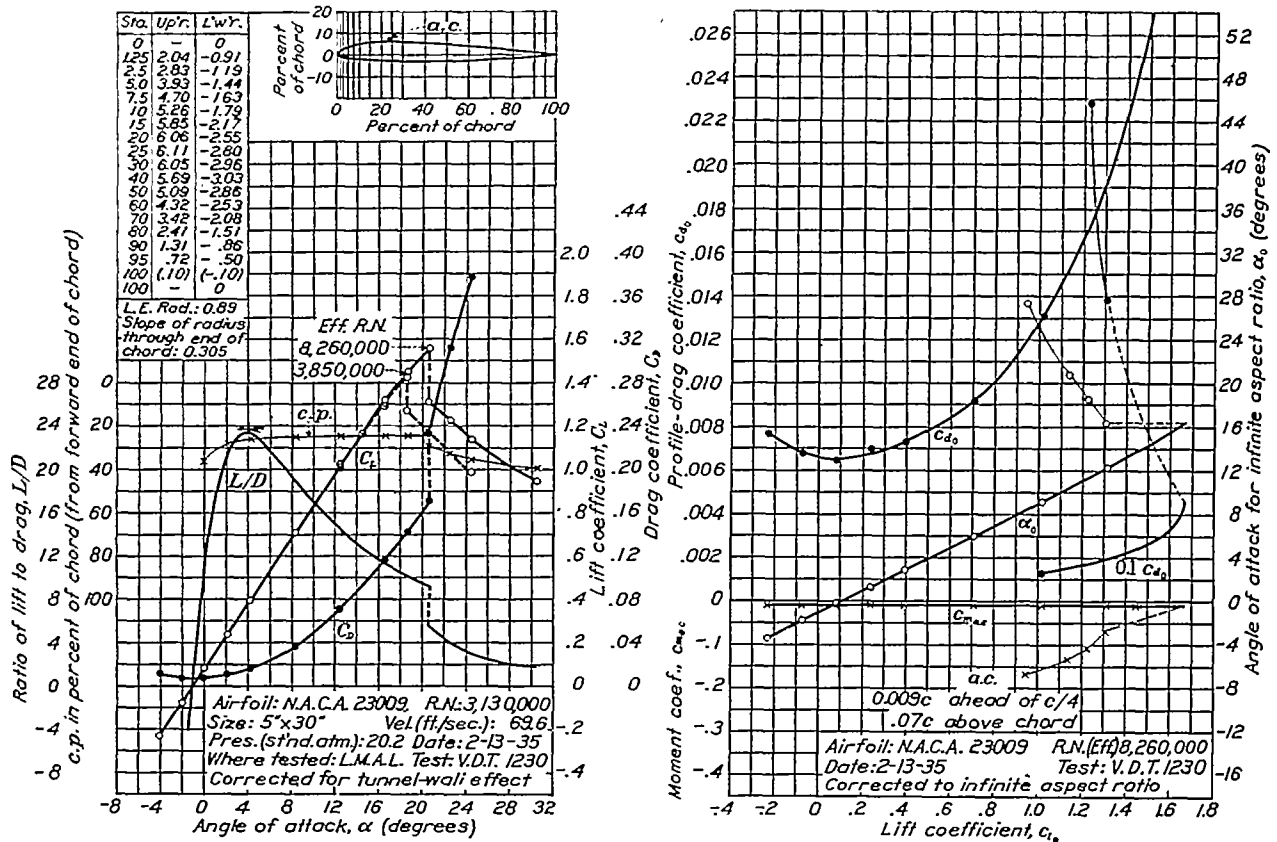


FIGURE 14.—N. A. C. A. 23009 airfoil.

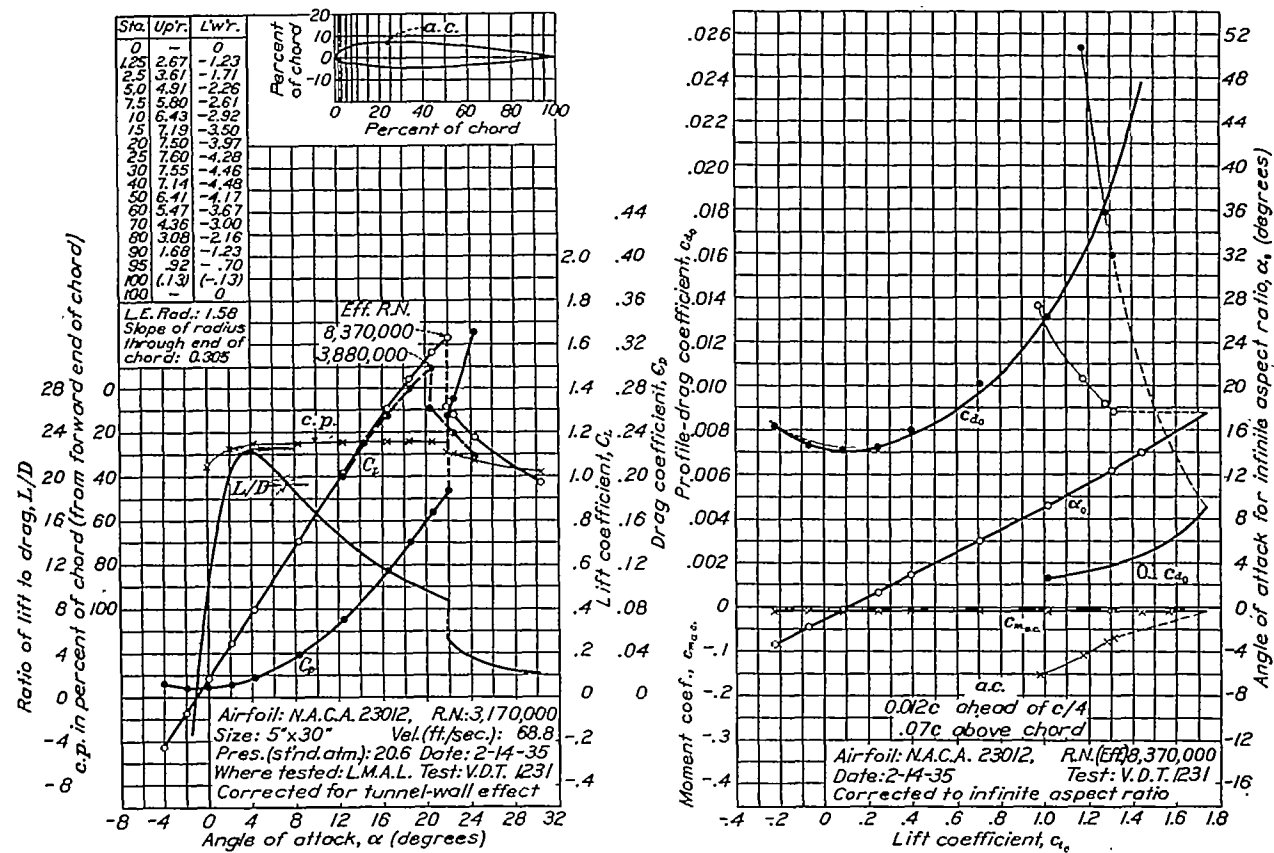


FIGURE 15.—N. A. O. A. 23012 airfoil.

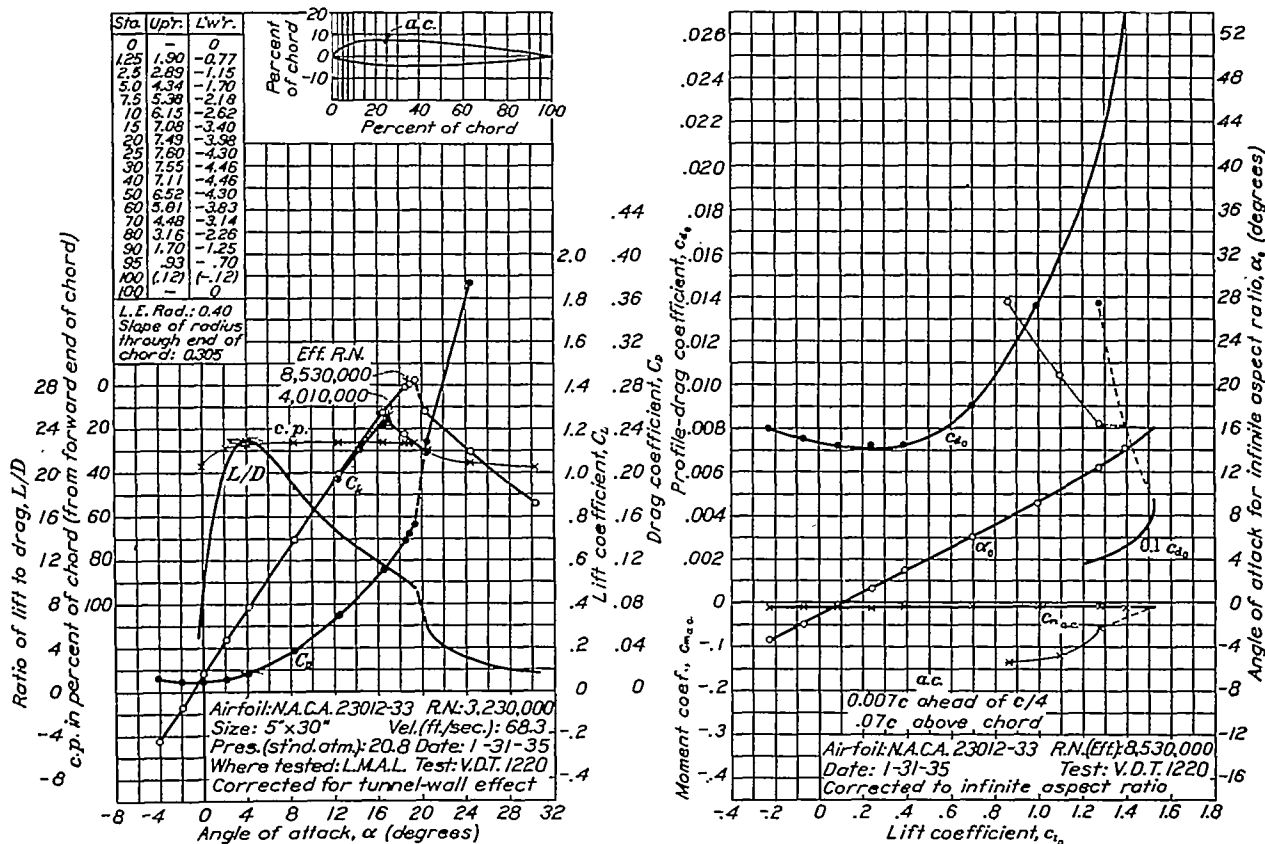


FIGURE 16.—N. A. C. A. 23012-33 airfoil.

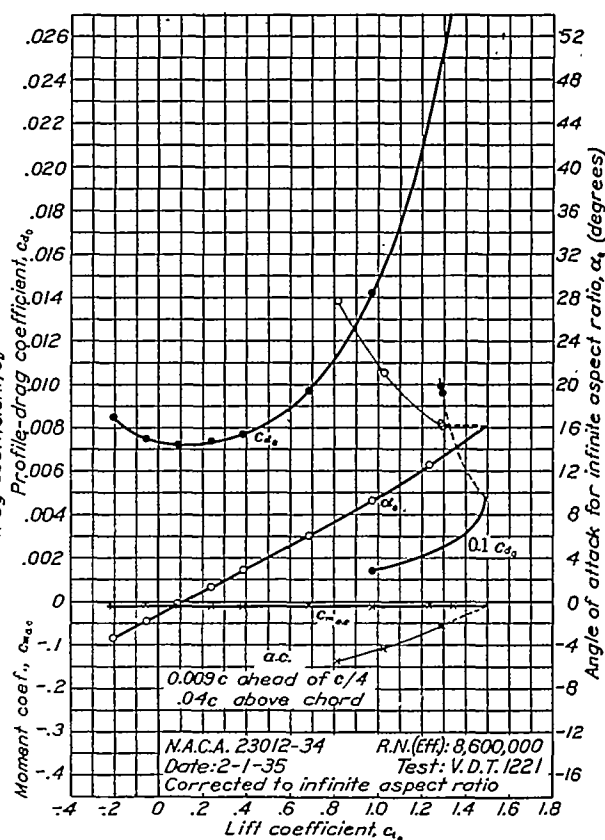
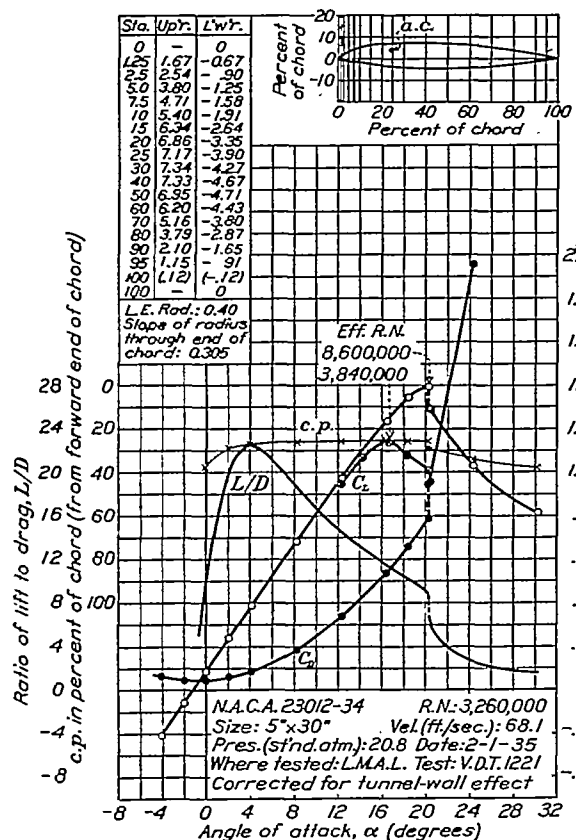


FIGURE 17.—N. A. C. A. 23012-34 airfoil.

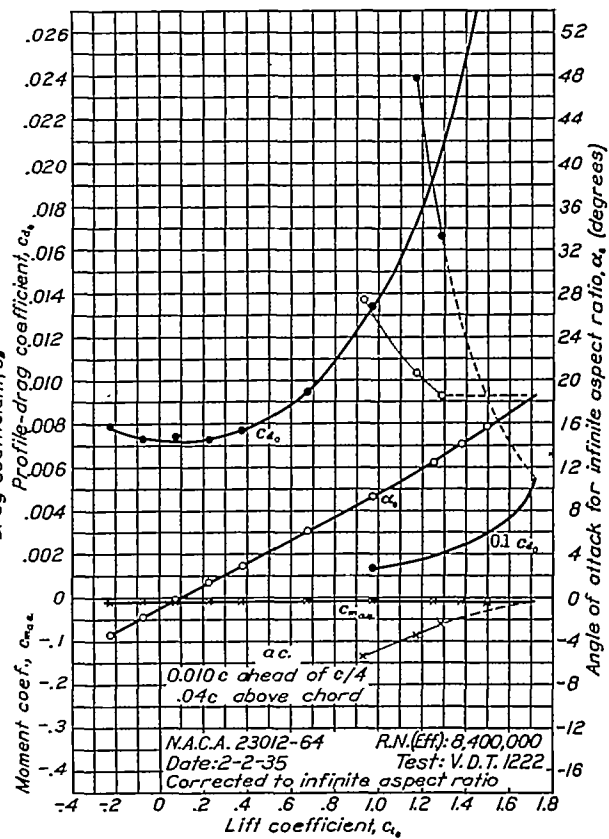
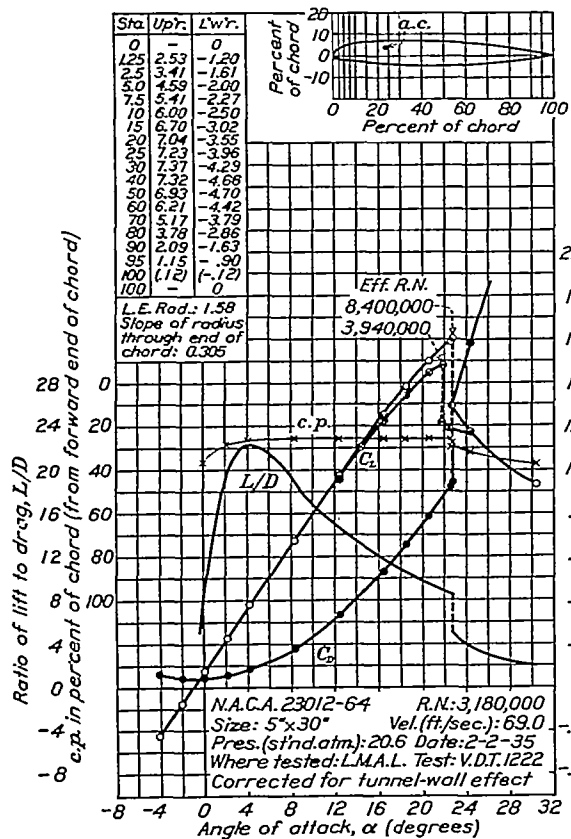


FIGURE 18.—N. A. C. A. 23012-64 airfoil.

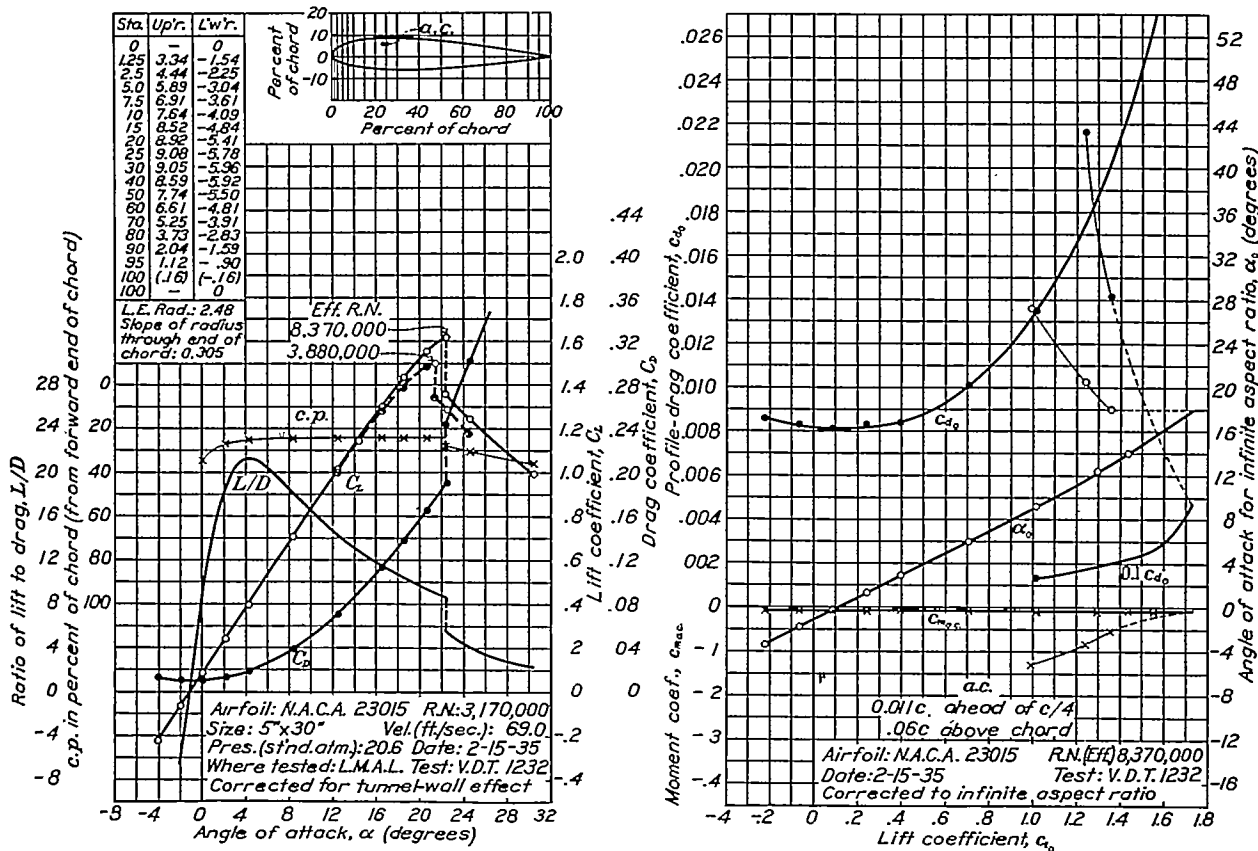


FIGURE 19.—N. A. C. A. 23015 airfoil.

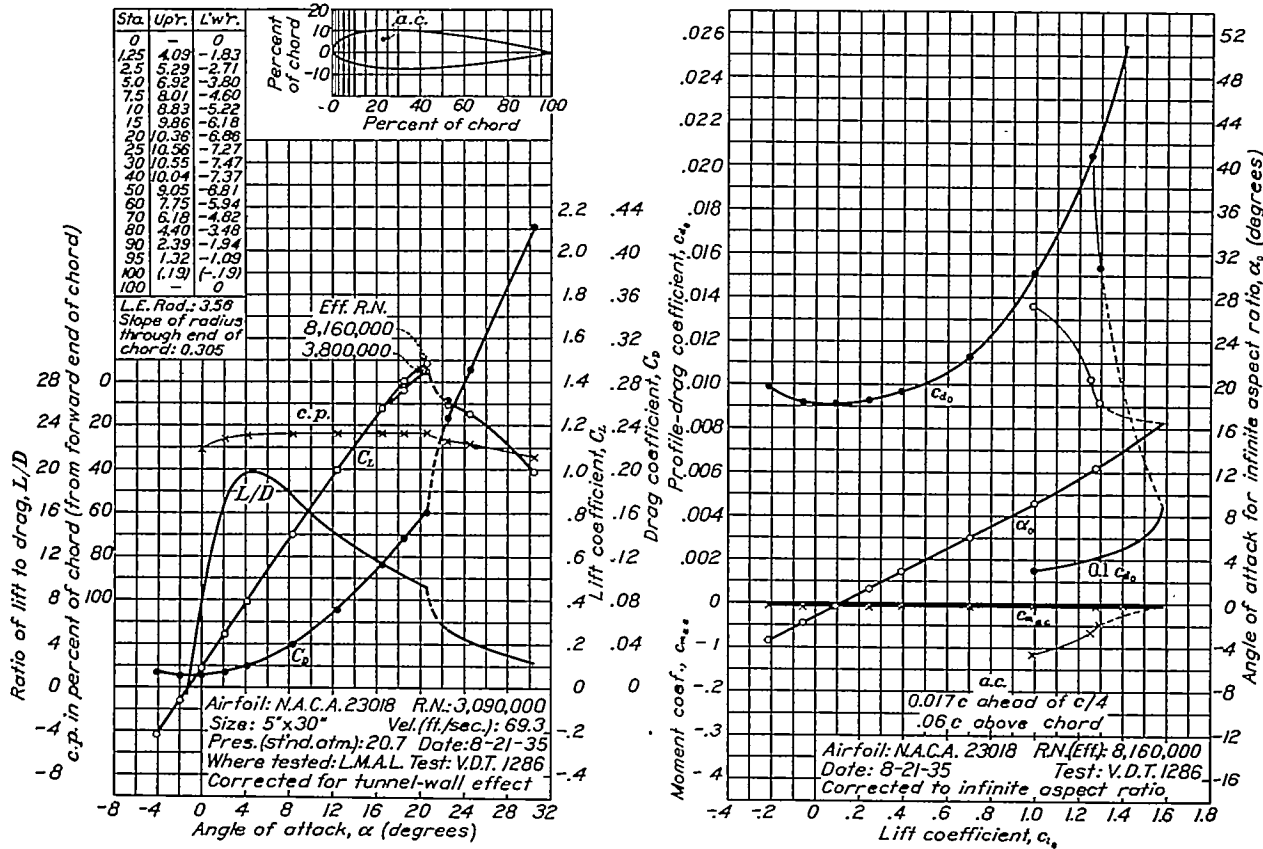


FIGURE 20.—N. A. C. A. 23018 airfoil.

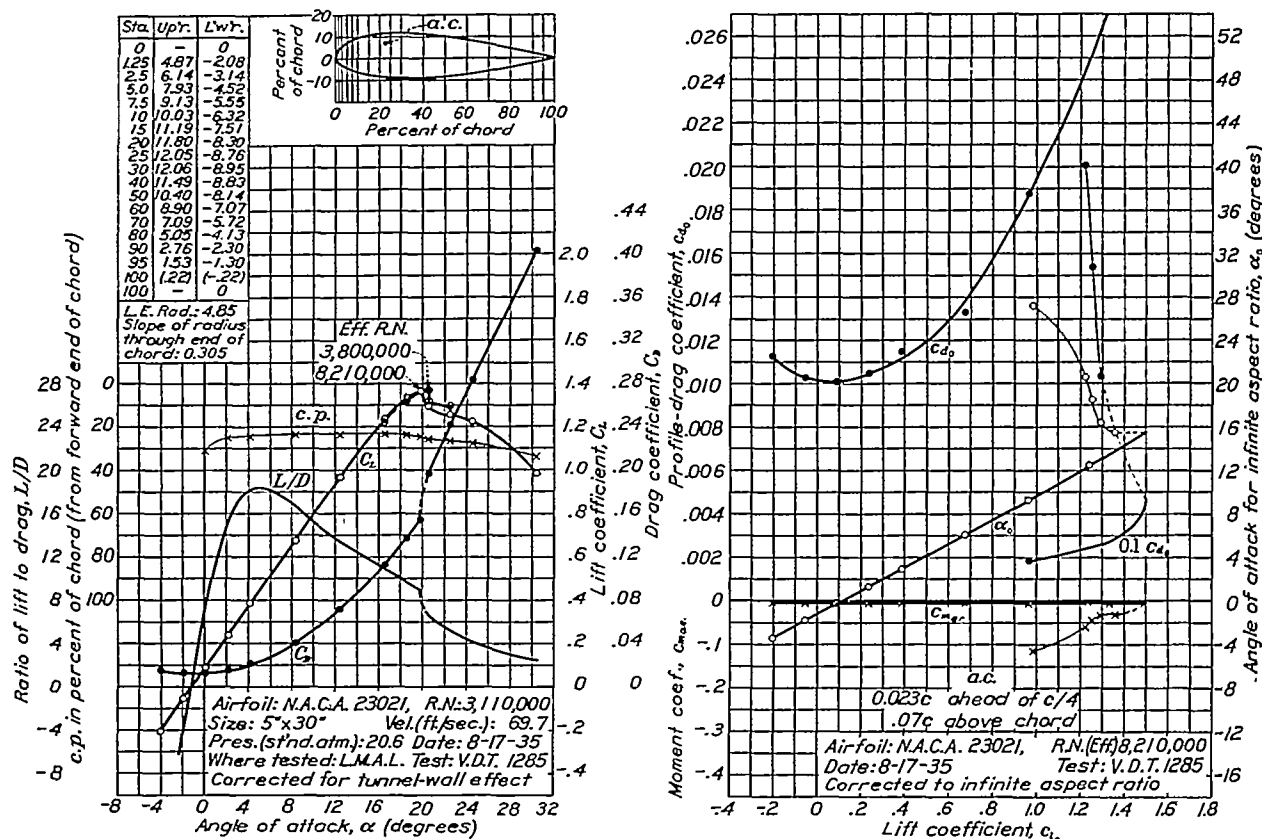


FIGURE 21.—N. A. C. A. 23021 airfoil.

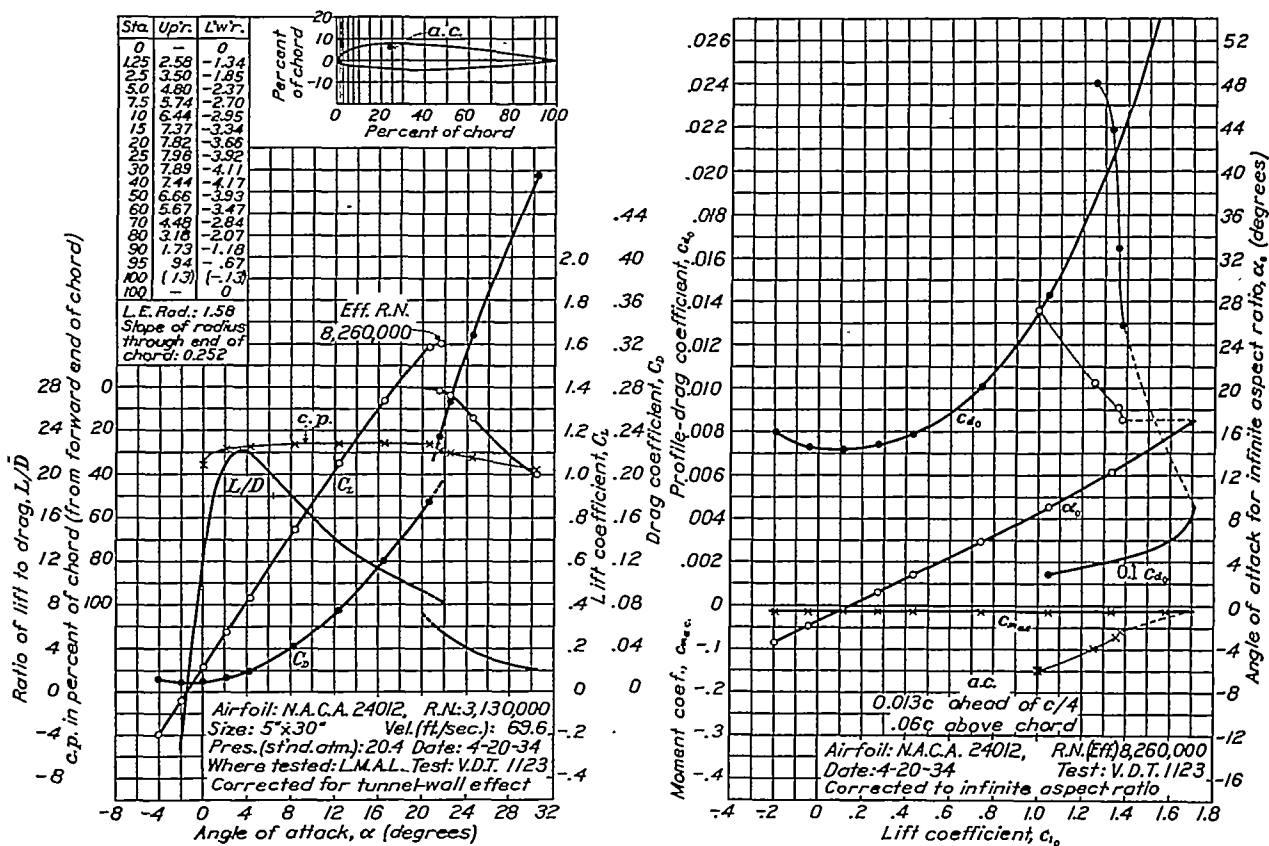


FIGURE 22.—N. A. C. A. 24012 airfoil.

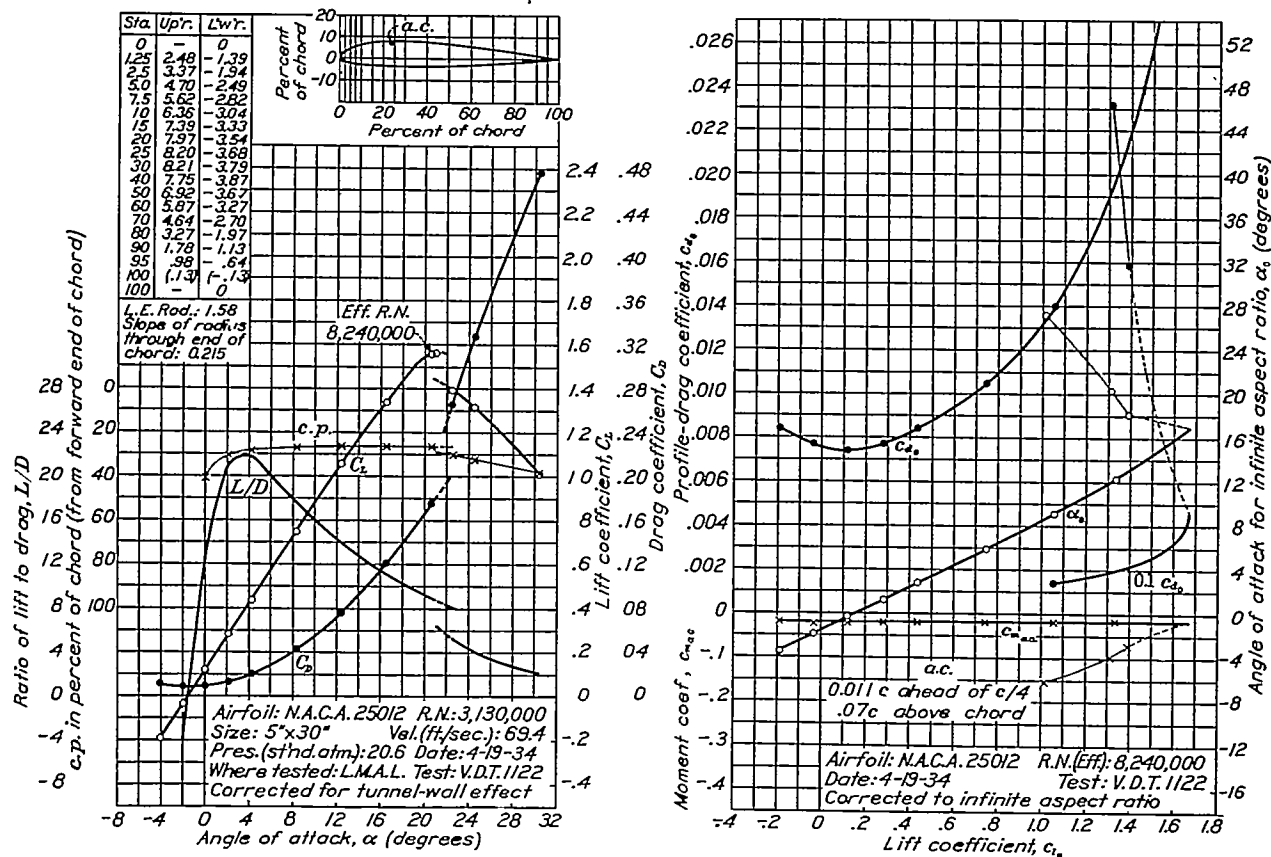


FIGURE 23.—N. A. C. A. 25012 airfoil.

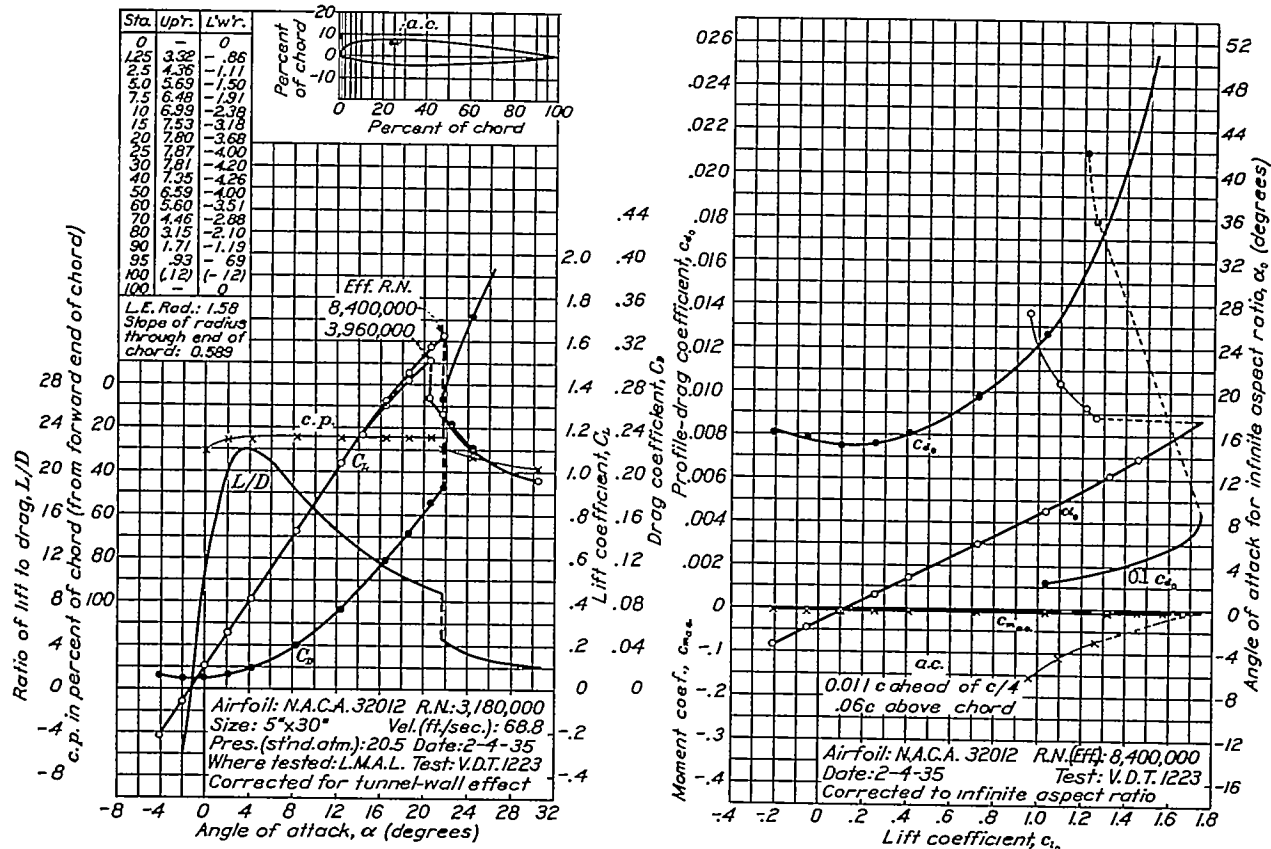


FIGURE 24.—N. A. C. A. 32012 airfoil.

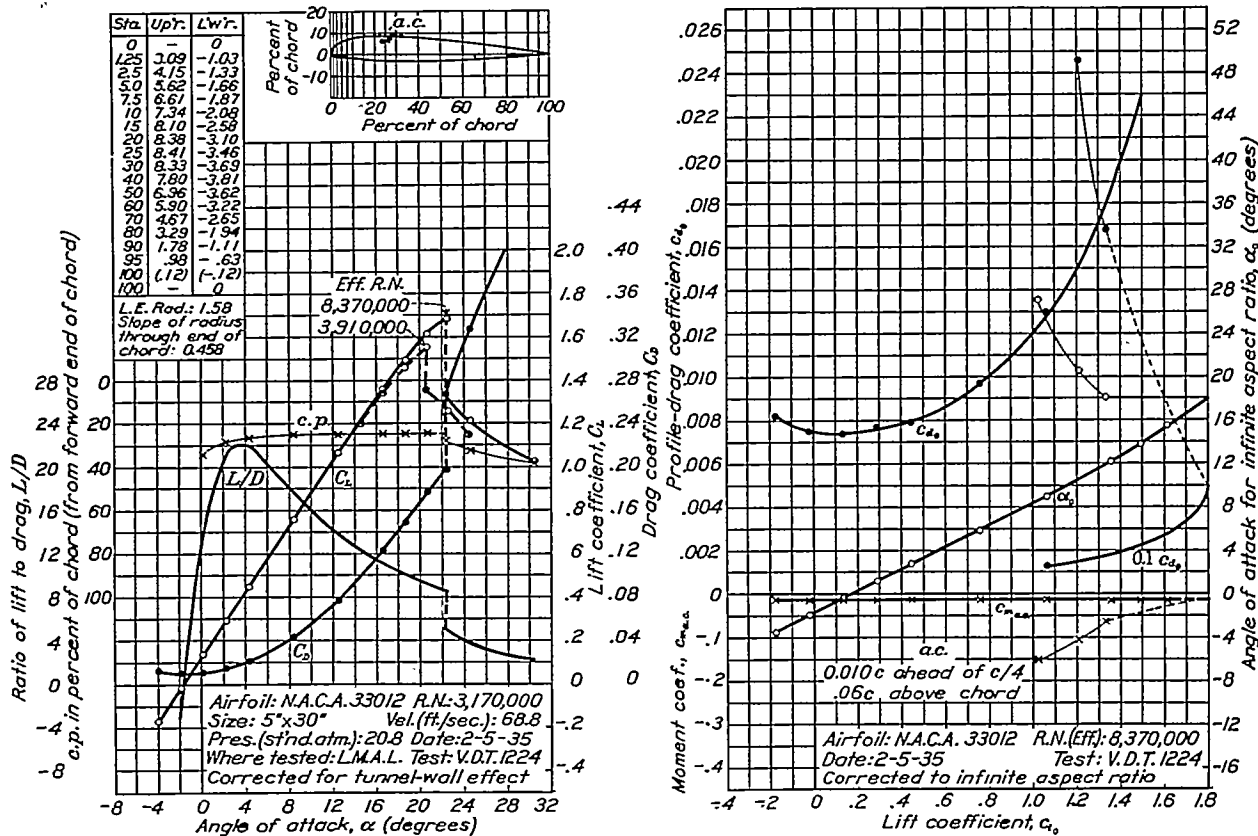


FIGURE 25.—N. A. C. A. 33012 airfoil.

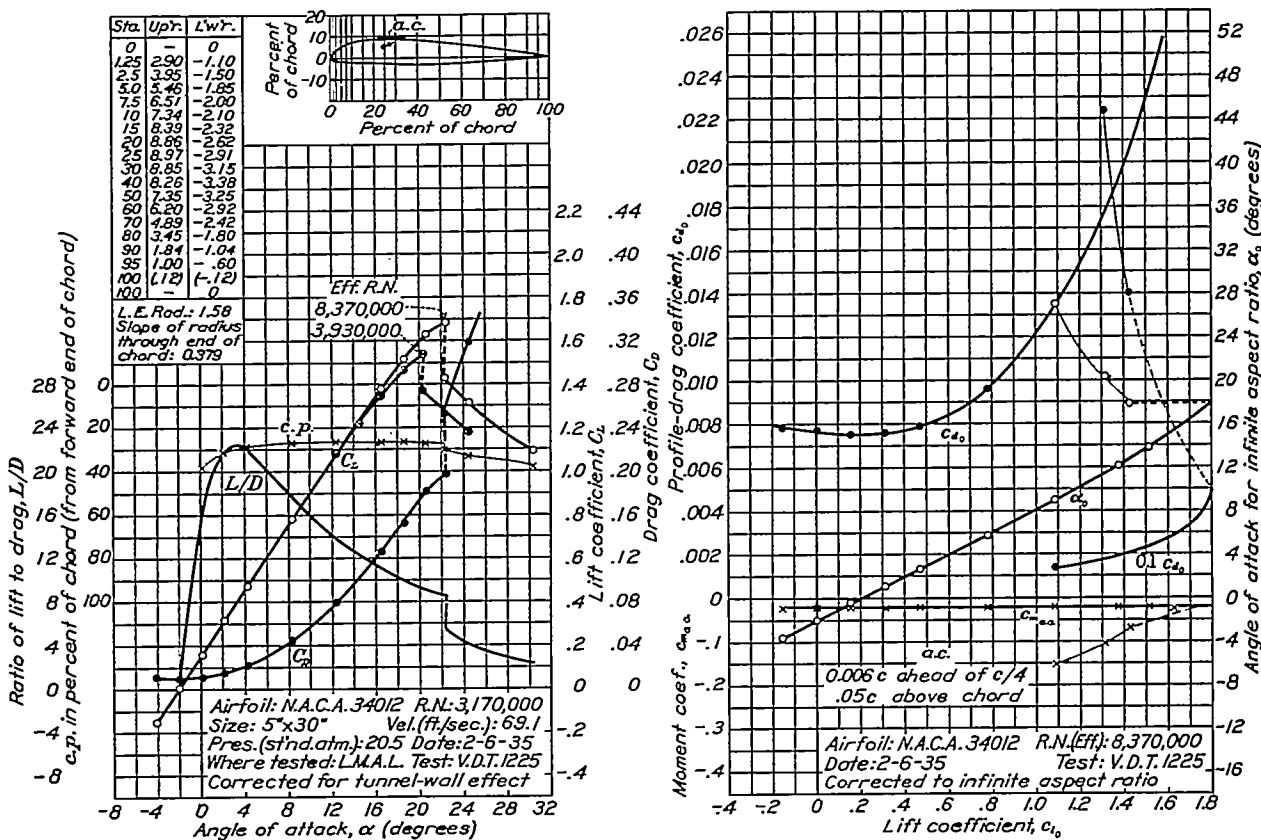


FIGURE 26.—N. A. C. A. 34012 airfoil.

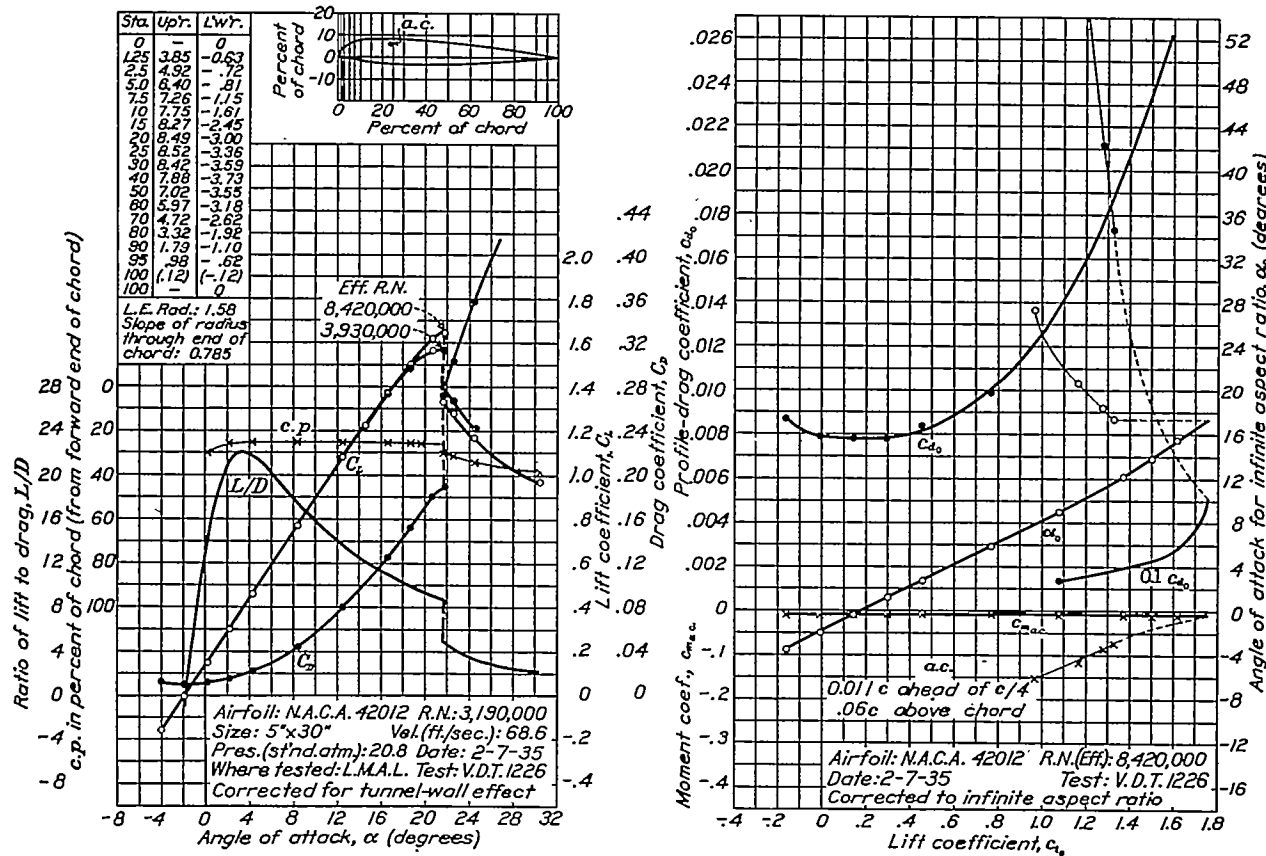


FIGURE 27.—N. A. O. A. 42012 airfoil.

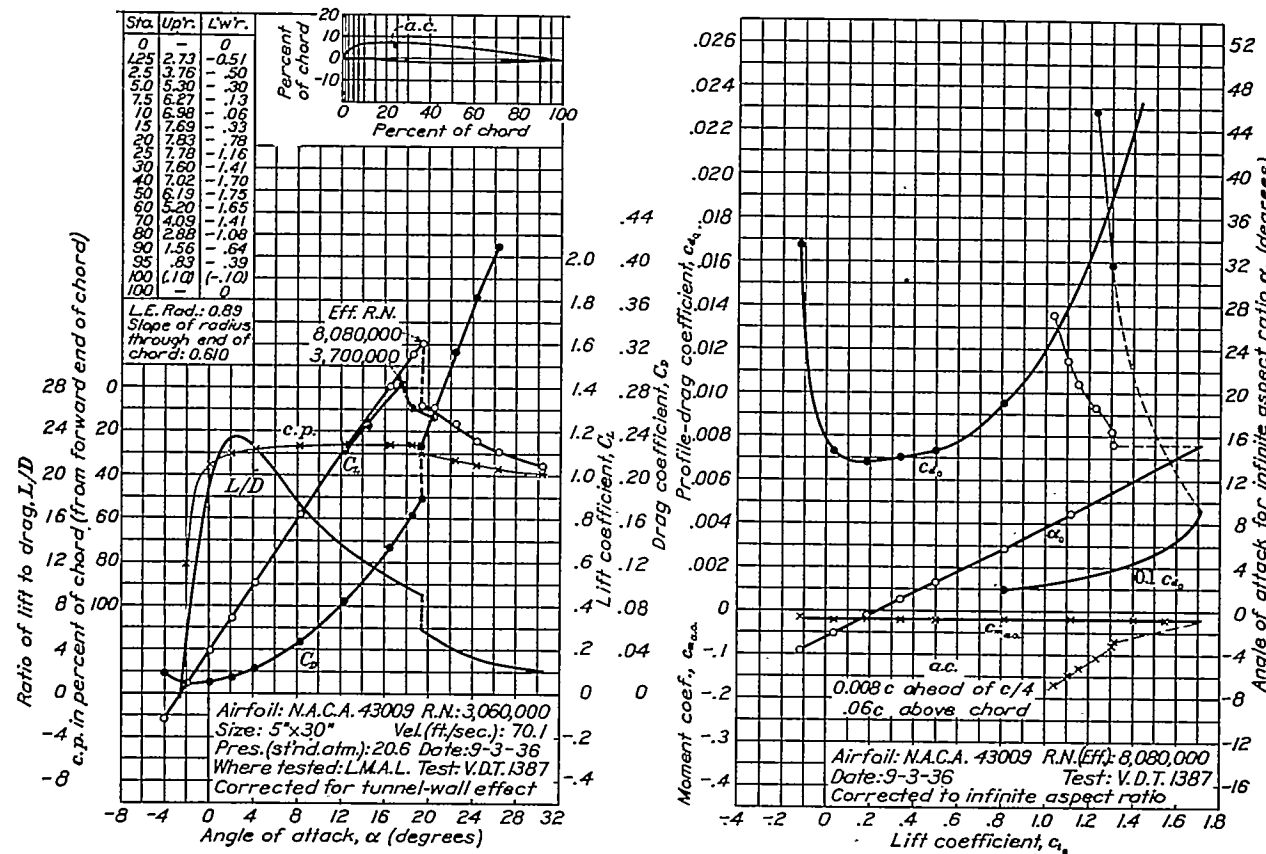


FIGURE 28.—N. A. O. A. 43009 airfoil.

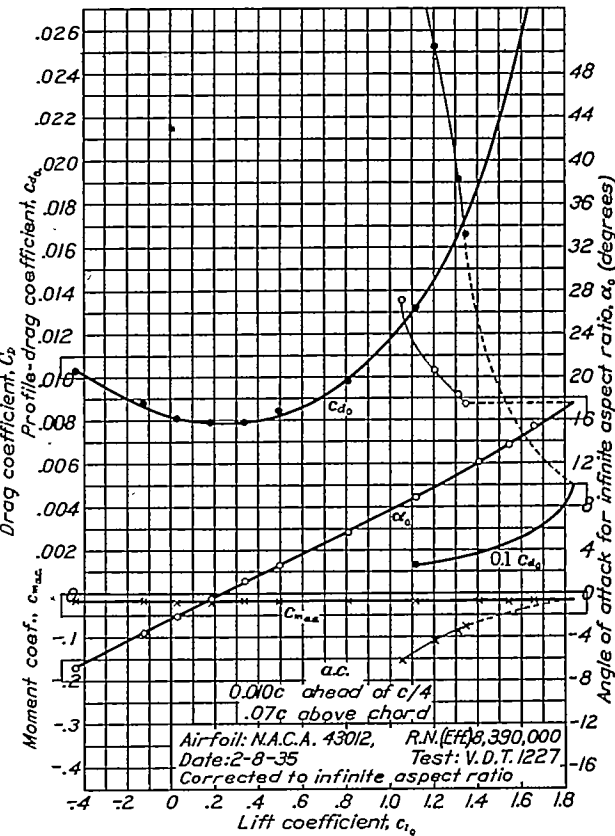
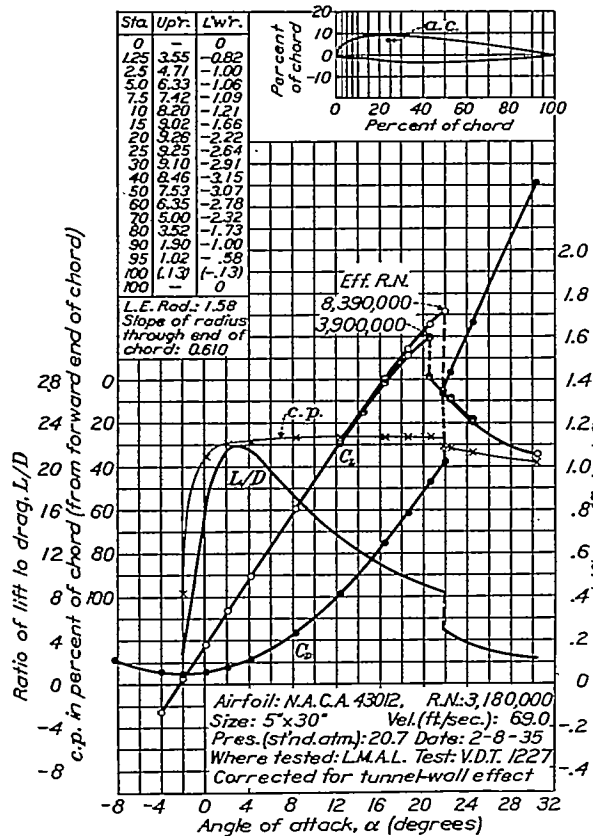


FIGURE 29.—N. A. C. A. 43012 airfoil.

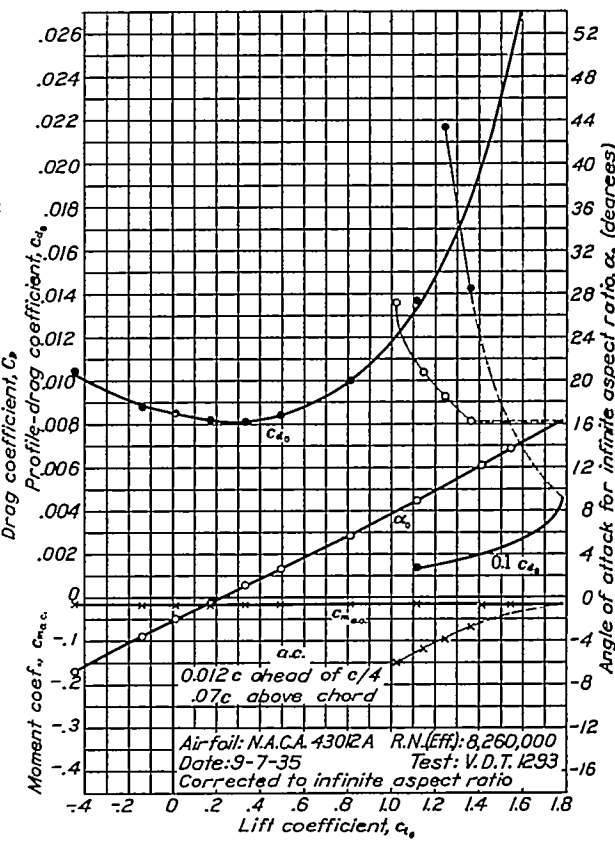
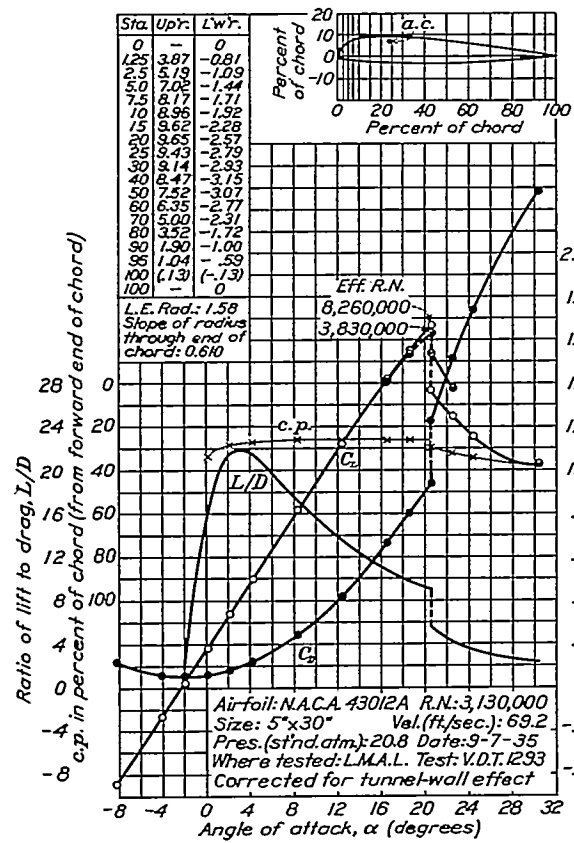


FIGURE 30.—N. A. C. A. 43012A airfoil.

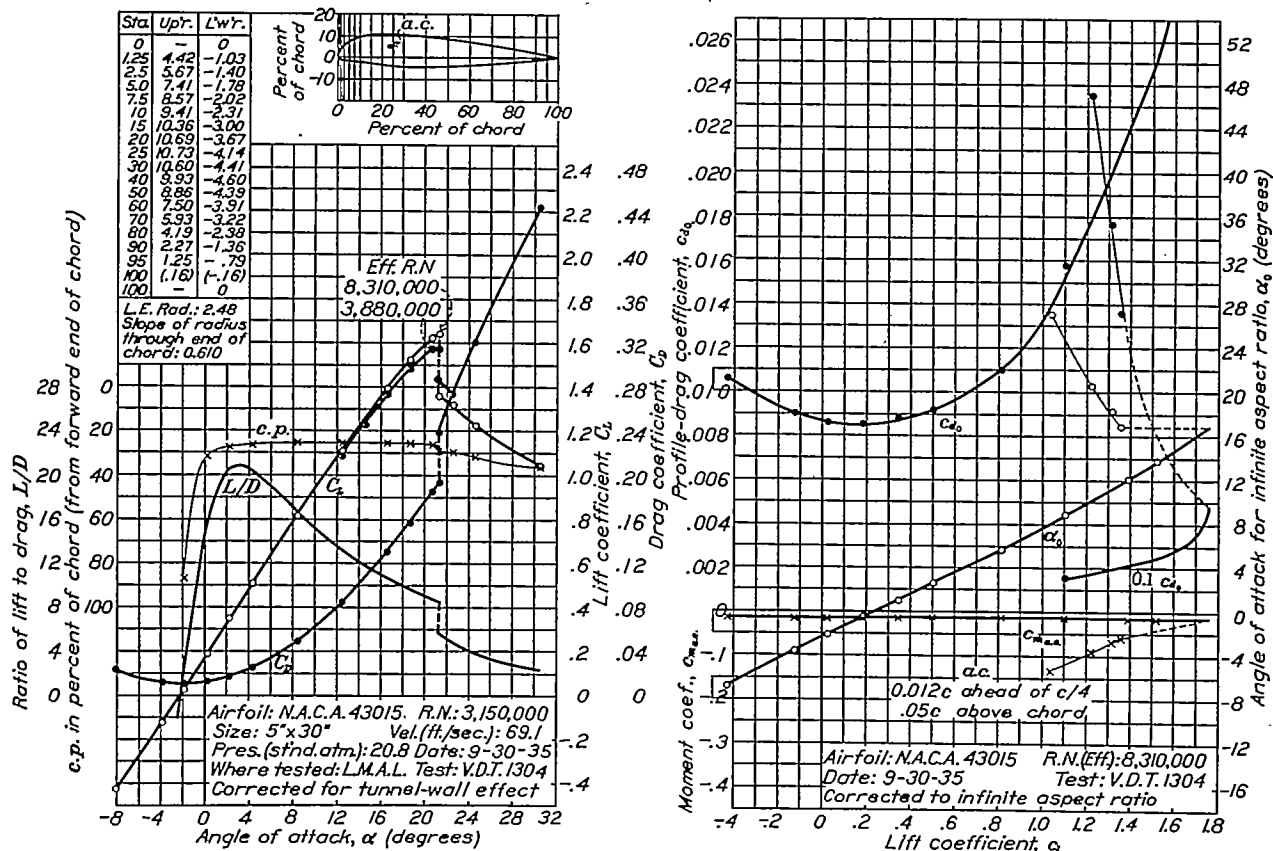


FIGURE 31.—N. A. C. A. 43015 airfoil.

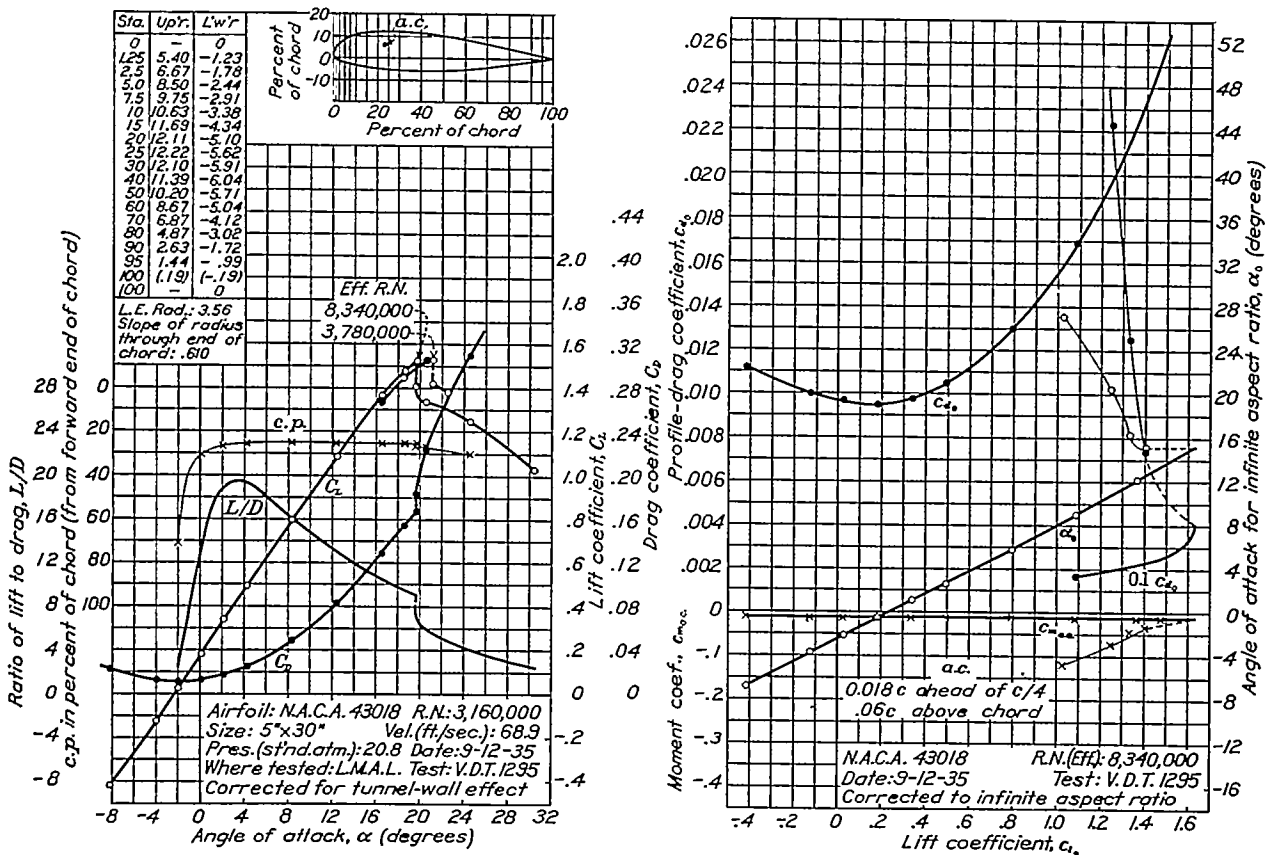


FIGURE 32.—N. A. C. A. 43018 airfoil.

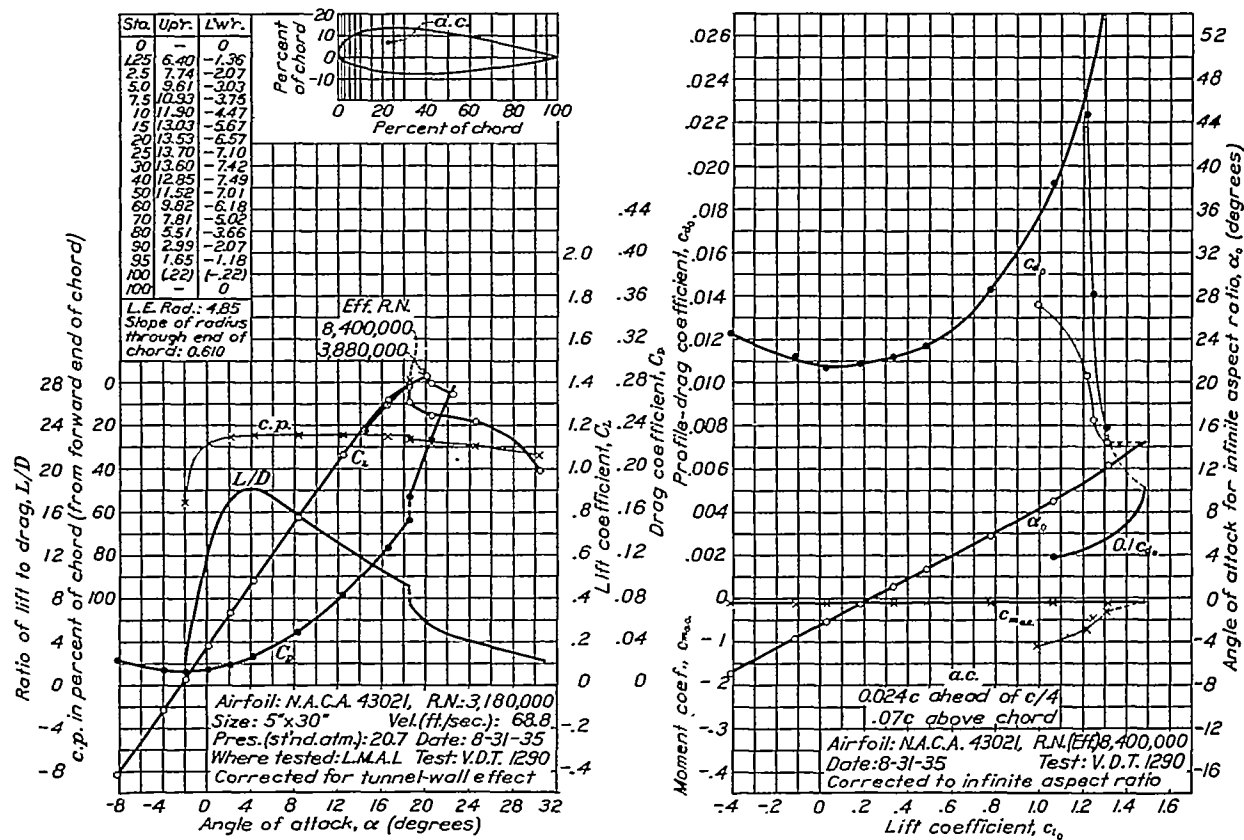


FIGURE 33.—N. A. C. A. 43021 airfoil.

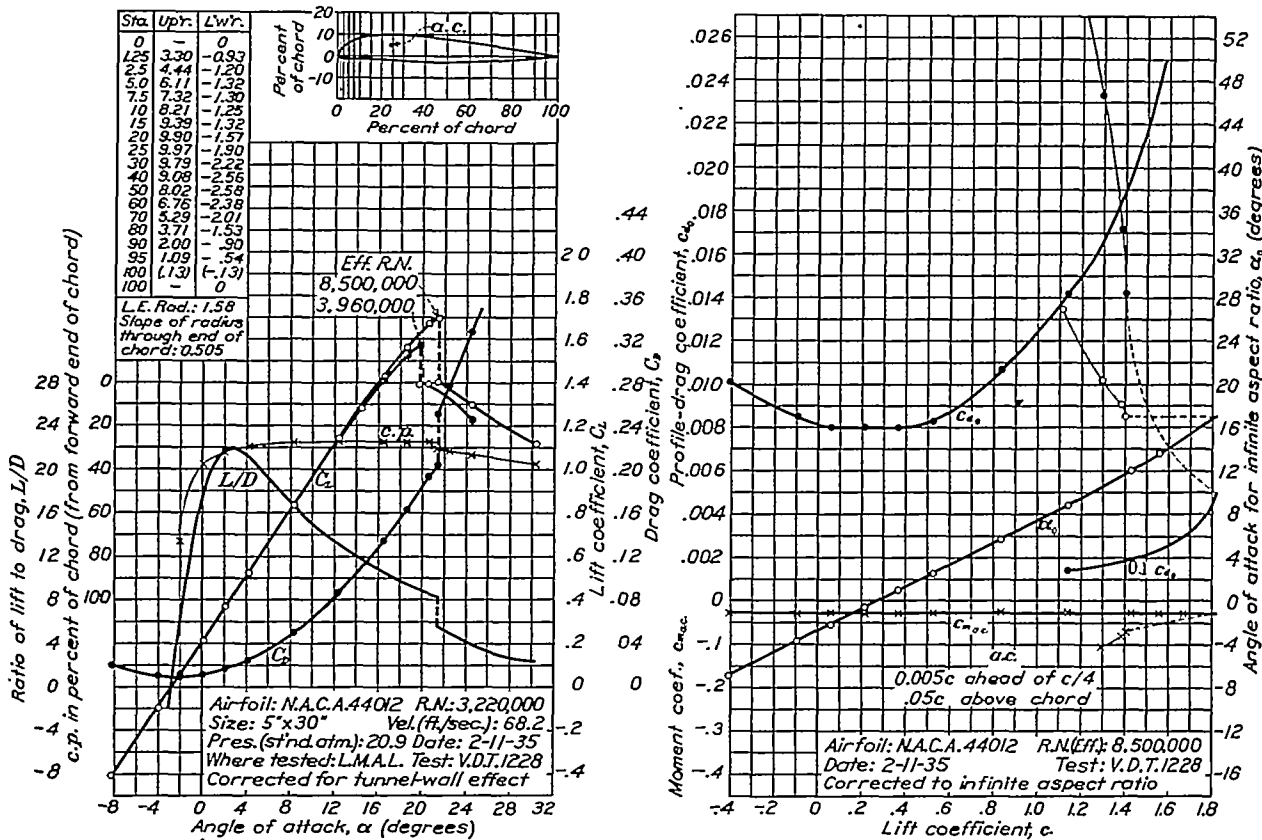


FIGURE 34.—N. A. C. A. 44012 airfoil.

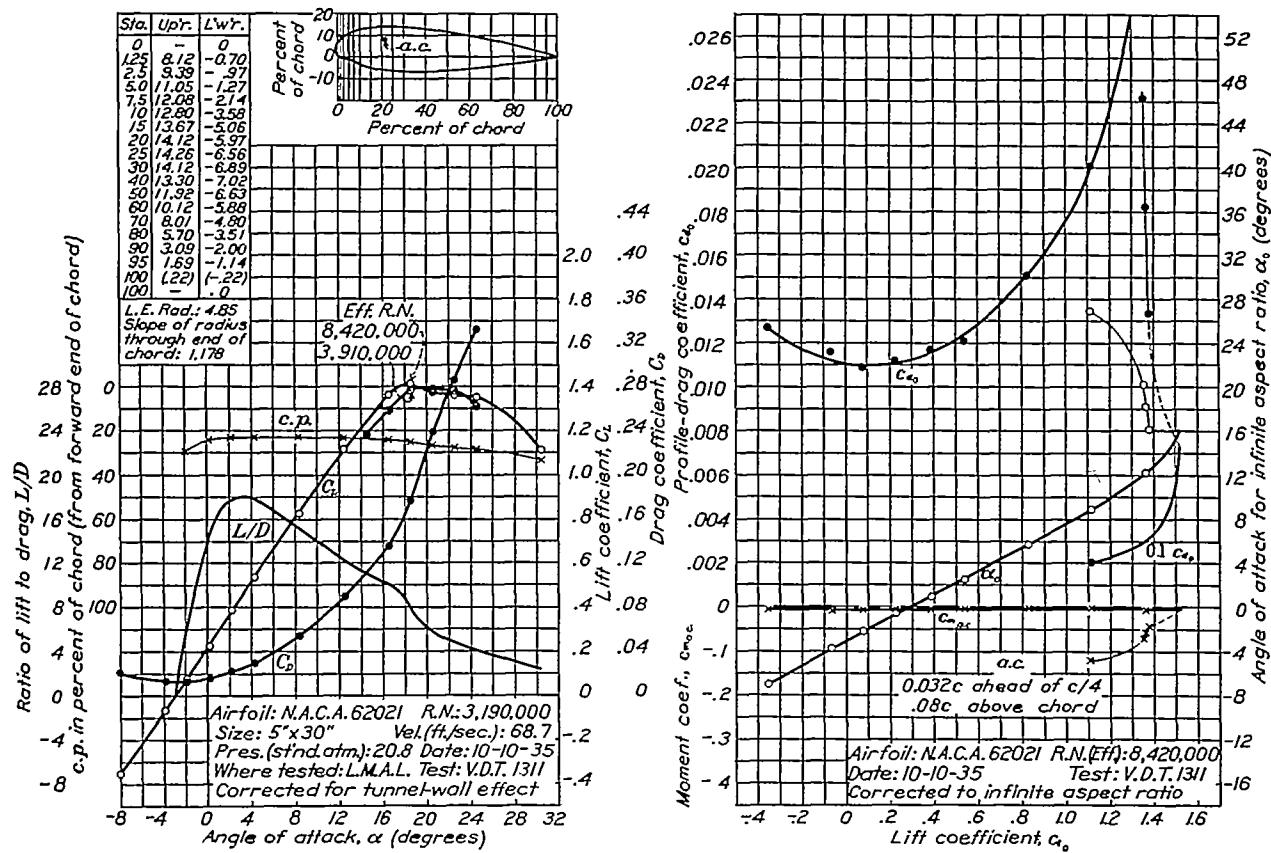


FIGURE 35.—N. A. C. A. 62021 airfoil.

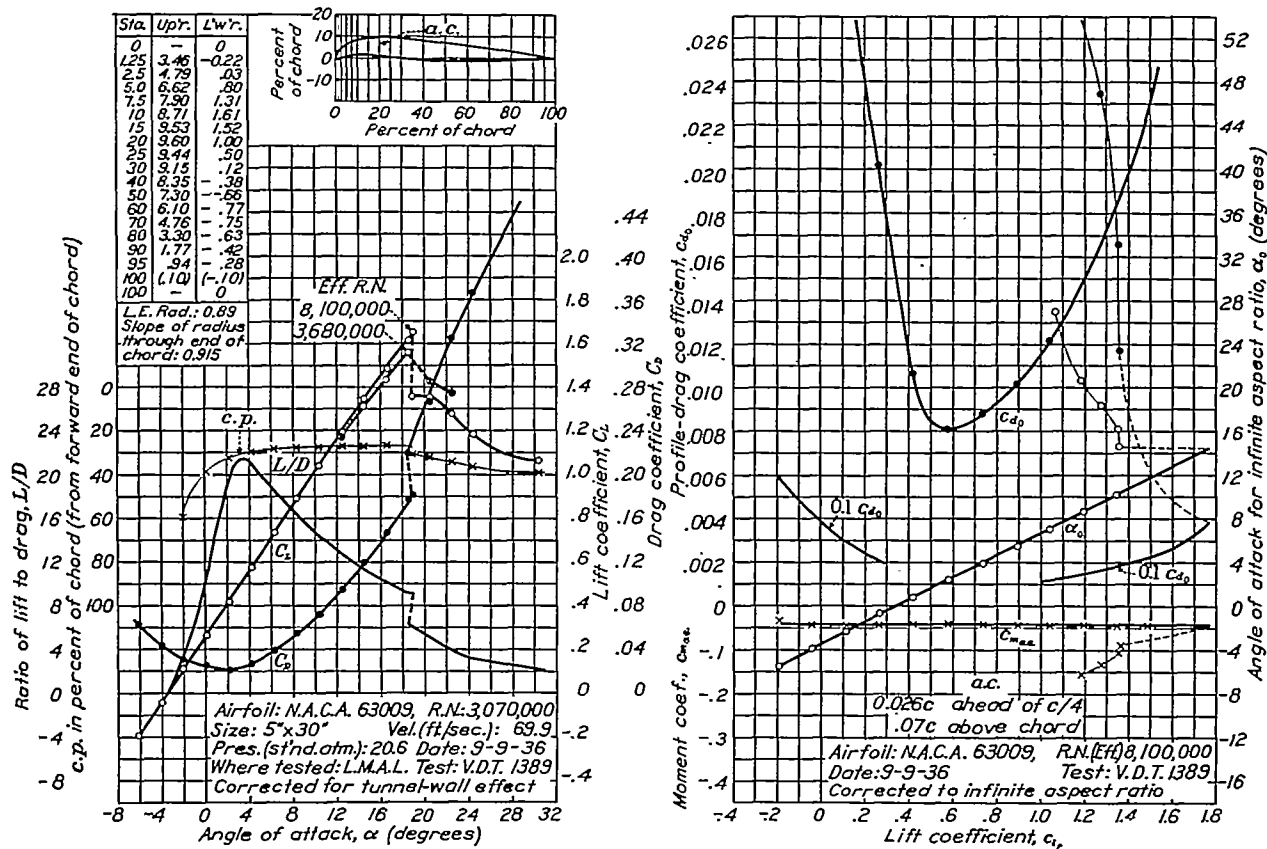


FIGURE 36.—N. A. C. A. 63009 airfoil.

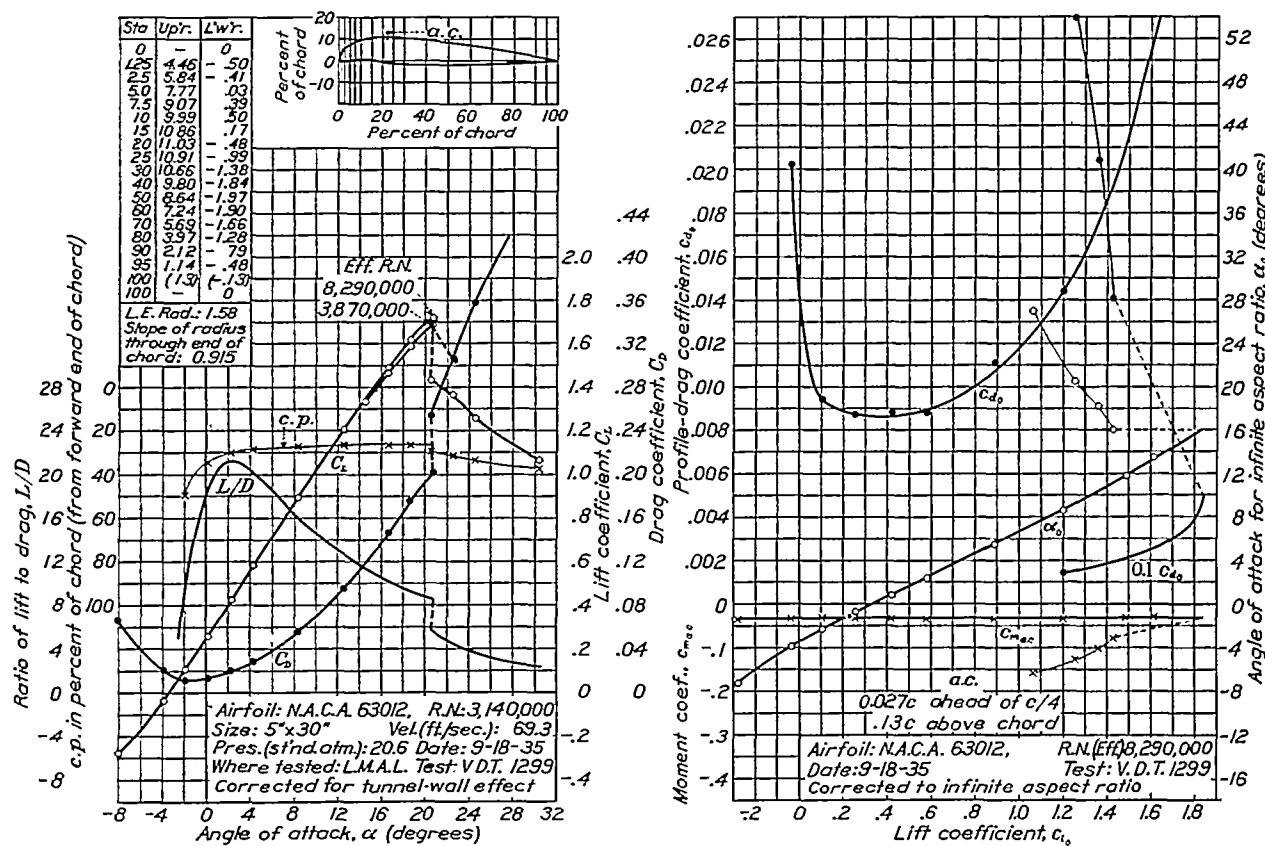


FIGURE 37.—N. A. C. A. 63012 airfoil.

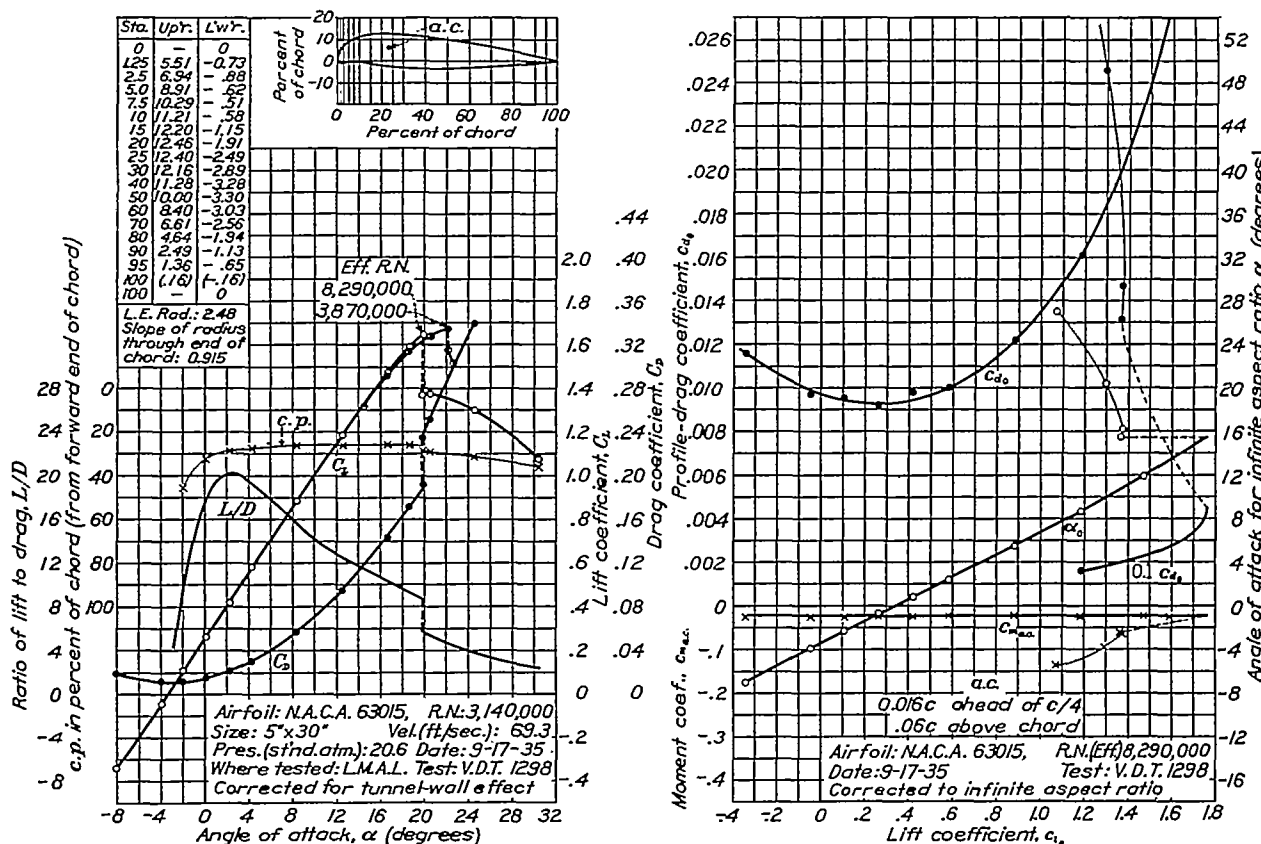


FIGURE 38.—N. A. C. A. 63015 airfoil.

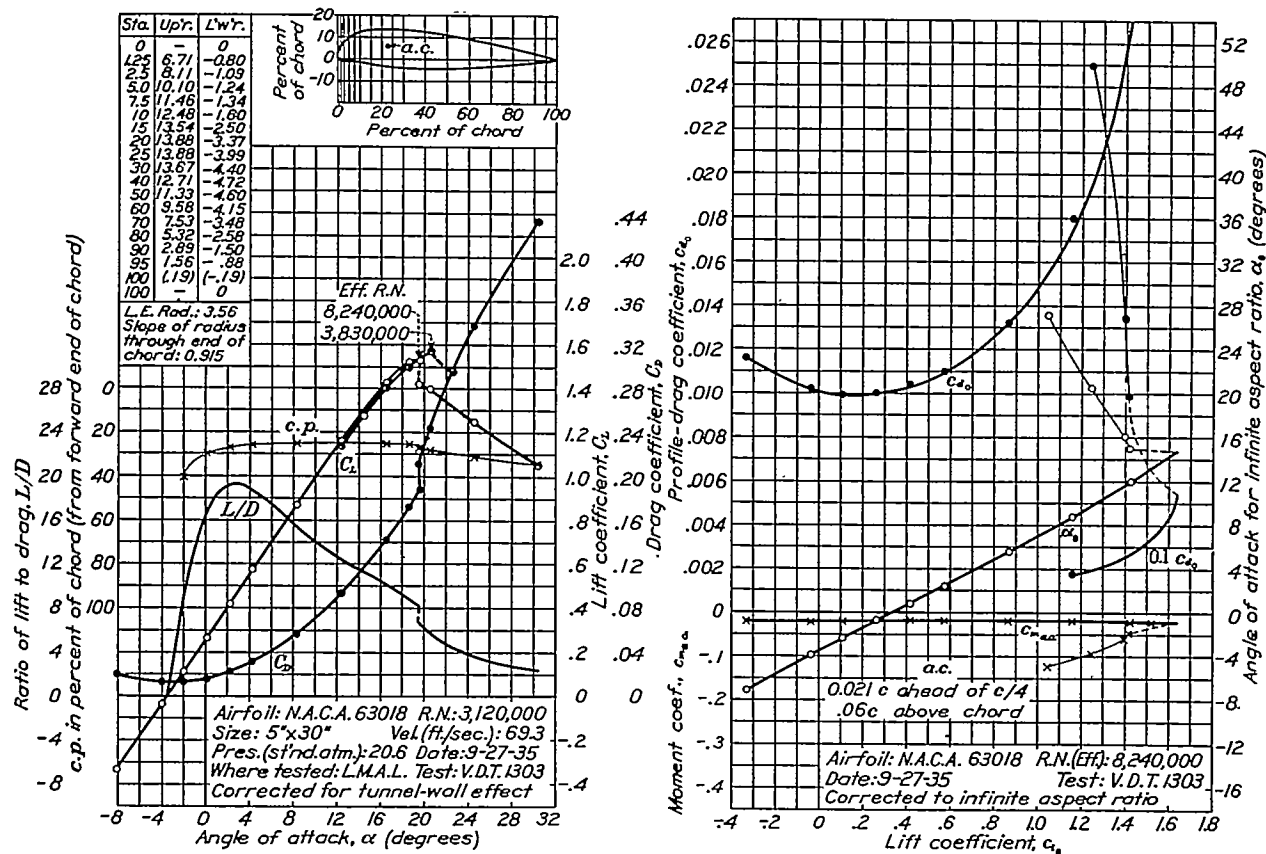


FIGURE 39.—N. A. C. A. 63018 airfoil.

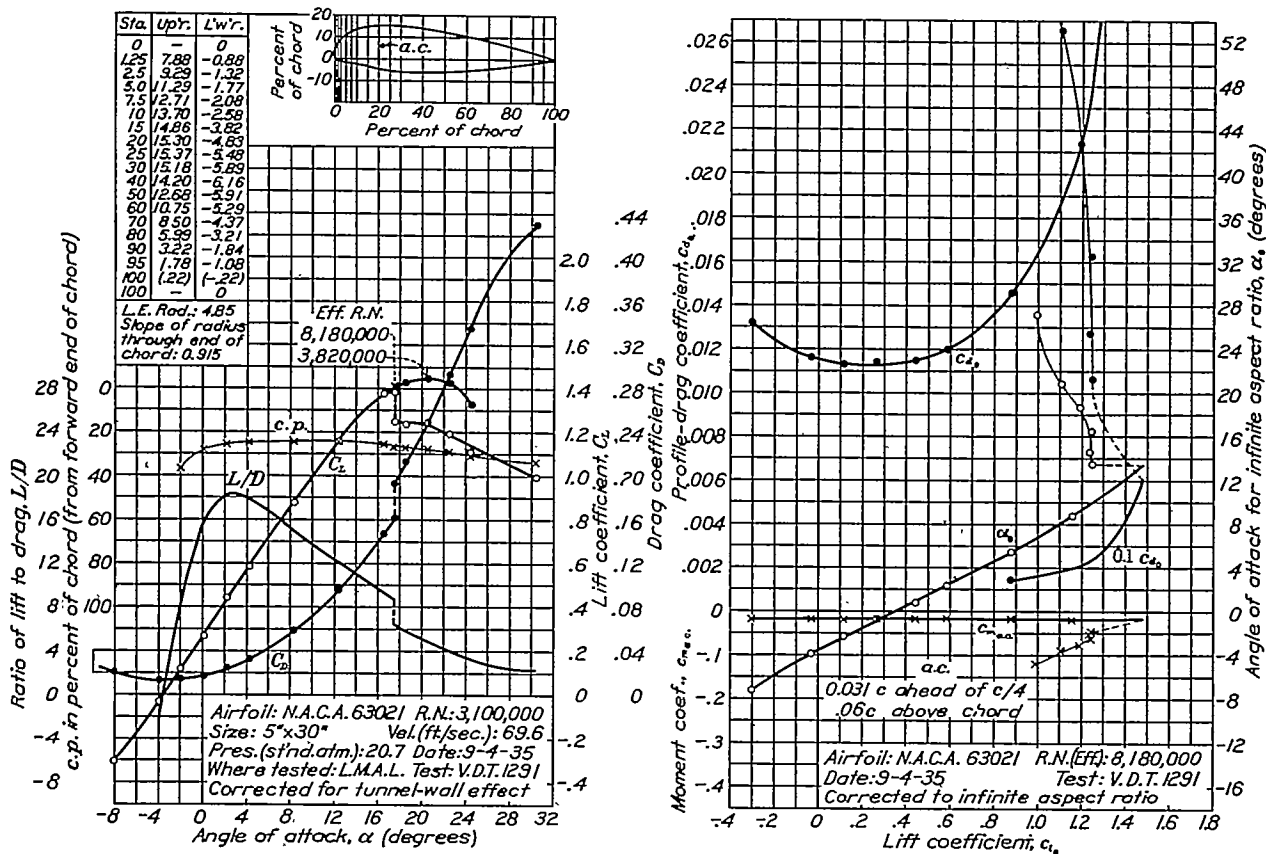


FIGURE 40.—N. A. C. A. 63021 airfoil.

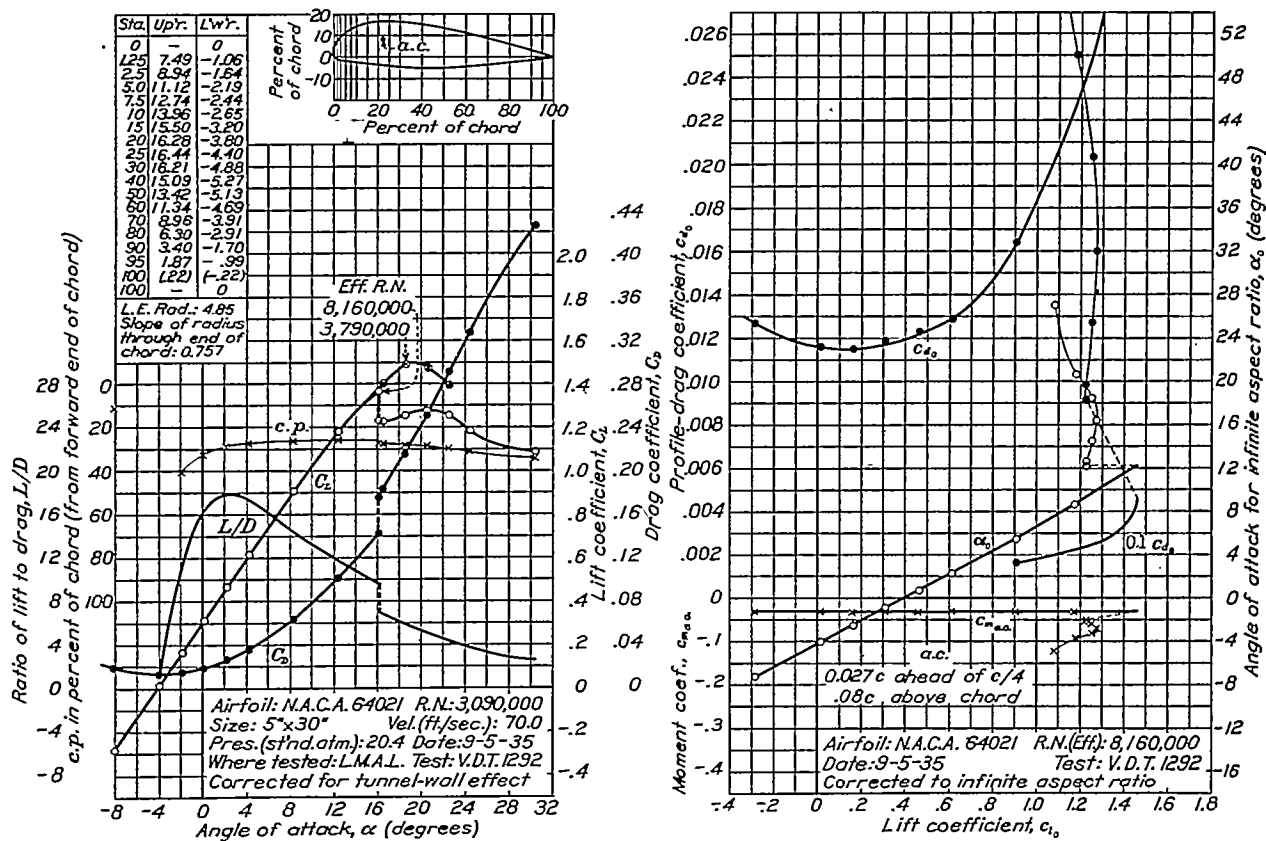


FIGURE 41.—N. A. C. A. 64021 airfoil.

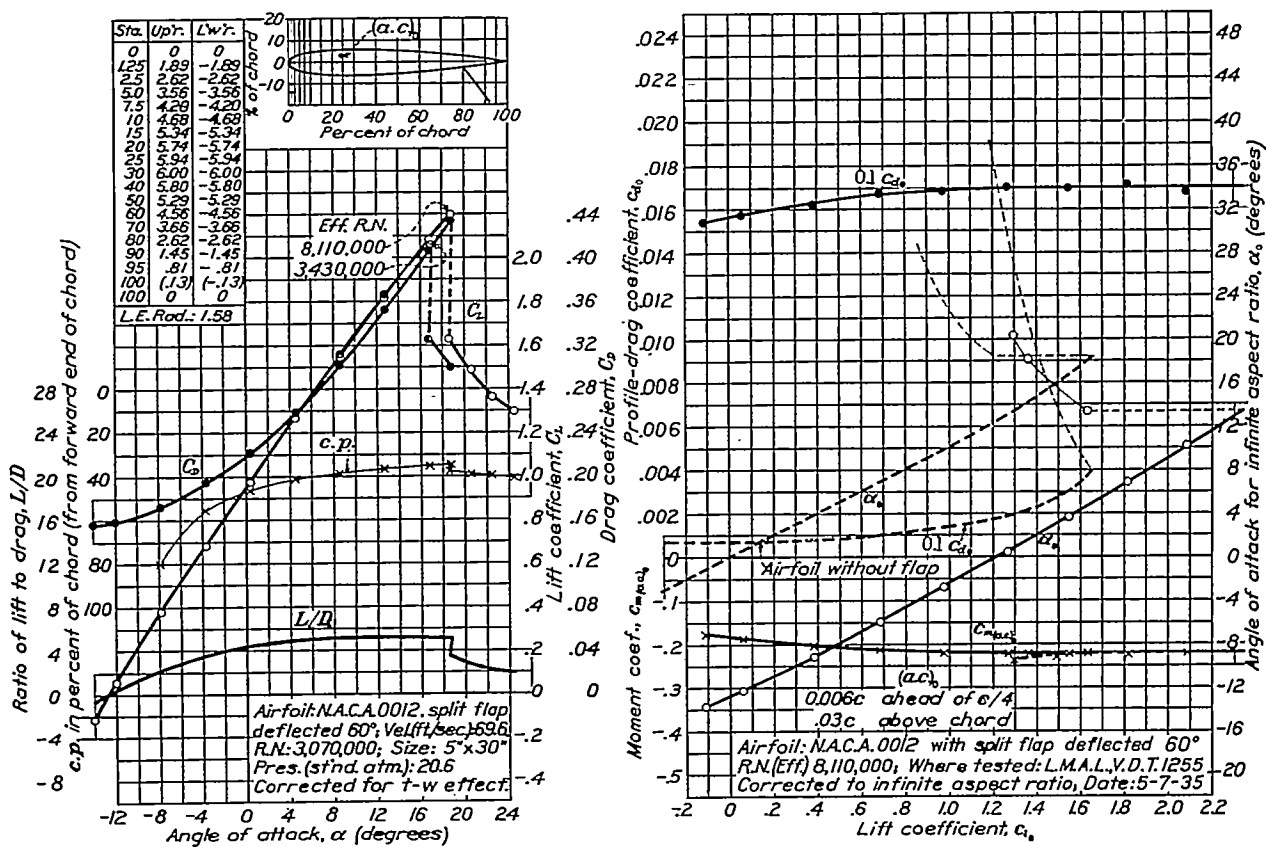


FIGURE 42.—N. A. C. A. 0012 airfoil with 0.2c split flap deflected 60°.

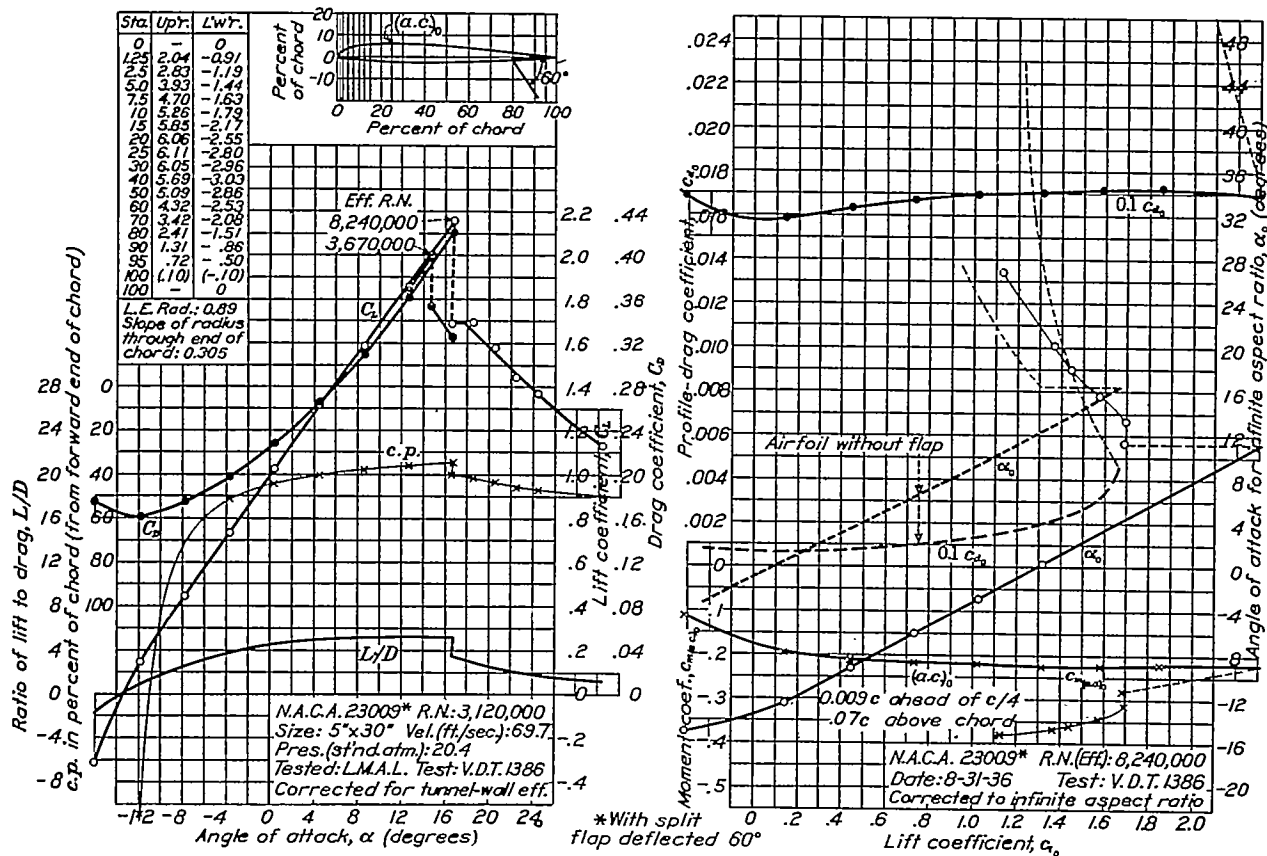


FIGURE 43.—N. A. C. A. 23009 airfoil with 0.2c split flap deflected 60°.

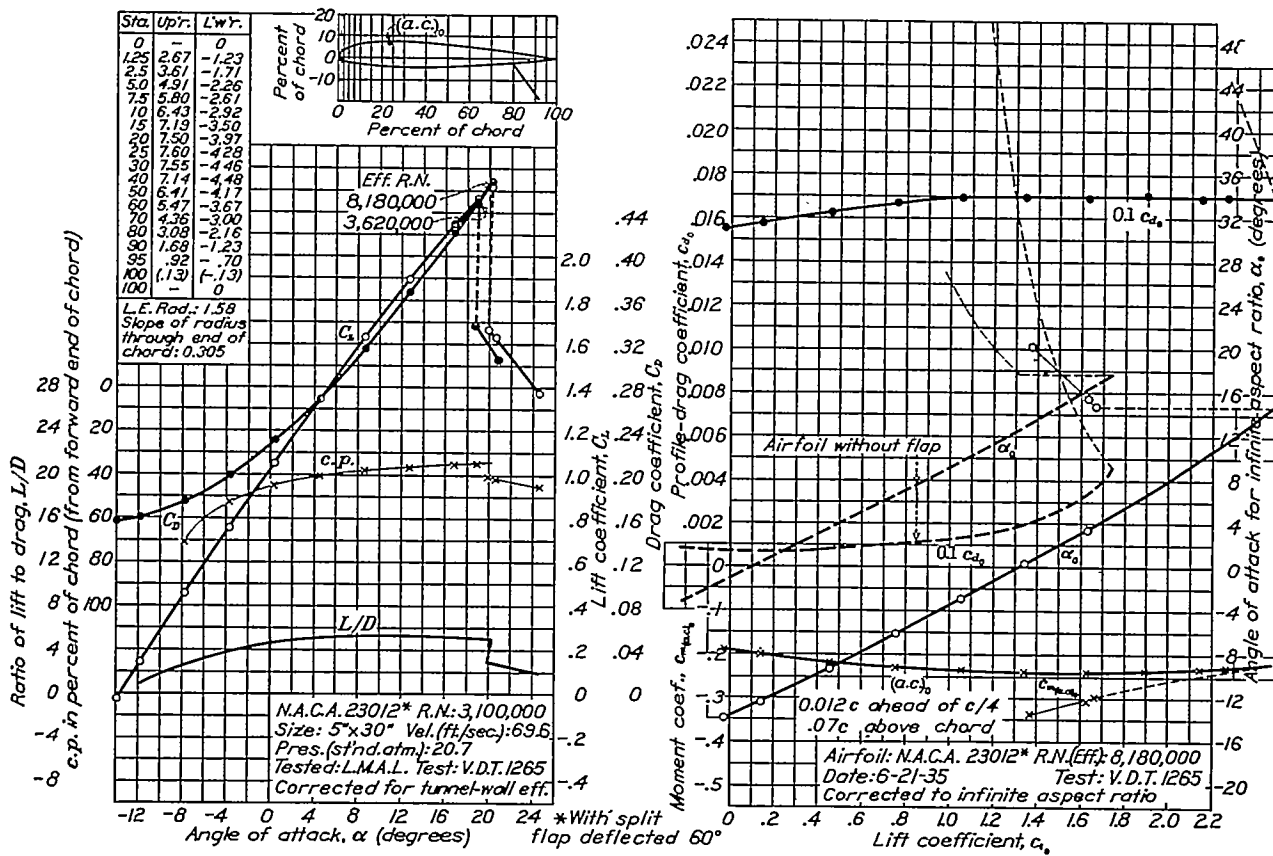
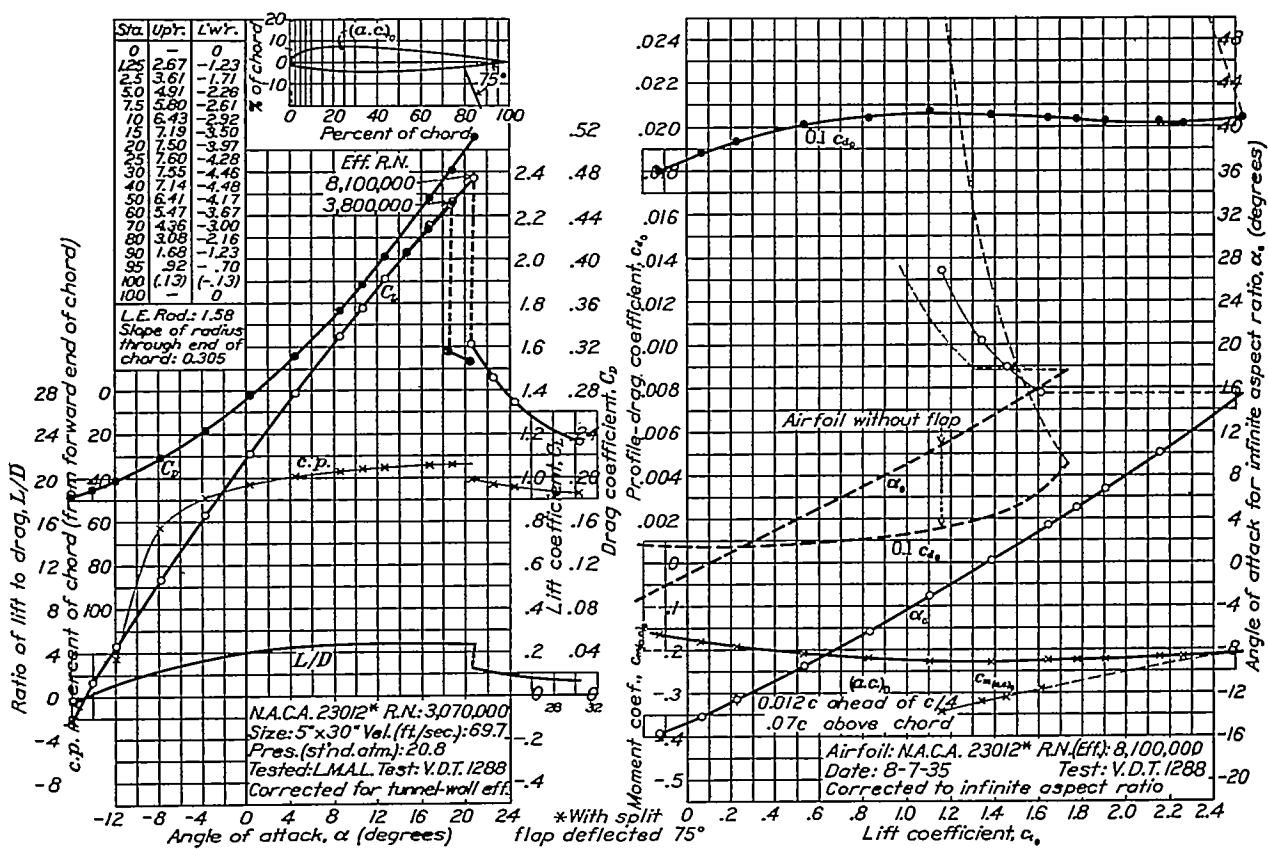
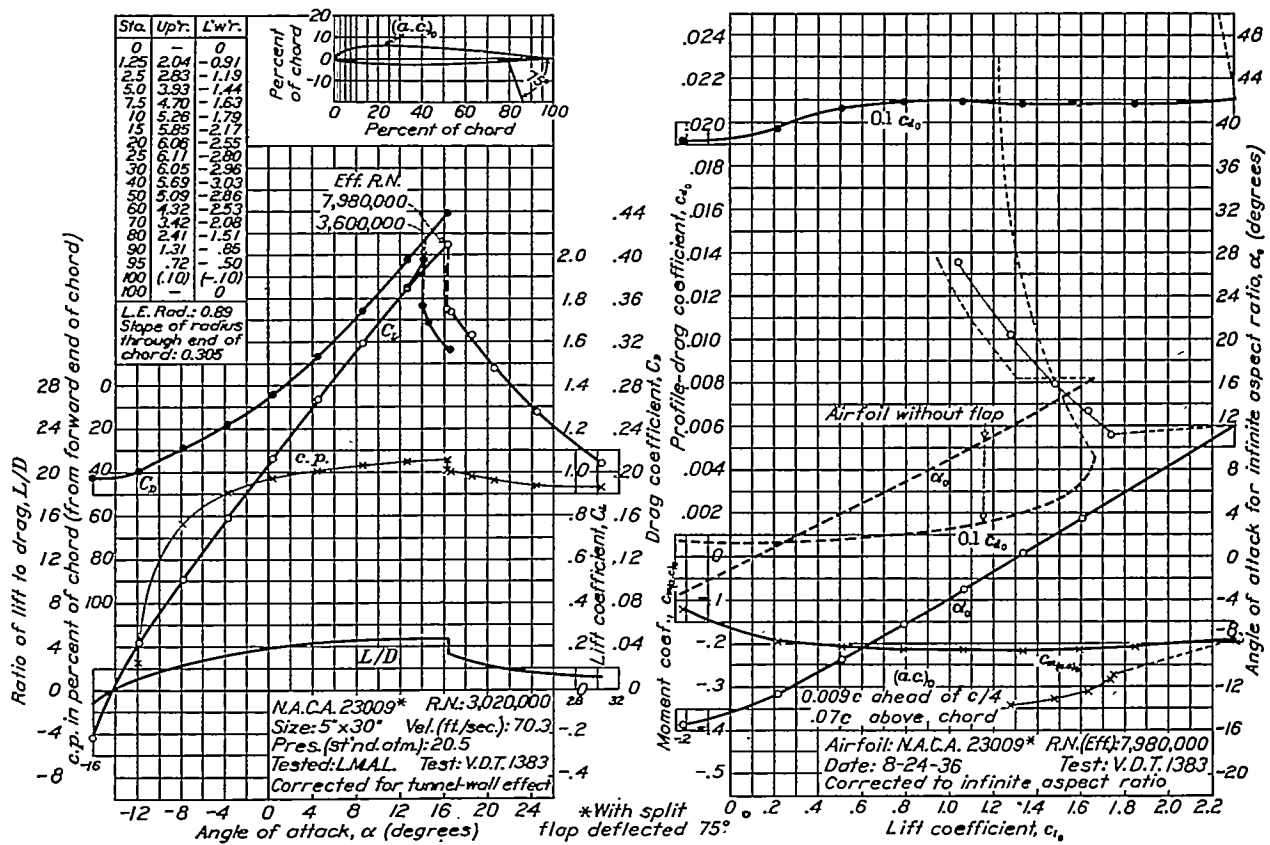


FIGURE 44.—N. A. C. A. 23012 airfoil with 0.2c split flap deflected 60°.



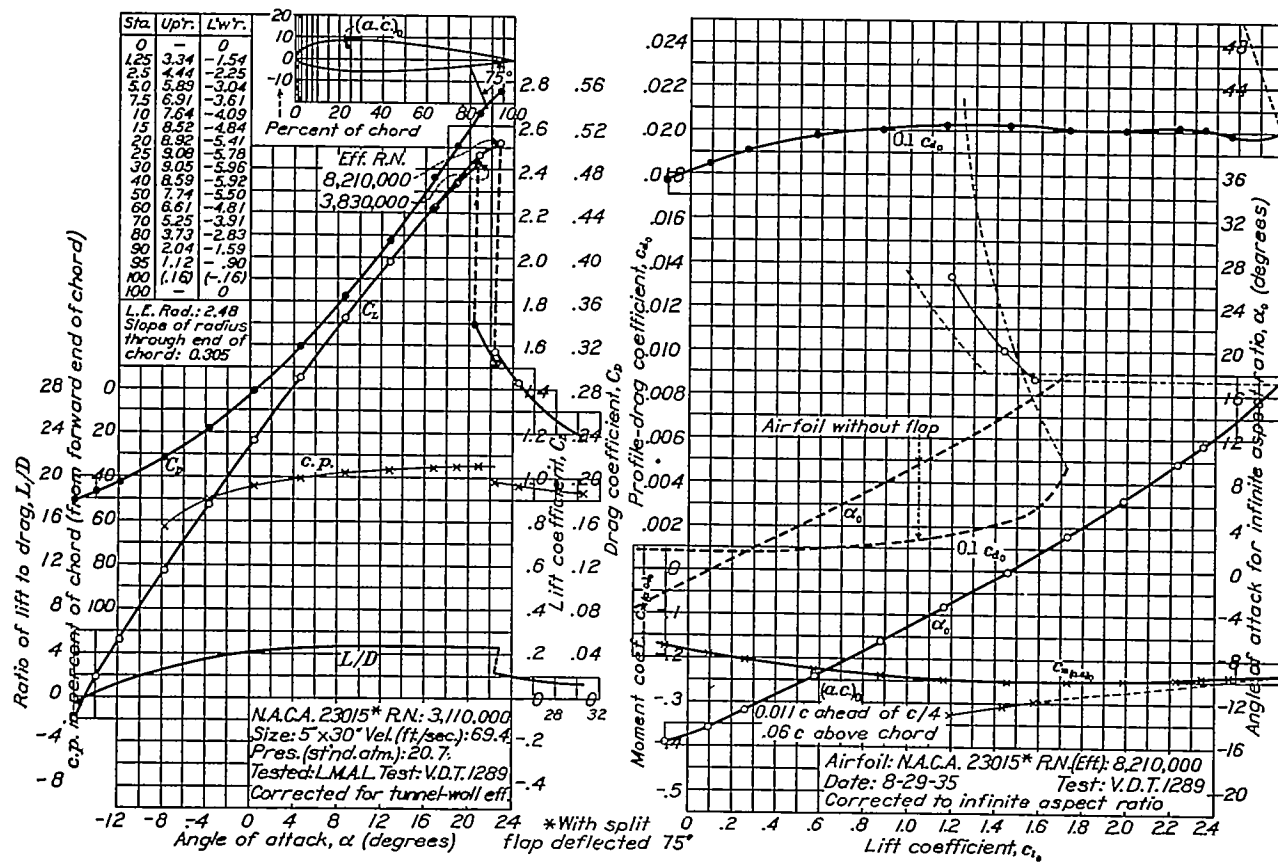


FIGURE 47.—N. A. C. A. 23015 airfoil with 0.2c split flap deflected 75°.

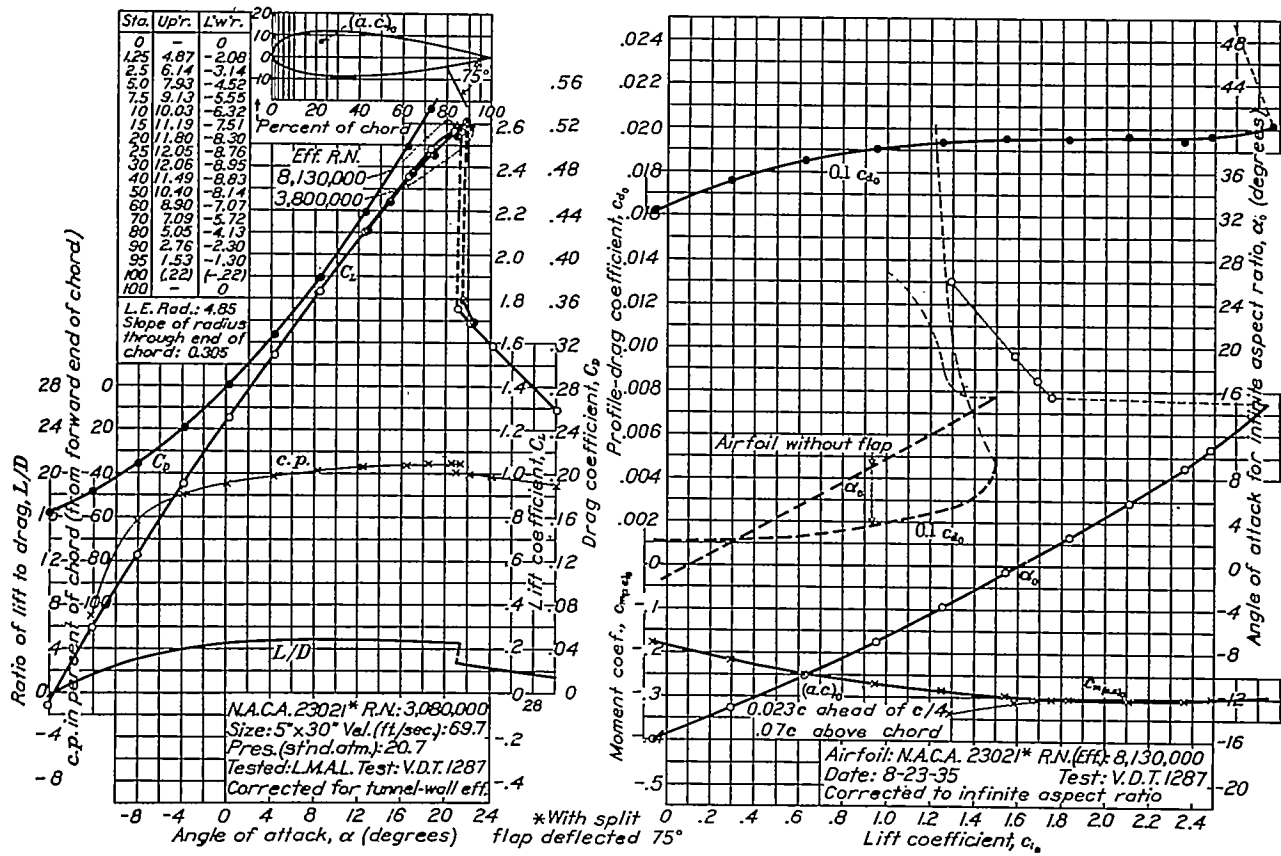
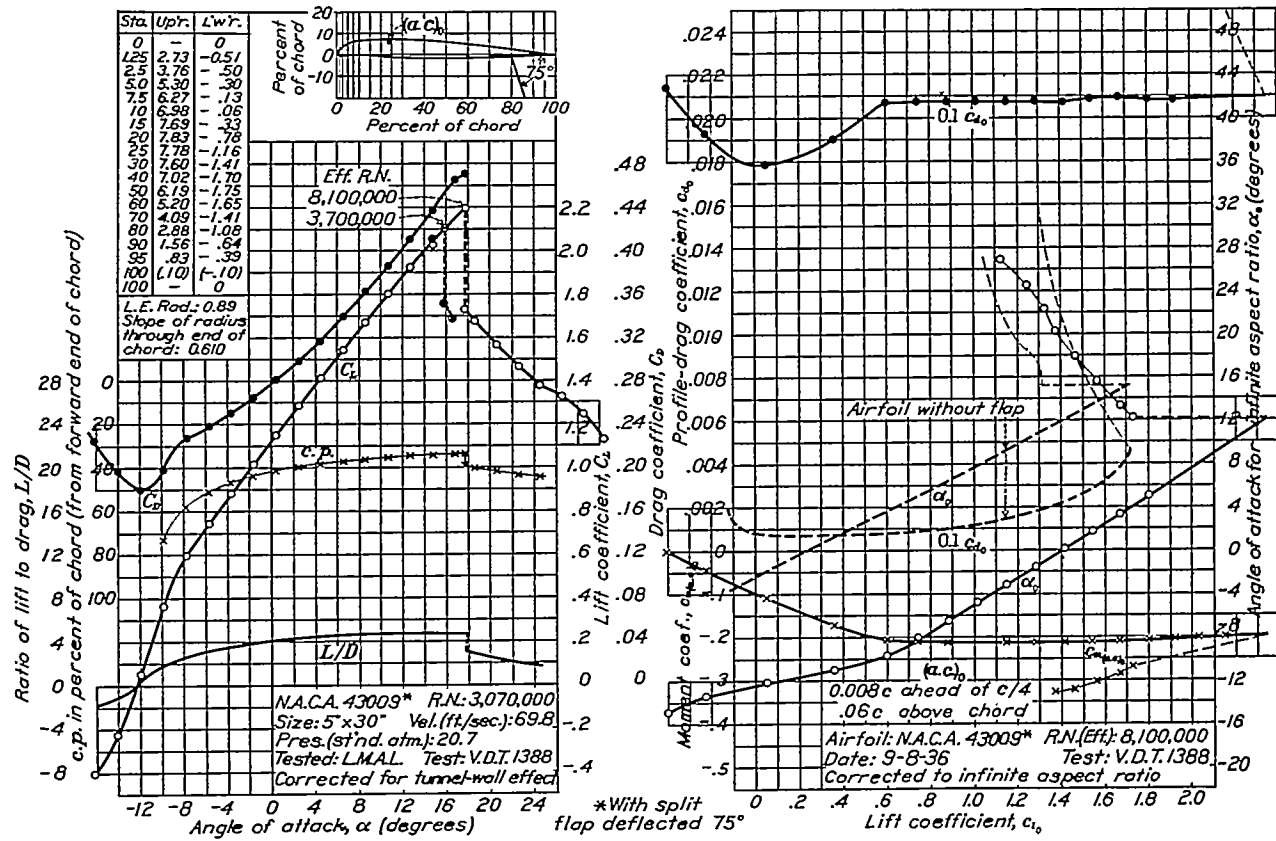
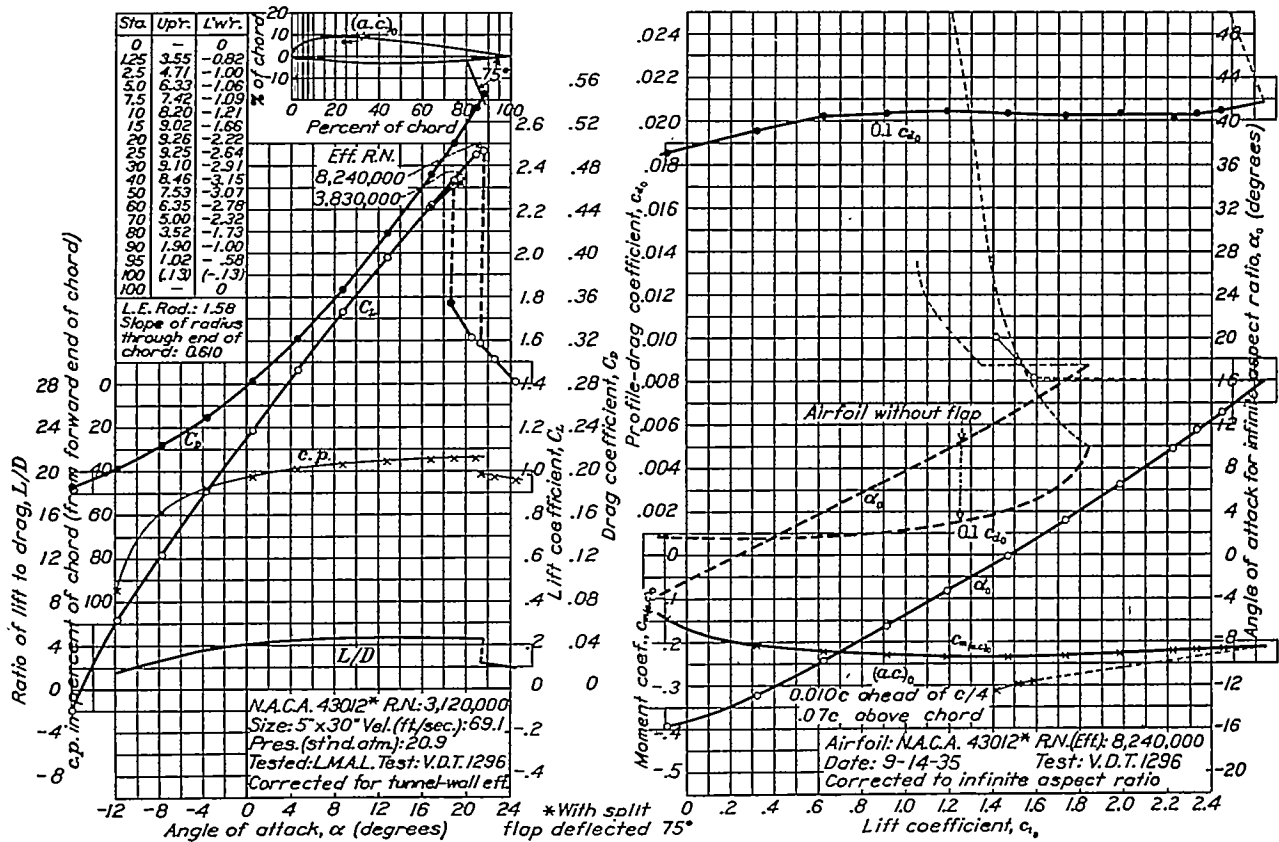
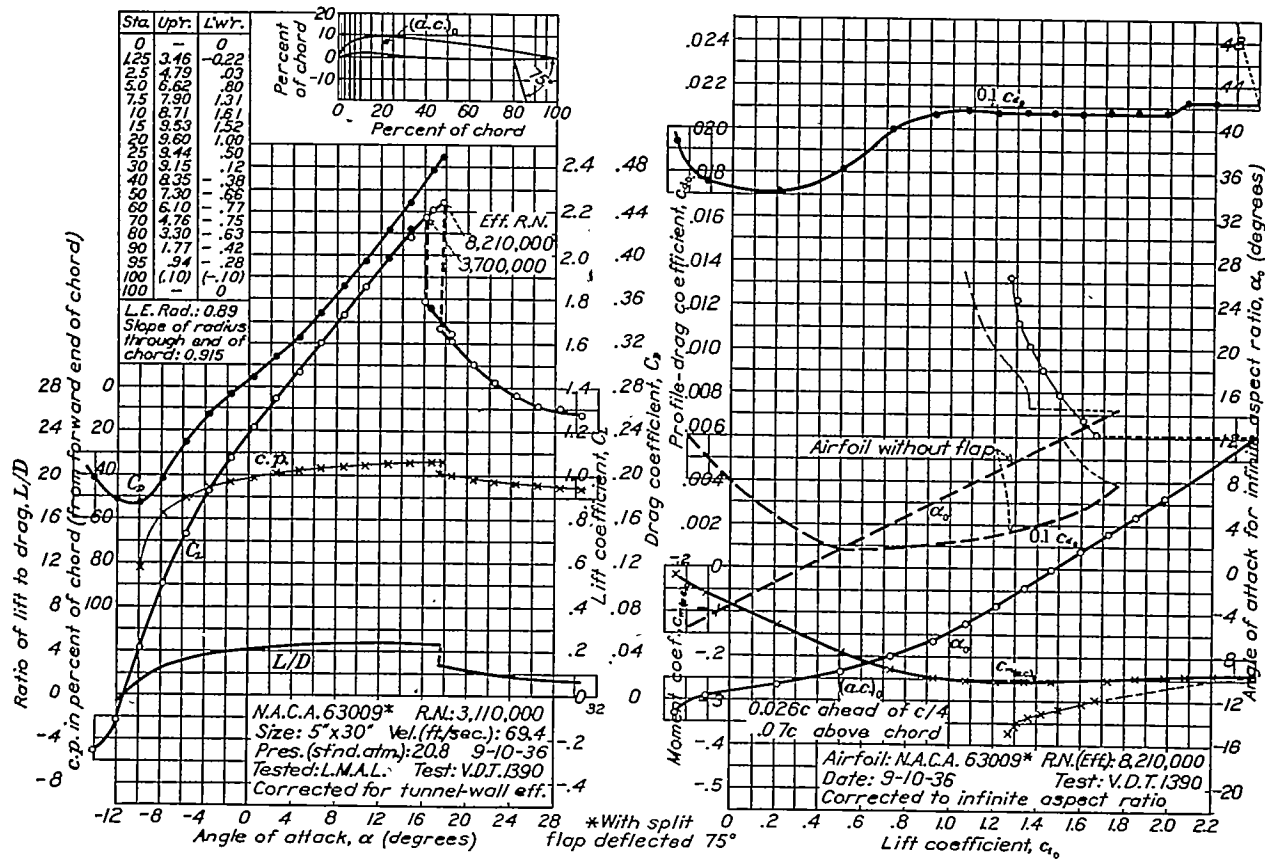


FIGURE 48.—N. A. C. A. 23021 airfoil with 0.2c split flap deflected 75°.

FIGURE 49.—N. A. C. A. 43009 airfoil with $0.2c$ split flap deflected 75° .FIGURE 50.—N. A. C. A. 43012 airfoil with $0.2c$ split flap deflected 75° .

FIGURE 51.—N. A. C. A. 63009 airfoil with $0.2c$ split flap deflected 75° .

CHOICE OF BEST CAMBER POSITION

The first results of an investigation of the effects of placing the camber forward of normal positions were reported in reference 2. These results showed that airfoils with the camber well forward had improved characteristics and that the $0.15c$ position was probably the best except for the apparently high maximum lift of the N. A. C. A. 21012 airfoil. (See fig. 15 and table II of reference 2.) Subsequently, the investigation was extended to higher cambers. These results (fig. 52) indicate that the $0.15c$ position is best for airfoils of moderate thickness (12 percent c). Furthermore, when the data for this report (including the data in references 2 and 3) were being prepared, an error was discovered in figure 15 and table II of reference 2. The value of the uncorrected maximum lift for the N. A. C. A. 21012 airfoil plotted in figure 15 should have been 1.52 instead of 1.62 and the corresponding value of $C_{L_{max}}$ in table II corrected for the tip effect should have been 1.57 instead of 1.67. The basis for the qualified conclusion of reference 2 that stated the maximum lift coefficient of simple mean-line airfoils to be unaffected by positions of camber less than $0.15c$ is thus removed. The optimum position of camber may now be definitely placed at $0.15c$; that is, the position corresponding to the mean-line shape designation 30.

The rest of this discussion will therefore be concerned with the effects of airfoil shape on the aerodynamic characteristics of those airfoils whose camber position

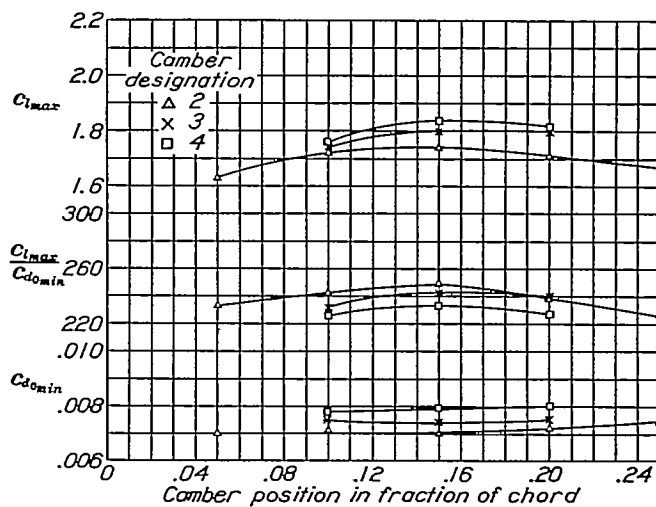


FIGURE 52.—Variation with camber position of maximum lift, minimum drag, and the ratio of maximum lift to minimum drag for the 12 percent thick airfoils.

is at 15 percent of the chord back of the leading edge and will be concluded with a discussion of the choice of the best thickness and camber.

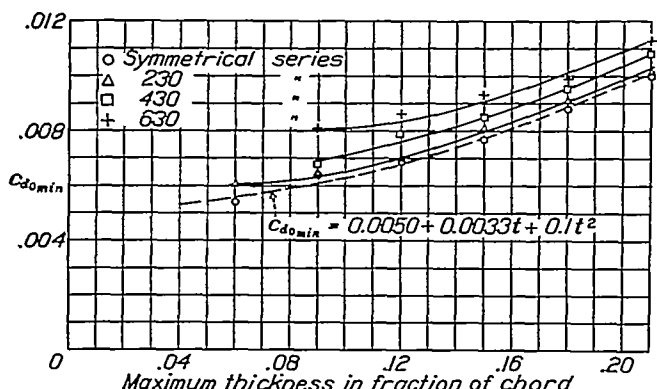


FIGURE 53.—Variation of minimum drag with thickness.

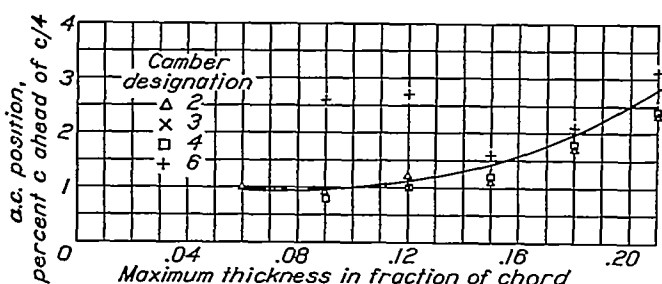


FIGURE 54.—Variation of position of aerodynamic center with thickness.

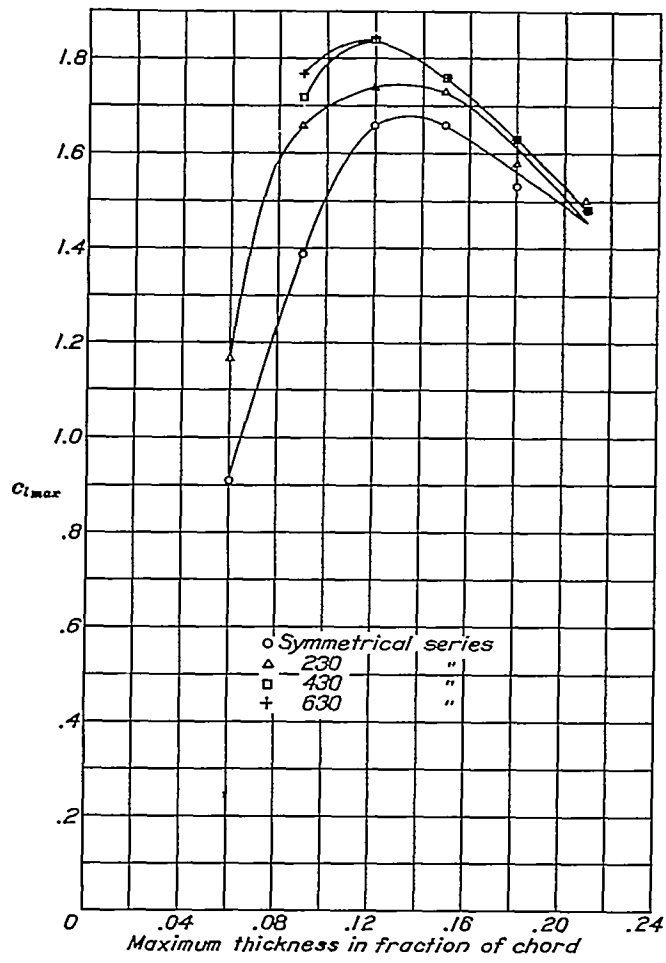


FIGURE 55.—Variation of maximum lift with thickness.

VARIATION OF AERODYNAMIC CHARACTERISTICS WITH SECTION SHAPE

The variation with thickness of the characteristics of the airfoils reported herein agrees approximately with previous findings, although the present results are slightly different owing to their greater accuracy. The added accuracy of the section characteristics is principally the result of corrections for turbulence and tip effects (reference 6), which may also be applied to the results presented in reference 1. The minimum drag coefficient increases in accordance with the relation $c_{d_{min}} = k + 0.0050 + 0.0033t + 0.1t^2$ (fig. 53), where t is the thickness ratio and k (which is approximately constant for sections having the same mean line) represents the increase in $c_{d_{min}}$ above that of the symmetrical section of corresponding thickness. The lift-curve slope decreases slightly for the thicker airfoils, and the position of the aerodynamic center moves slightly forward with increasing thickness (fig. 54). The pitching-moment coefficient and the optimum lift coefficient decrease numerically with increasing thickness.

The maximum lift coefficient is highest for moderately thick sections, as shown in figure 55. The greatest value of maximum lift occurs at a thickness near 13 percent for the symmetrical and 230 series but at a lower thickness for the 430 and 630 series.

Tests made to determine the optimum position of maximum thickness for an airfoil showed that the usual N. A. C. A. thickness distribution is better than thickness distributions having positions of maximum thickness farther back. This conclusion is substantiated by the results shown in figure 56.

The effect of filling out the concave portion of the lower surface near the nose of the N. A. C. A. 43012 airfoil and thickening the upper surfaces so that the mean line is unchanged may be seen by examining the data given in table I. The N. A. C. A. 43012 is seen to be aerodynamically better than the N. A. C. A. 43012A. A comparison of the results given in table I for the N. A. C. A. 23012 with the N. A. C. A. 23012-33 and those for the N. A. C. A. 23012-64 with the N. A. C. A. 23012-34 shows that the effect of decreasing the leading-edge radius below its normal value is to decrease the maximum lift, which confirms the results of reference 1.

The effects of camber changes upon the aerodynamic characteristics of the airfoils shown in figure 1 also agree with previous findings. The minimum drag increases with camber. (See fig. 53.) The angle of zero lift is proportional to camber and agrees with the theoretical value (see reference 1) to within 0.2° for airfoils of moderate thickness. The comparison of the angle of zero lift with the computed theoretical value is shown in figure 57. The diving moment is proportional to the camber and increases with a rearward movement of the position of the camber as predicted by

theory but is smaller in magnitude than the theoretical value (fig. 58). These and other differences between theory and experiment agree with the findings in reference 1 but have since been adequately explained. (See reference 10.)

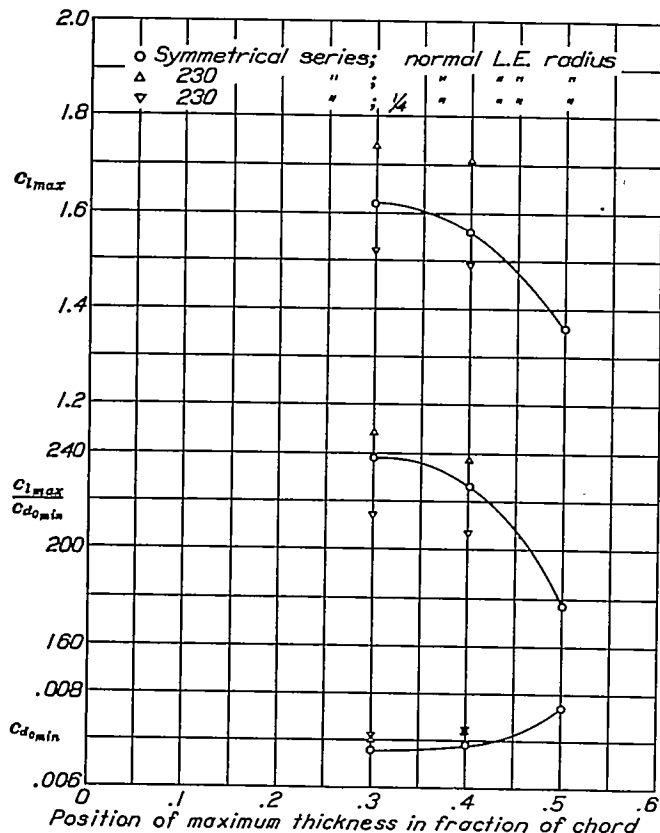


FIGURE 56.—Variation with position of maximum thickness of maximum lift, minimum drag, and the ratio of maximum lift to minimum drag.

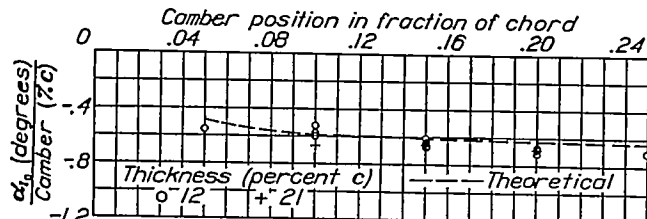


FIGURE 57.—Variation of angle of zero lift with camber position.

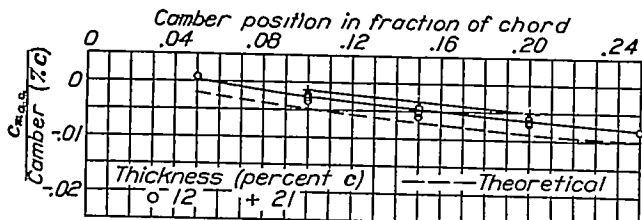


FIGURE 58.—Variation of pitching moment with camber position.

The maximum lift increases for moderate amounts of camber, but this effect is less noticeable with thicker airfoils (fig. 59). It may be mentioned that the increase of maximum lift with camber is more pronounced at reduced values of the Reynolds Number. (See reference 6.)

The addition of the split flap may be considered as giving a maximum-lift increment. This maximum-lift increment increases with thickness, as shown in figure 60, but does not change appreciably with camber.

CHOICE OF BEST THICKNESS AND CAMBER

In the selection of a member of this airfoil family for a given application, the choice of the best thickness and camber to be used depends on several factors. The Reynolds Number at which the airfoil is to be used will be one of these factors. By means of the scale-

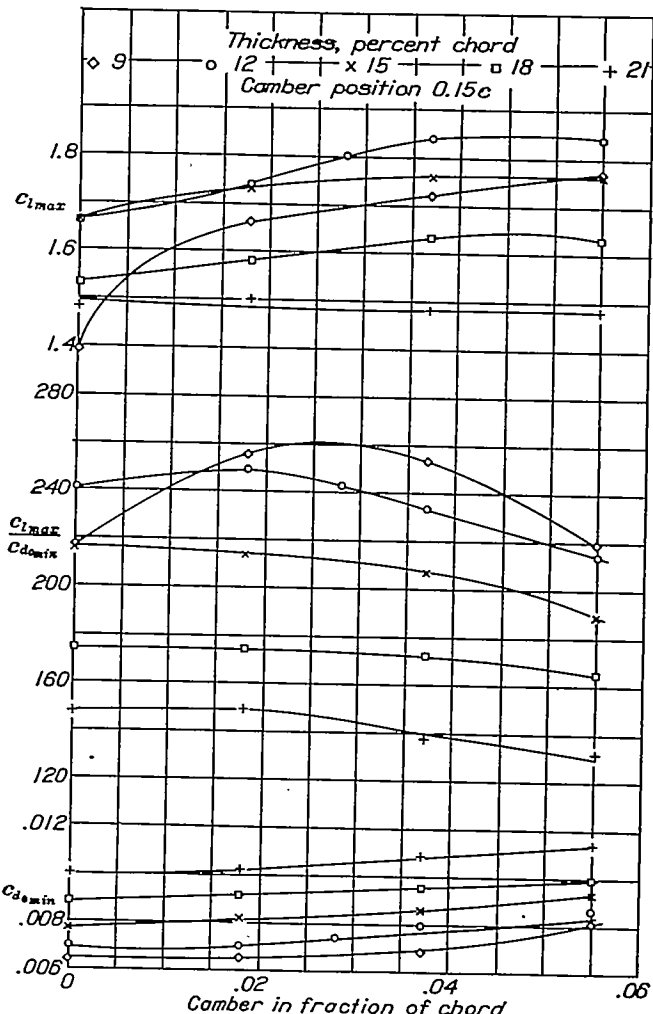


FIGURE 59.—Variation with camber of maximum lift, minimum drag, and the ratio of maximum lift to minimum drag.

effect classification given in table I and explained in references 6 and 9, the variation of maximum lift and other characteristics with Reynolds Number for any airfoil can be found.

For simplicity, the following discussion is based on airfoil section characteristics corresponding to the standard conditions (effective Reynolds Number, 8,000,000). Such an analysis will apply approximately to an airplane such as a medium-size transport, which lands at Reynolds Numbers near 8,000,000.

If a high cruising speed for a given landing speed is of primary importance, the ratio of maximum lift to the drag at cruising speed $c_{l_{max}}/c_{d_0}$, known as the "speed-range index," is a useful criterion of airfoil efficiency.

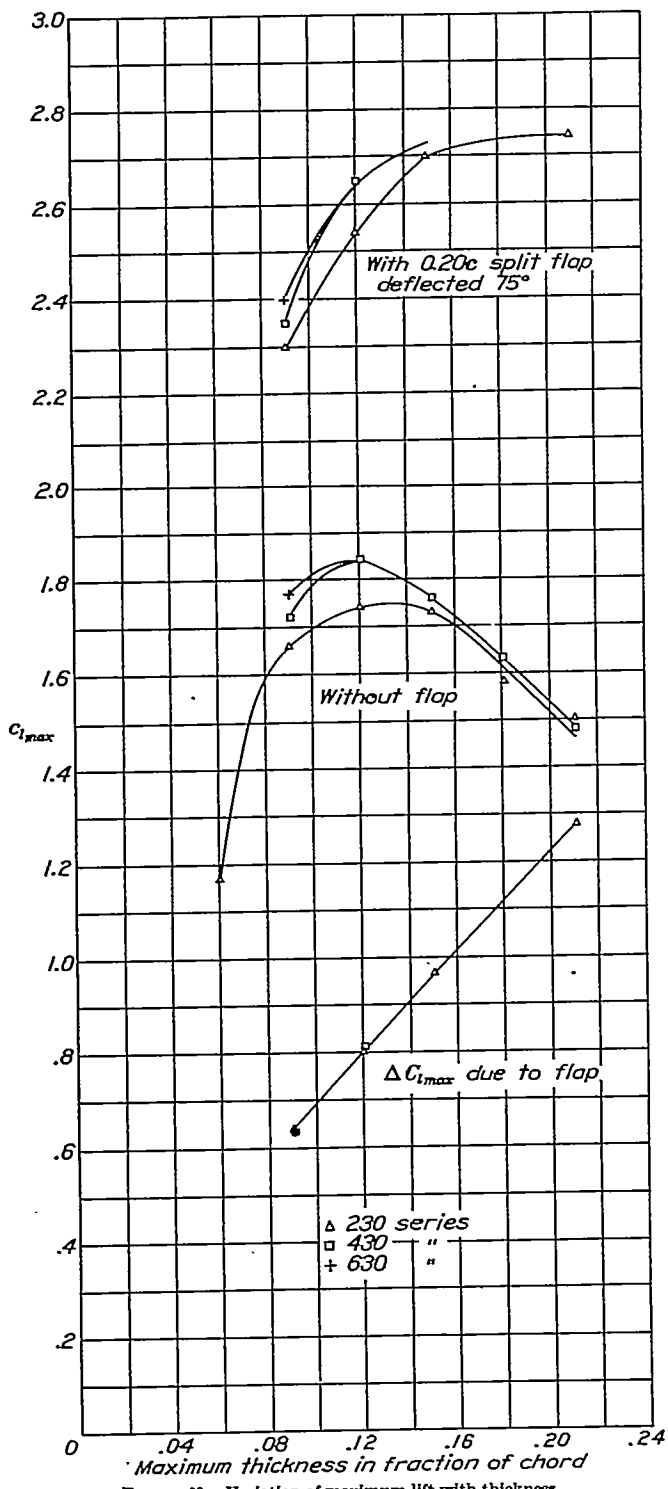


FIGURE 60.—Variation of maximum lift with thickness.

Although other performance characteristics, such as rate of climb and length of take-off run, depend less on the airfoil section characteristics than does the speed

range, the same criterion may also serve as a rough indication of these characteristics. In such cases, the drag coefficient in the ratio $c_{l_{max}}/c_{d_0}$ should be taken at a lift coefficient corresponding to the best rate of climb or to the shortest take-off run, respectively.

Inasmuch as the cruising speed generally occurs near the lift coefficient corresponding to the attitude of minimum profile drag, the ratio $c_{l_{max}}/c_{d_{0\min}}$ may be used as a measure of merit. The variation of this ratio with thickness and camber is shown in figure 61, which indicates that for thicknesses near the optimum (that is, somewhat less than 12 percent c) the N. A. C. A. airfoils can be arranged in the following decreasing

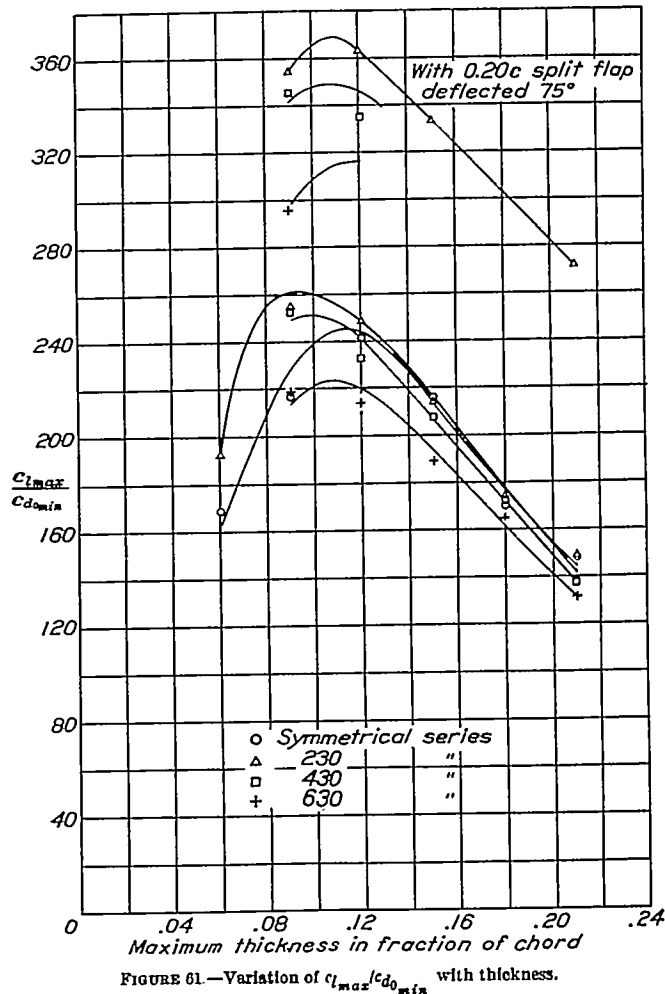


FIGURE 61.—Variation of $c_{l_{max}}/c_{d_{0\min}}$ with thickness.

order of merit as shown by the speed-range index: 230 series, 430 series, symmetrical series, and 630 series. For thicknesses only slightly greater than the optimum, however, the index for the symmetrical series becomes greater than for the 430 series and nearly equal to that of the 230 series. Attention should perhaps be called to the fact that the curves presented in figures 61, 62, and 63 are drawn to agree with cross plots of the characteristics against thickness. Points are included to show the experimental values.

Owing to the wide use of split flaps and other high-lift devices in landing, the speed-range index should preferably be derived from the maximum lift coefficient with the high-lift device. Figures 61, 62, and 63 each include curves showing the ratio of the maximum lift coefficient with flap deflected to the drag coefficient with flap neutral. The addition of split flaps does not affect the optimum camber of the airfoils since the maximum-lift increment is practically independent of camber at flap deflections of 60° and 75° . The addition of split flaps will tend, however, to increase the optimum thickness of the airfoils, since the maximum-lift incre-

A comparison of the N. A. C. A. forward-camber airfoils, based on their drags at a lift coefficient of 0.4, is given in figure 62. The order of decreasing merit for thicknesses between 10 and 12 percent is then changed and becomes 430 series, 230 series, 630 series, and symmetrical series. As before, the addition of a flap will not markedly affect the relative merit of the airfoils for any given thickness but will increase the value of optimum thickness for any given camber.

It may also be desirable to compare these airfoils on the basis of a cruising speed corresponding to a lift coefficient of 0.6. The results, which are shown in

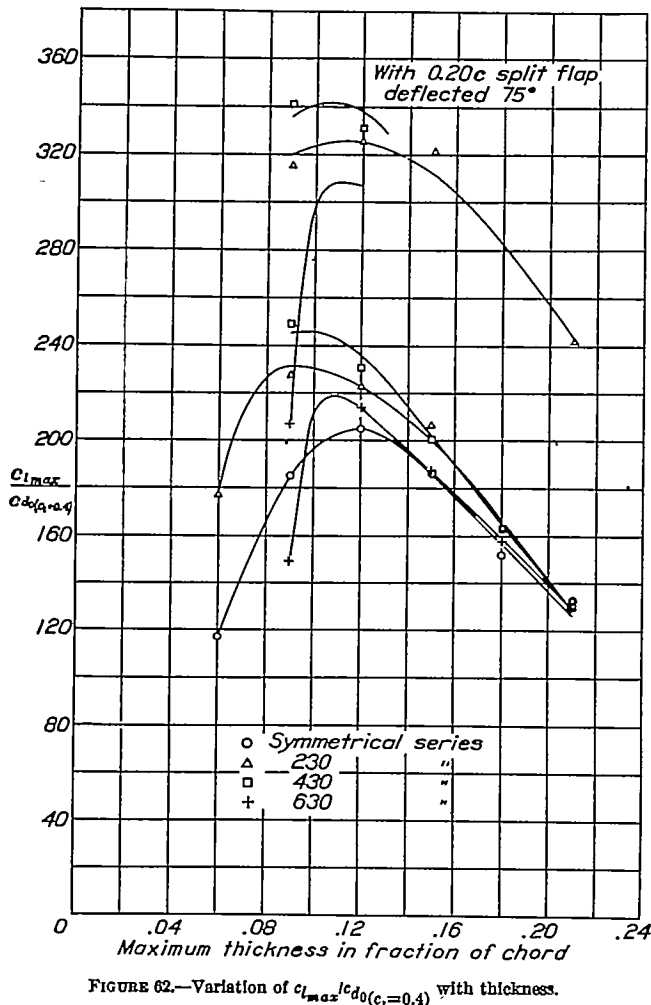


FIGURE 62.—Variation of $c_{l_{\max}}/c_{d_0}(c_l=0.4)$ with thickness.

ment with flaps increases with thickness. (See fig. 60.) Thus the thickness for the highest value of $c_{l_{\max}}/c_{d_0}$ for the 230 series increases from 9 to 11 percent (approximately) with the addition of the flap. (See fig. 61.)

Particular design conditions, such as high-altitude flight, high wing loadings, and long-range flight, require that the airplane fly most efficiently at a certain lift coefficient that may be higher than $c_{l_{opt}}$. For such applications the useful criterion is the ratio $c_{l_{\max}}/c_{d_0}$ where c_{d_0} is taken as the value corresponding to this certain lift coefficient.

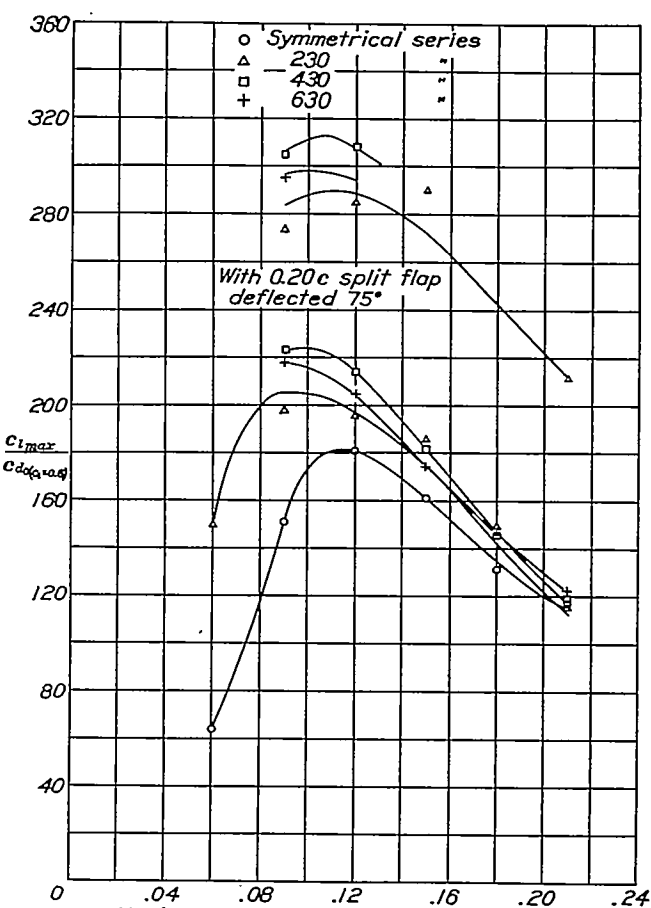


FIGURE 63.—Variation of $c_{l_{\max}}/c_{d_0}(c_l=0.6)$ with thickness.

figure 63, indicate that the 430 series now becomes superior to the 230 series over the entire range of thicknesses tested and the symmetrical series becomes definitely inferior.

Finally, structural considerations will dictate the choice of an airfoil thickness and a wing shape that will efficiently support the aerodynamic loads. This requirement will lead to the choice of an airfoil that is thicker, in general, than one selected solely on the basis of aerodynamic requirements. The final selection of the best thickness and camber will result in a compromise between the demands of aerodynamic and structural efficiency.

The general factors determining the choice of the best thickness and camber have been only briefly discussed. The requirements of any particular airplane design will determine exactly what airfoil will be best suited to that application. It should be emphasized, for instance, that for small airplanes landing at Reynolds Numbers much below 8,000,000, section characteristics should be corrected by means of the method given in reference 6 to the design Reynolds Number before comparisons to determine the optimum sections are made. Such a comparison will show that the optimum camber is considerably higher at the lower Reynolds Number than that indicated by the preceding analysis. For most purposes, a camber of 2 to 4 percent and a thickness slightly above that of the maximum speed-range index will usually be chosen. Some unpublished investigations of particular cases indicate that it is inadvisable, in any case, to depart very much from the optimum airfoil shape dictated by purely aerodynamic considerations unless structural considerations definitely justify the departure.

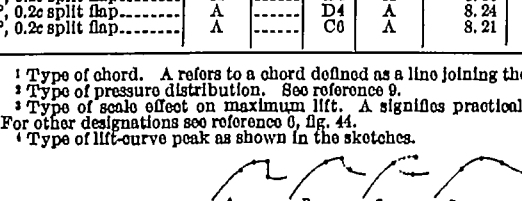
REFERENCES

1. Jacobs, Eastman N., Ward, Kenneth E., and Pinkerton, Robert M.: The Characteristics of 78 Related Airfoil Sections from Tests in the Variable-Density Wind Tunnel. T. R. No. 460, N. A. C. A., 1933.
2. Jacobs, Eastman N., and Pinkerton, Robert M.: Tests in the Variable-Density Wind Tunnel of Related Airfoils Having the Maximum Camber Unusually Far Forward. T. R. No. 537, N. A. C. A., 1935.
3. Jacobs, Eastman N., and Pinkerton, Robert M.: Tests of N. A. C. A. Airfoils in the Variable-Density Wind Tunnel. Series 230. T. N. No. 567, N. A. C. A., 1936.
4. Jacobs, Eastman N., and Clay, William C.: Characteristics of the N. A. C. A. 23012 Airfoil from Tests in the Full-Scale and Variable-Density Tunnels. T. R. No. 530, N. A. C. A., 1935.
5. Platt, Robert C.: Turbulence Factors of N. A. C. A. Wind Tunnels as Determined by Sphere Tests. T. R. No. 558, N. A. C. A., 1936.
6. Jacobs, Eastman N., and Sherman, Albert: Airfoil Section Characteristics as Affected by Variations of the Reynolds Number. T. R. No. 586, N. A. C. A., 1937.
7. Stack, John, and von Doenhoff, Albert E.: Tests of 16 Related Airfoils at High Speeds. T. R. No. 492, N. A. C. A., 1934.
8. Jacobs, Eastman N., and Abbott, Ira H.: The N. A. C. A. Variable-Density Wind Tunnel. T. R. No. 416, N. A. C. A., 1932.
9. Jacobs, Eastman N., and Rhode, R. V.: Airfoil Section Characteristics as Applied to the Prediction of Air Forces and Their Distribution on Wings. T. R. to be published, N. A. C. A., 1938.
10. Pinkerton, Robert M.: Calculated and Measured Pressure Distributions over the Midspan Section of the N. A. C. A. 4412 Airfoil. T. R. No. 563, N. A. C. A., 1936.

LANGLEY MEMORIAL AERONAUTICAL LABORATORY,
NATIONAL ADVISORY COMMITTEE FOR AERONAUTICS,
LANGLEY FIELD, VA., December 5, 1936.

TABLE I.—CHARACTERISTICS OF FORWARD-CAMBER AIRFOILS

Airfoil	Classification				Fundamental section characteristics							Derived and additional characteristics that may be used for structural design							Camber (percent c)		
	Chord	PD	SE	$C_{L_{max}}$	Effective Reynolds number (millions)	$c_{l_{max}}$	α_{l_0} (deg.)	a_0 (per deg.)	$c_{l_{opt}}$	$c_{d_0 \min}$	$c_{m_{a.c.}}$	a. c. (percent c from $c/4$)		$\frac{c_{l_{max}}}{c_{d_0 \min}}$	c. p. at $c_{l_{max}}$ (per cent c)	Wing characteristics $A=6$, round tips		Thickness (percent c) at—			
												Ahead	Above			m_t (per radian)	$C_D \min$	0.15 c	0.65 c	Maximum	
N. A. O. A.																					
0006	(1) A	(2) A10	(3) A	(4) D	(5) 8.47	(6) 0.91	(7) 0	(8) 0.008	(9) 0.00	(10) 0.0054	(11) 0	(12) 0.7	(13) 2	(14) 189	(15) 35	(16) 4.28	(17) 0.0054	(18) 5.35	(19) 4.13	(20) 6	0.00 0.00
0009	A	B10	B0	A	8.29	1.39	0	.098	.00	.0004	0	1.0	5	217	26	4.28	.0064	8.02	8.20	9	0.00 0.00
0012	A	C10	C0	A	8.37	1.68	0	.090	.00	.0009	0	.6	3	241	26	4.32	.0069	10.69	8.27	12	0.00 0.00
0012-03	A	C10	C0	A	7.87	1.62	0	.098	.00	.0008	0	1.0	6	238	25	4.28	.0068	10.82	8.58	12	0.00 0.00
0012-04	A	C10	C0	C	7.95	1.56	0	.094	.00	.0069	0	1.5	5	220	24	4.14	.0069	0.72	9.87	12	0.00 0.00
0012-05	A	C10	B8	C	8.21	1.38	0	.084	.00	.0077	0	3.5	0	177	23	3.78	.0077	9.01	11.22	12	0.00 0.00
0015	A	D10	D0	A	8.81	1.66	0	.097	.00	.0077	0	1.2	4	216	25	4.24	.0077	13.36	10.33	16	0.00 0.00
0018	A	E10	E0	A	7.84	1.53	0	.096	.00	.0083	0	1.7	4	174	25	4.20	.0088	10.04	12.40	18	0.00 0.00
0021	A	F10	E1	A	8.34	1.48	0	.093	.00	.0100	0	3.0	6	148	24	4.11	.0100	18.71	14.46	21	0.00 0.00
21012	A	O12	D3	C	8.37	1.63	-1.6	.099	.04	.0070	.001	1.5	6	233	25	4.32	.0070	10.69	8.26	12	1.1
22012	A	C12	D2	C	8.32	1.72	-1.9	.100	.10	.0071	-.005	1.3	5	242	25	4.34	.0072	10.69	8.24	12	1.5
23006	A	A12	A	D	8.29	1.17	-1.2	.100	.15	.0061	-.012	1.0	8	192	20	4.34	.0062	5.34	4.13	6	1.8
23009	A	B12	G2	A	8.26	1.60	-1.1	.099	.08	.0065	-.009	.9	7	256	25	4.32	.0068	8.02	6.21	9	1.8
23012	A	C12	D2	A	8.37	1.74	-1.2	.100	.08	.0070	-.006	1.2	7	249	25	4.34	.0071	10.69	8.25	12	1.8
23012-33	A	B12	B6	B	8.53	1.52	-1.2	.097	.25	.0071	-.010	.7	7	214	27	4.24	.0073	10.48	8.80	12	1.8
23012-34	A	B12	B3	C	8.00	1.49	-1.2	.094	.13	.0072	-.011	.9	4	207	26	4.14	.0073	8.98	9.87	12	1.8
23012-04	A	C12	D2	A	8.40	1.71	-1.0	.095	.10	.0073	-.010	1.0	4	237	26	4.18	.0073	9.72	9.88	12	1.8
23015	A	D12	D2	A	8.37	1.73	-1.1	.098	.10	.0081	-.008	1.1	6	214	24	4.28	.0082	13.30	10.35	15	1.8
23018	A	E12	E2	B	8.16	1.58	-1.2	.097	.03	.0091	-.008	1.7	6	174	24	4.24	.0091	16.04	12.39	18	1.8
23021	A	F12	E2	B	8.21	1.50	-1.2	.092	.07	.0101	-.005	2.3	7	149	24	4.07	.0102	18.70	14.44	21	1.8
24012	A	C12	C3	C	8.28	1.71	-1.5	.100	.08	.0072	-.013	1.3	0	238	26	4.34	.0073	10.71	8.25	12	2.1
25012	A	C12	C3	C	8.24	1.67	-1.6	.100	.10	.0074	-.019	1.1	7	226	27	4.34	.0075	10.73	8.28	12	2.3
32012	A	C12	D3	A	8.40	1.74	-1.2	.100	.15	.0075	-.005	1.1	6	232	24	4.34	.0077	10.69	8.23	12	2.3
33012	A	C12	D3	A	8.37	1.80	-1.7	.090	.10	.0074	-.014	1.0	6	243	25	4.32	.0075	10.68	8.28	12	2.8
34012	A	C12	D3	A	8.37	1.80	-2.1	.100	.20	.0075	-.023	.6	5	240	27	4.34	.0077	10.71	8.25	12	3.1
42012	A	C12	D4	A	8.42	1.70	-1.8	.100	.20	.0078	-.009	1.1	6	226	26	4.34	.0079	10.72	8.28	12	3.1
43009	A	B12	B4	A	8.08	1.72	-2.4	.100	.18	.0068	-.021	.8	0	253	26	4.34	.0073	8.02	6.21	9	3.7
43012	A	C12	D4	A	8.39	1.84	-2.3	.100	.26	.0079	-.010	1.0	7	233	27	4.34	.0081	10.69	8.26	12	3.7
43012A	A	C12	D4	A	8.28	1.78	-2.2	.102	.29	.0081	-.017	1.2	7	220	26	4.41	.0085	11.90	8.28	12	3.7
43015	A	D12	D4	A	8.31	1.76	-2.3	.101	.18	.0086	-.015	1.2	5	207	26	4.37	.0086	13.30	10.32	15	3.7
43018	A	E12	E4	C	8.34	1.63	-2.4	.096	.16	.0095	-.013	1.8	0	172	26	4.20	.0097	10.03	12.40	18	3.7
43021	A	F12	E6	A	8.40	1.48	-2.4	.093	.10	.0108	-.010	2.4	7	137	25	4.11	.0108	18.70	14.50	21	3.7
44012	A	C12	D4	A	8.50	1.82	-2.8	.098	.25	.0080	-.028	.5	5	227	28	4.28	.0081	10.70	8.24	12	4.3
46021	A	F12	E4	D	8.42	1.52	-3.1	.094	.12	.0110	-.006	3.2	8	188	25	4.14	.0111	18.73	14.47	21	4.6
83009	A	B12	C6	A	8.10	1.77	-3.5	.098	.57	.0081	-.042	2.6	7	210	27	4.28	.0204	11.05	6.22	9	5.5
03012	A	C12	D6	A	8.29	1.84	-3.5	.100	.40	.0086	-.033	2.7	13	214	26	4.34	.0100	11.03	8.27	12	5.5
63015	A	D12	E6	A	8.29	1.76	-3.5	.098	.25	.0093	-.024	1.0	6	180	20	4.28	.0097	13.35	10.33	15	5.5
03018	A	E12	E7	A	8.24	1.63	-3.4	.097	.16	.0099	-.020	2.1	6	165	20	4.24	.0100	16.04	12.44	18	5.5
03021	A	F12	E8	A	8.18	1.48	-3.6	.097	.21	.0113	-.018	3.1	6	131	25	4.24	.0115	18.68	14.52	21	5.5
04021	A	F12	E11	A	8.16	1.46	-4.2	.094	.13	.0115	-.031	2.7	8	127	26	4.14	.0110	18.68	14.53	21	5.2
0012; 0°, 0.2e split flap	A	—	C0	A	8.11	2.35	-13.1	.091	—	.107	-.220	.0	3	341	35	4.04	—	10.69	8.27	12	0
23009; 60°, 0.2e split flap	A	—	C2	A	8.24	2.31	-14.0	.092	—	.106	-.223	.9	7	355	35	4.07	—	8.02	0.21	9	1.8
23012; 60°, 0.2e split flap	A	—	D2	A	8.18	2.48	-14.3	.088	—	.106	-.236	1.2	7	354	35	3.03	—	10.69	8.25	12	1.8
23009; 75°, 0.2e split flap	A	—	C2	A	7.98	2.30	-15.1	.089	—	.205	-.210	.0	7	364	34	3.08	—	8.02	0.21	9	1.8
23012; 75°, 0.2e split flap	A	—	D2	A	8.10	2.54	-15.0	.085	—	.201	-.228	1.2	7	303	34	3.82	—	10.69	8.25	12	1.8
23015; 75°, 0.2e split flap	A	—	D2	A	8.21	2.70	-16.2	.080	—	.198	-.245	1.1	6	333	35	3.86	—	13.36	10.35	15	1.8
23021; 75°, 0.2e split flap	A	—	E2	A	8.13	2.74	-16.5	.084	—	.191	-.300	2.3	7	271	35	4.14	—	18.70	14.44	21	1.8
43009; 75°, 0.2e split flap	A	—	B4	A	8.10	2.35	-17.5	.080	—	.207	-.208	.8	6	340	34	3.04	—	7.62	0.20	9	3.7
43012; 75°, 0.2e split flap	A	—	D4	A	8.24	2.05	-17.3	.082	—	.200	-.225	1.0	7	335	34	3.72	—	10.68	8.20	12	3.7
63009; 75°, 0.2e split flap	A	—	C6	A	8.21	2.40	-10.0	.078	—	.207	-.230	2.6	7	295	34	3.67	—	11.05	0.23	9	5.5



For other designations see reference 6, fig. 44.
* Type of lift-curve peak as shown in the sketches.

¹ Type of chord. A refers to chord defined as a line joining the extremities of the mean line.
² Type of pressure distribution. See reference 9.
³ Type of scale effect on maximum lift. A signifies practically no scale effect.
⁴ Turbulence factor is 2.64.
⁵ These data have been corrected for tip effect.
⁶ Angle of zero lift obtained from linear lift curve approximating experimental lift curve.
⁷ Slope obtained from linear lift curve approximating experimental lift curve.
⁸ Value of the drag that applies approximately over the entire useful range of lift coefficients.
⁹ The value of $c_{m_{a.c.}}$ is taken about the aerodynamic center of the airfoil without the flap.
¹⁰ Values of $c_{d_0 \min}$ used in computing this ratio are taken from tests of the airfoil without the flap.